Stacked Intelligent Metasurfaces

Communication, Computing and Sensing in the Wave Domain

Marco Di Renzo

CNRS Research Director – CentraleSupélec, Paris-Saclay University, France
Chair Professor in Telecom Engineering, King's College London, UK
marco.di-renzo@universite-paris-saclay.fr, marco.di_renzo@kcl.ac.uk

HE-MSCA-DN-2021

ANR-23
CHR-2022

HE-JU-SNS-2023

COST ACTION

Télécom Paris – IP Paris
Seminaire ICE
May 6, 2025

Outline: Wireless Evolution

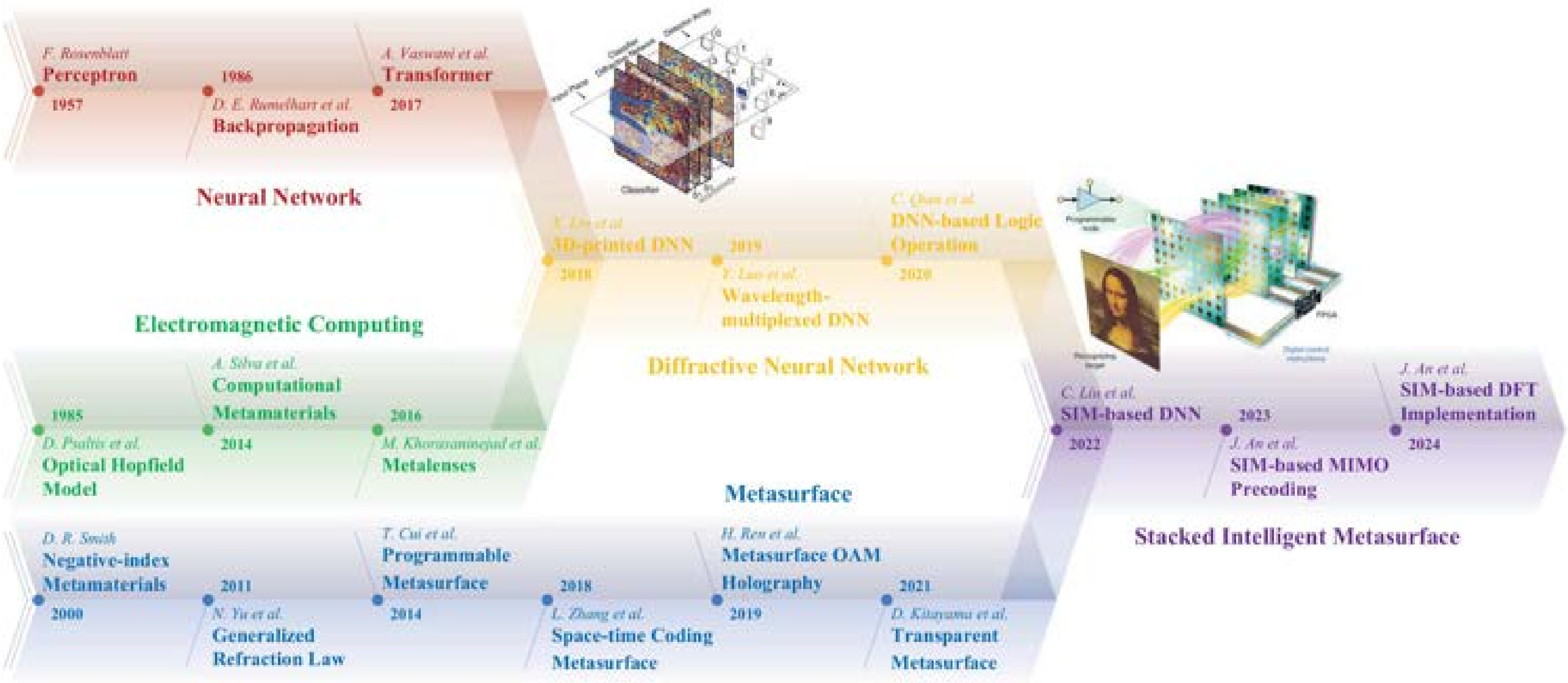

Radio

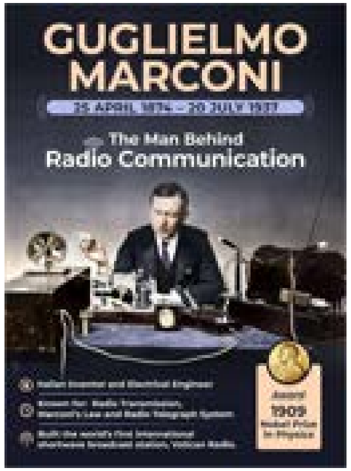

Smart Radio

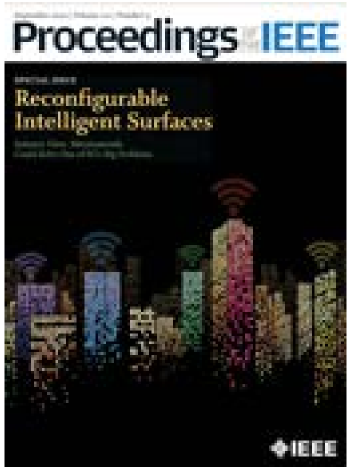

Deep Diffractive Radio

Reconfigurable Intelligent Surface

Reconfigurable Intelligent Surface

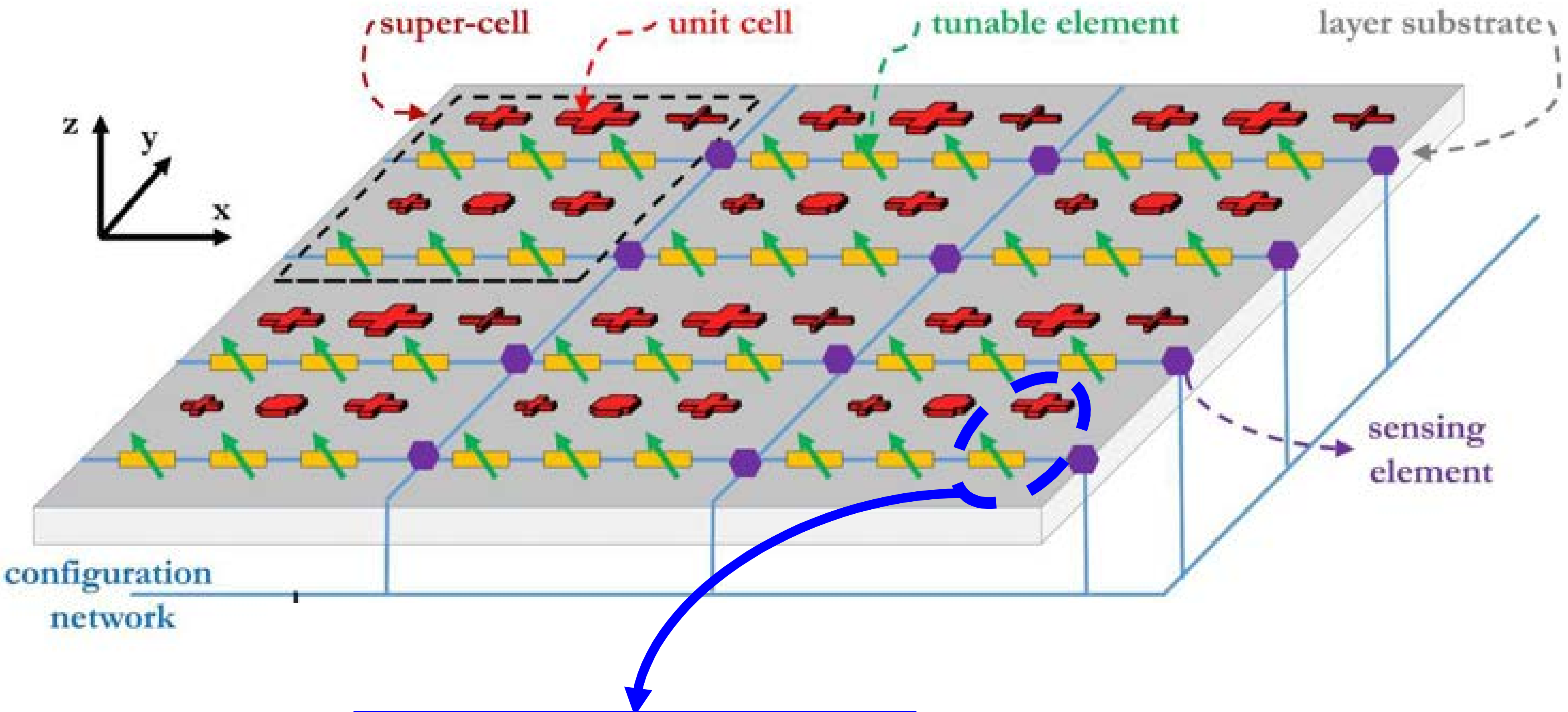

$$x \longrightarrow \boxed{\boldsymbol{\Theta}(i,i) = \beta_i \exp(\phi_i)} \longrightarrow y_i = \boldsymbol{\Theta}(i,i)\,x$$

M. Di Renzo et al. Smart radio environments empowered by reconfigurable intelligent surfaces: How it works, state of research, and the road ahead. **IEEE JSAC, Nov. 2020.**

Smart Radio Environments

Smart Radio Environment: Generalized Snell's Law

Mathematical Background

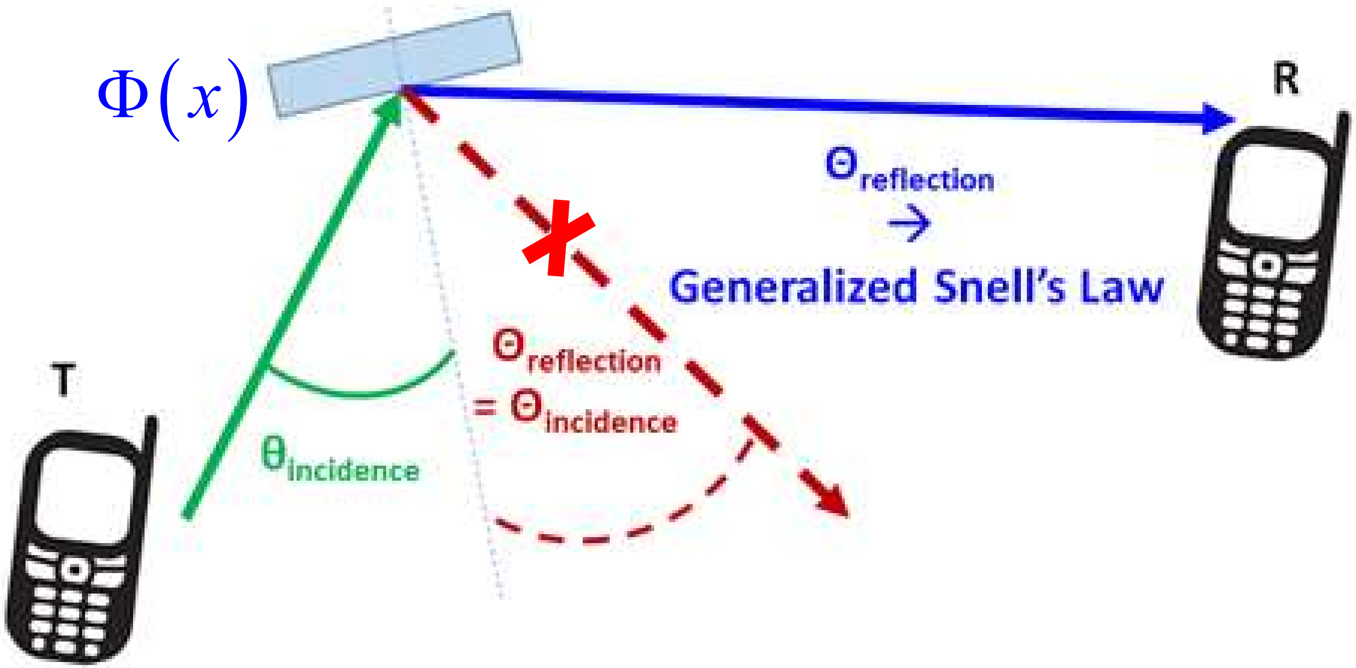

$$\sin(\theta_{\text{ref}}) - \sin(\theta_{\text{inc}}) = \frac{\lambda}{2\pi} \frac{d\Phi(x)}{dx}$$

$$\Phi(x) = \alpha x$$

$$\alpha = \frac{2\pi}{\lambda}\left(\sin(\theta_{\text{des}}) - \sin(\theta_{\text{inc}})\right)$$

$$\boxed{\theta_{\text{ref}} = \theta_{\text{des}}}$$

System-Level Evaluations

Large-Scale System-Level Simulations

Grid point calculation

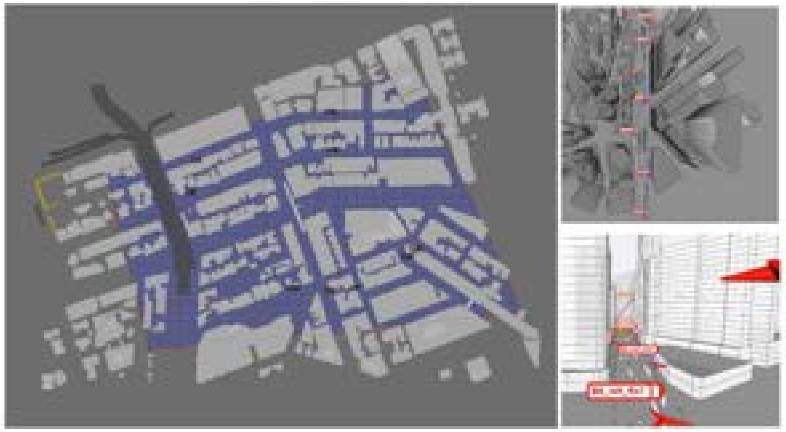

SNR map without RISs | SNR map with RISs

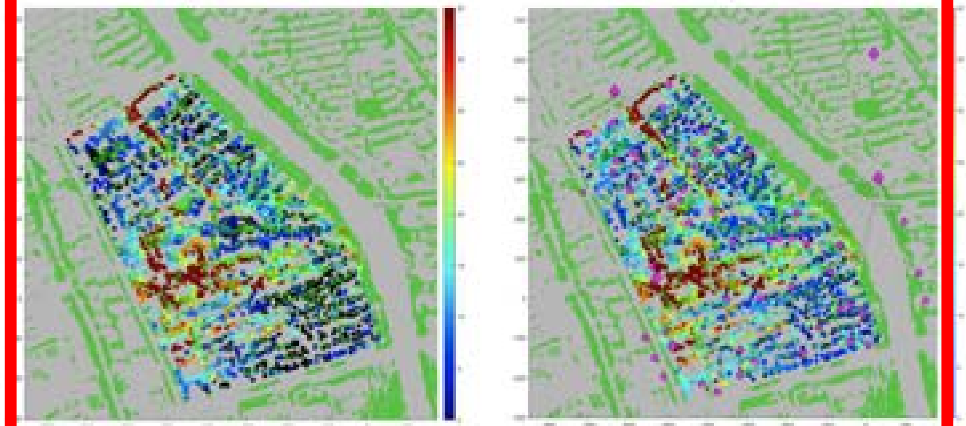

Size 1 at 28 GHz = 0.33x0.33 m^2

Size 3 at 28 GHz = 0.67x0.67 m^2

	Achievable Coverage [Required Number of RISs per BS]			
	No RIS	Few RISs		Total RISs
RIS – Size 1 at 3.5 GHz	77% [0]	80% [1]	88% [5]	95% [21]
RIS – Size 2 at 3.5 GHz	77% [0]	81% [1]	90% [5]	95% [12]
RIS – Size 3 at 3.5 GHz	77% [0]	83% [1]	92% [5]	95% [9]
RIS – Size 1 at 28 GHz	46% [0]	57% [1]	76% [5]	95% [20]
RIS – Size 2 at 28 GHz	46% [0]	63% [1]	86% [5]	95% [11.2]
RIS – Size 3 at 28 GHz	46% [0]	68% [1]	91% [5]	95% [7.4]

	Rate Improvement [Required Number of RISs per BS]			
	Cell-Edge			Cell-Average
	Few RISs		Total RISs	Total RISs
RIS – Size 1 at 3.5 GHz	3% [1]	34% [5]	253% [21]	12% [21]
RIS – Size 2 at 3.5 GHz	5% [1]	59% [5]	253% [12]	14% [12]
RIS – Size 3 at 3.5 GHz	11% [1]	115% [5]	258% [9]	16% [9]
RIS – Size 1 at 28 GHz	0% [1]	38% [5]	2508% [20]	45% [20]
RIS – Size 2 at 28 GHz	8% [1]	238% [5]	2508% [11.2]	53% [11.2]
RIS – Size 3 at 28 GHz	46% [1]	700% [5]	2508% [7.4]	62% [7.4]

Today:
46% of
users get a
good signal

With RIS:
95% of
users get a
good signal

3GPP-Compliant System-Level Simulations

Table 1 Simulation set up and parameters.

Parameter	**Value**
Number of cells	7 (e.g., 21 sectors), hexagonal macro
Operating band	2.6 GHz
Site-to-site dist.	500 m
Number of RIS panels per sector	4, 8, or 24, min distance of 25 m between RIS panels, uniformly distributed or at cell edges (e.g., 0.9~1.0 cell radius)
RIS antenna orientation	Facing towards its serving BS (azimuth)
Number of mobiles per sector	50 (100% outdoor), uniformly distributed or at cell edges (e.g., 0.85~0.9 cell radius
BS antenna height	25 m
BS antenna down-tilt	0° (mechanical) and 4° (electronic)
RIS panel height	15 m
RIS panel down-tilt	10° (mechanical)
Mobile antenna height	1.5 m
BS transmit power	46 dBm
BS antenna gain	17 dBi for sector beam
Polarization	Vertical
MS antenna config	1×2, with random orientation
Pathloss model	ITU-Urban Macro for BS-RIS, RIS-UE and BS-UE links
RIS antenna pattern	BS antenna pattern in 3GPP TR 38.901, separately modeled for cascaded link, total gain of 5 dBi at boresight
Number of elements per RIS panel	16×16, or 40×40, with 0.4λ spacing both vertical and horizontal
Number of bits for RIS element phase	2 bits
Combining of RIS cascaded link and direct link	Non-coherent, e.g., gains added up

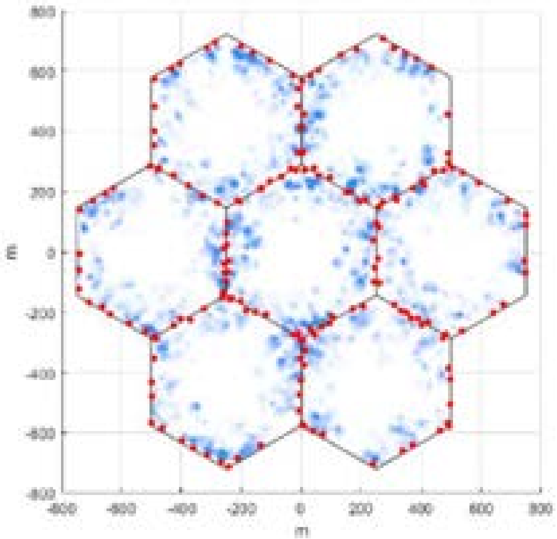

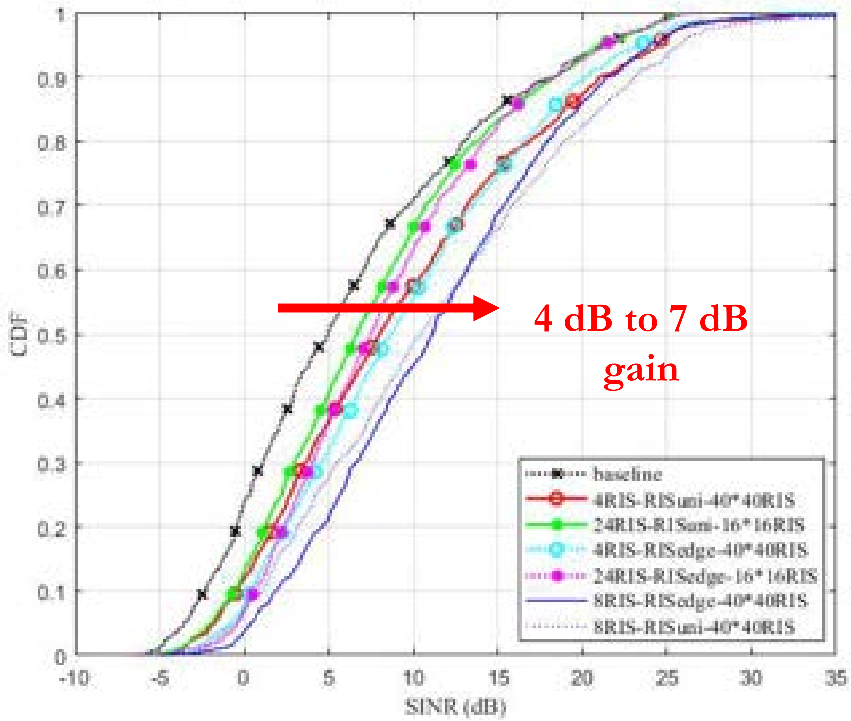

Ray Tracing Module for Reflecting Surfaces

Without RIS

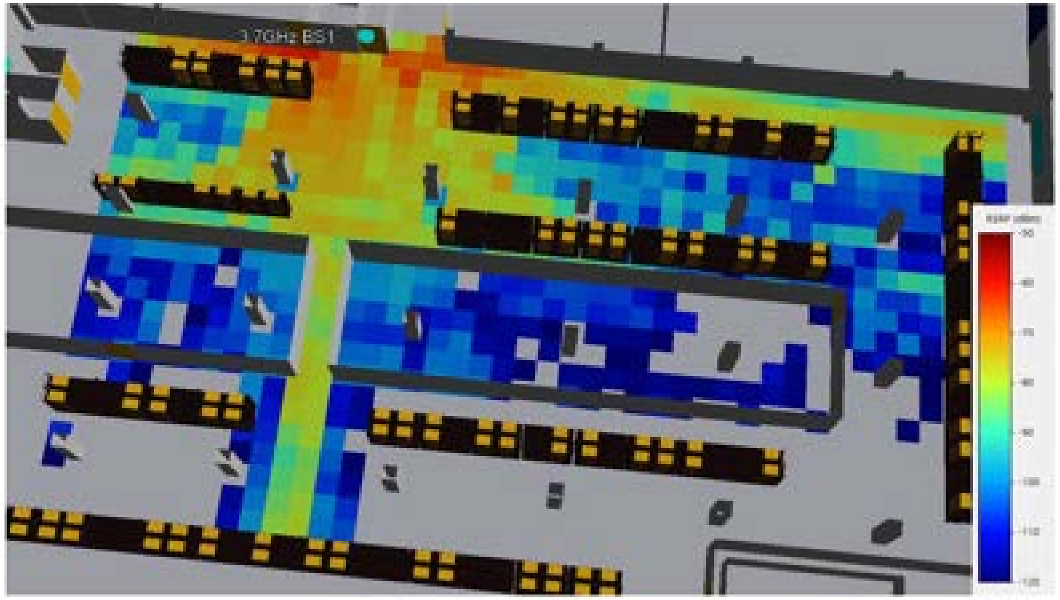

RIS-free RSRP coverage map of BS1 at 3.7 GHz.

With RIS

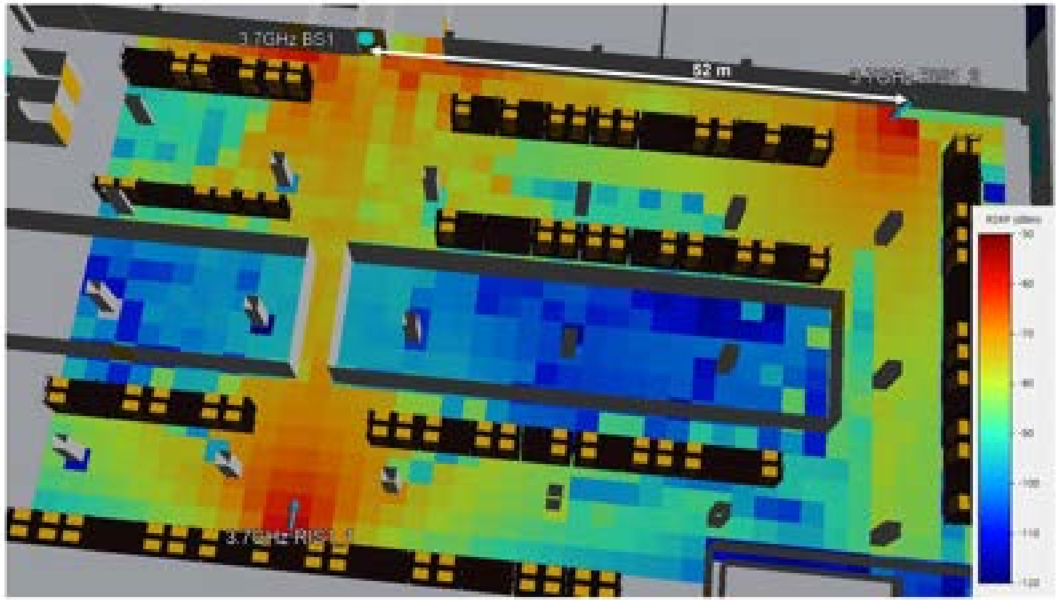

RIS-enhanced RSRP coverage map of BS1 with 64×64 RIS1_1 and 64×64 RIS1_2 at 3.7 GHz.

Pre-Standardization: ETSI ISG-RIS

- ETSI: European Telecommunications Standards Institute
- ISG: Industry Specification Group (ISG) on RIS – 30 sept. 2021
- Founder, Vice-President (elected) and Rapporteur (elected)

" *Provide an opportunity for ETSI members to coordinate their pre-standards research efforts on RIS technology across various EU/UK collaborative projects, extended with relevant global initiatives, towards paving the way for future standardization of the technology* "

60+ membres

Lessons Learnt

Rethinking Communication Models

Nearly-Passive Processing Without New Waves

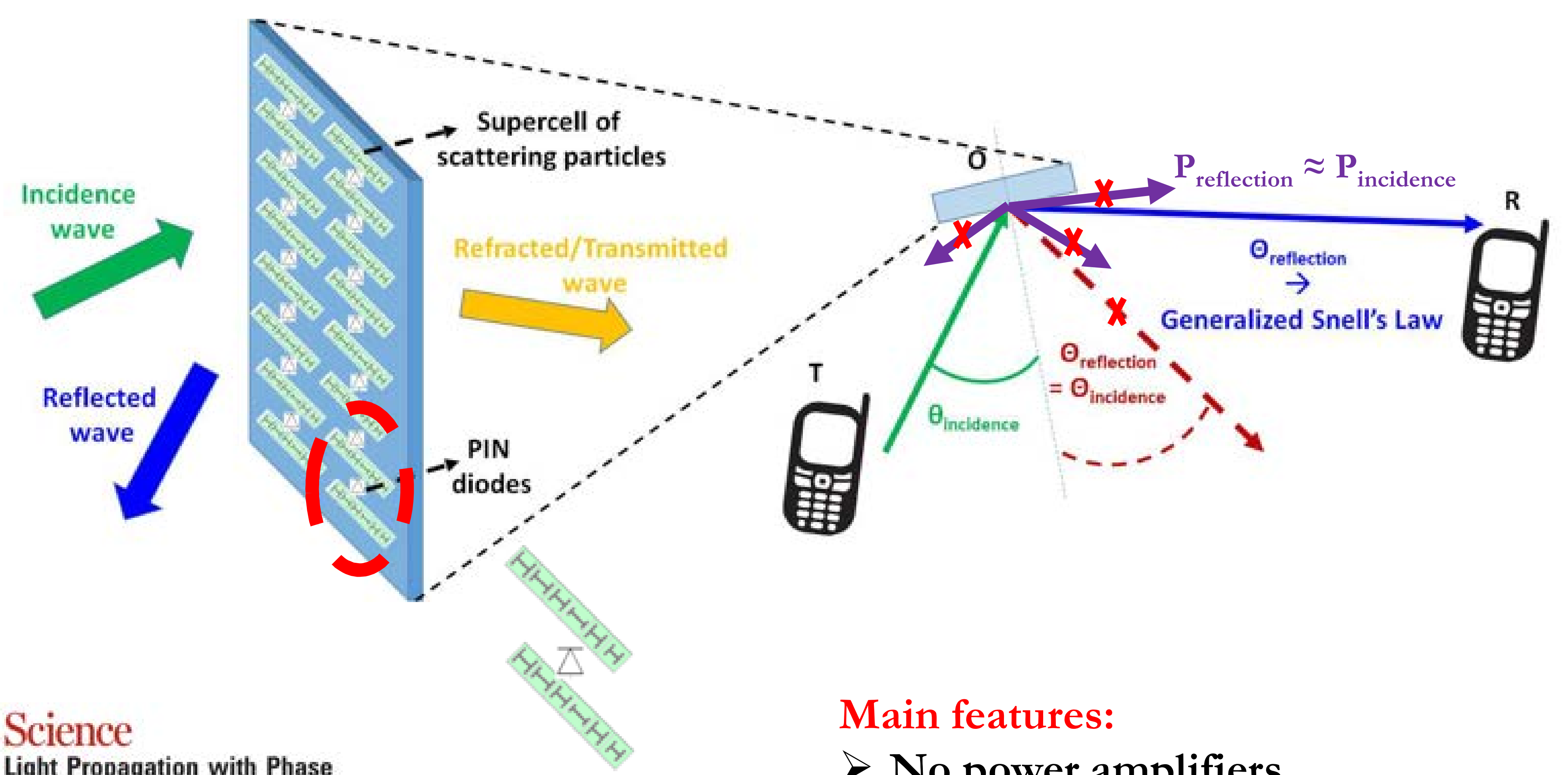

Science

Light Propagation with Phase Discontinuities: Generalized Laws of Reflection and Refraction

Nanfang Yu,[1] Patrice Genevet,[1,2] Mikhail A. Kats,[1] Francesco Aieta,[1,3] Jean-Philippe Tetienne,[1,4] Federico Capasso,[1]* Zeno Gaburro[1,5]*

Conventional optical components rely on gradual phase shifts accumulated during light propagation to shape light beams. New degrees of freedom are attained by introducing abrupt phase changes over the scale of the wavelength. A two-dimensional array of optical resonators with spatially varying phase response and subwavelength separation can imprint such phase discontinuities on propagating light as it traverses the interface between two media. Anomalous reflection and refraction phenomena are observed in this regime in optically thin arrays of metallic antennas on silicon with a linear phase variation along the interface, which are in excellent agreement with generalized laws derived from Fermat's principle. Phase discontinuities provide great flexibility in the design of light beams, as illustrated by the generation of optical vortices through use of planar designer metallic interfaces.

Main features:

- No power amplifiers
- No digital signal processing
- No radio frequency chains
- Better use of electromagnetic waves

RF Analog Domain Processing

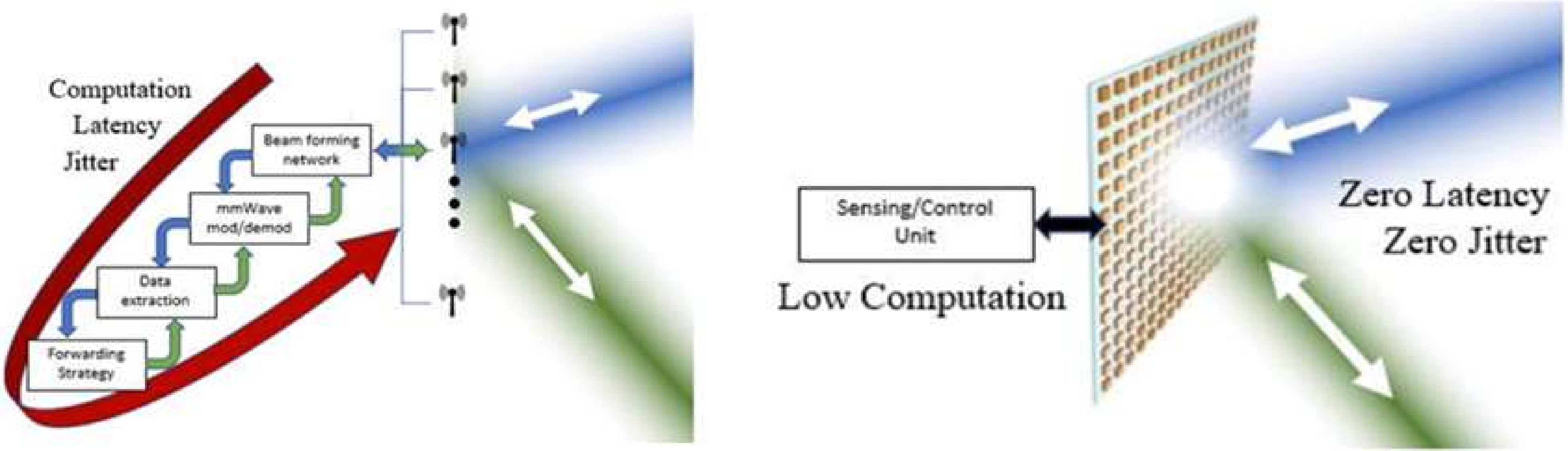

conventional digital-based radios

wave-domain processing

From Plane Waves for Spherical Waves

- **Paradigm #1: The wavefronts of the electromagnetic waves are (approximated as) locally planar on the antenna arrays**
  - **RIS and HoloS are electrically large, and the transmission distances are shrinking**

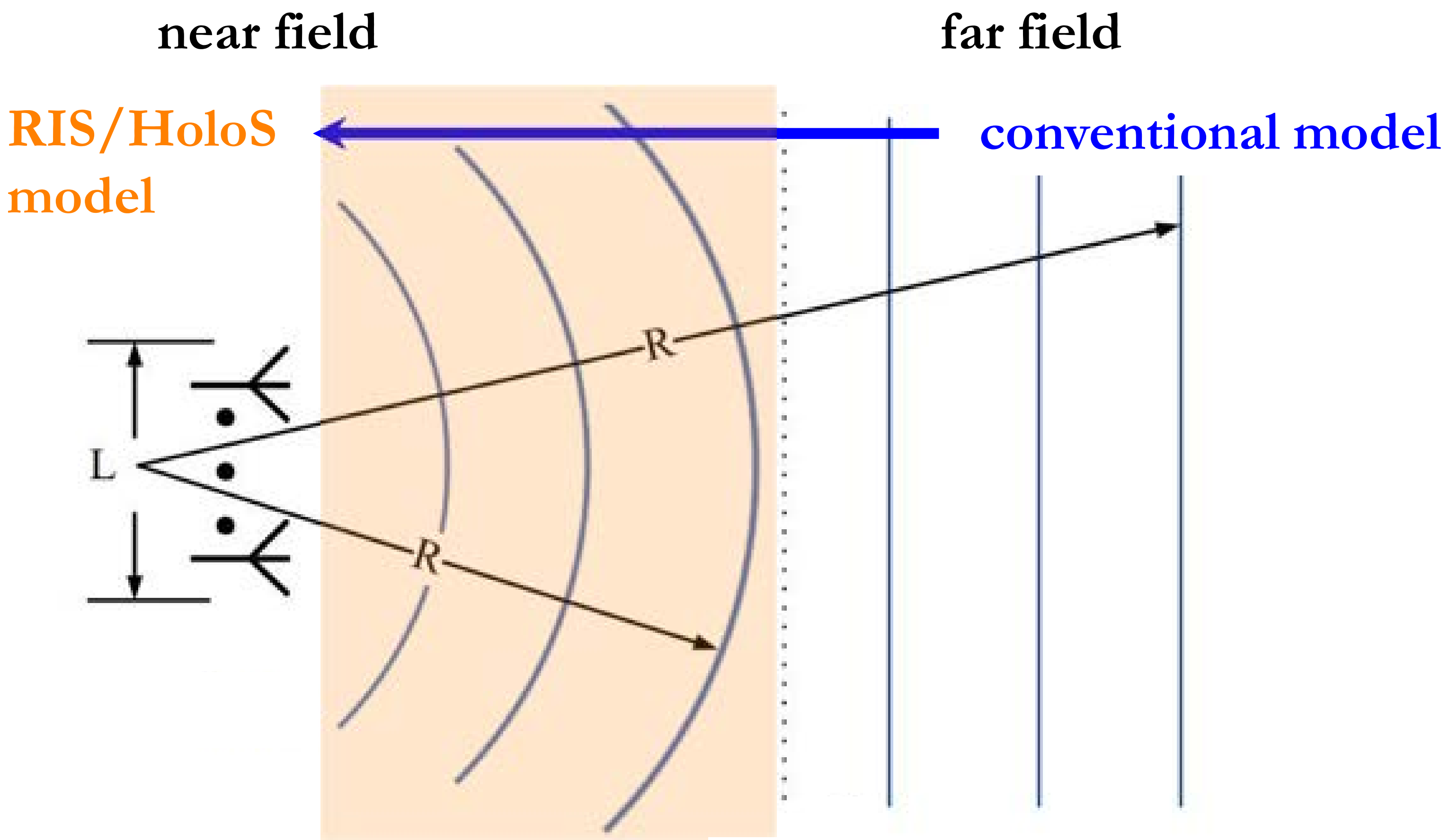

$$R \geq R_f = \frac{2L^2}{\lambda}$$

Densification of Radiating Elements

- **Paradigm #2: The radiating elements of antenna-arrays are decoupled electromagnetically**
  - **The inter-distances are smaller than the wavelength (< λ/2)**

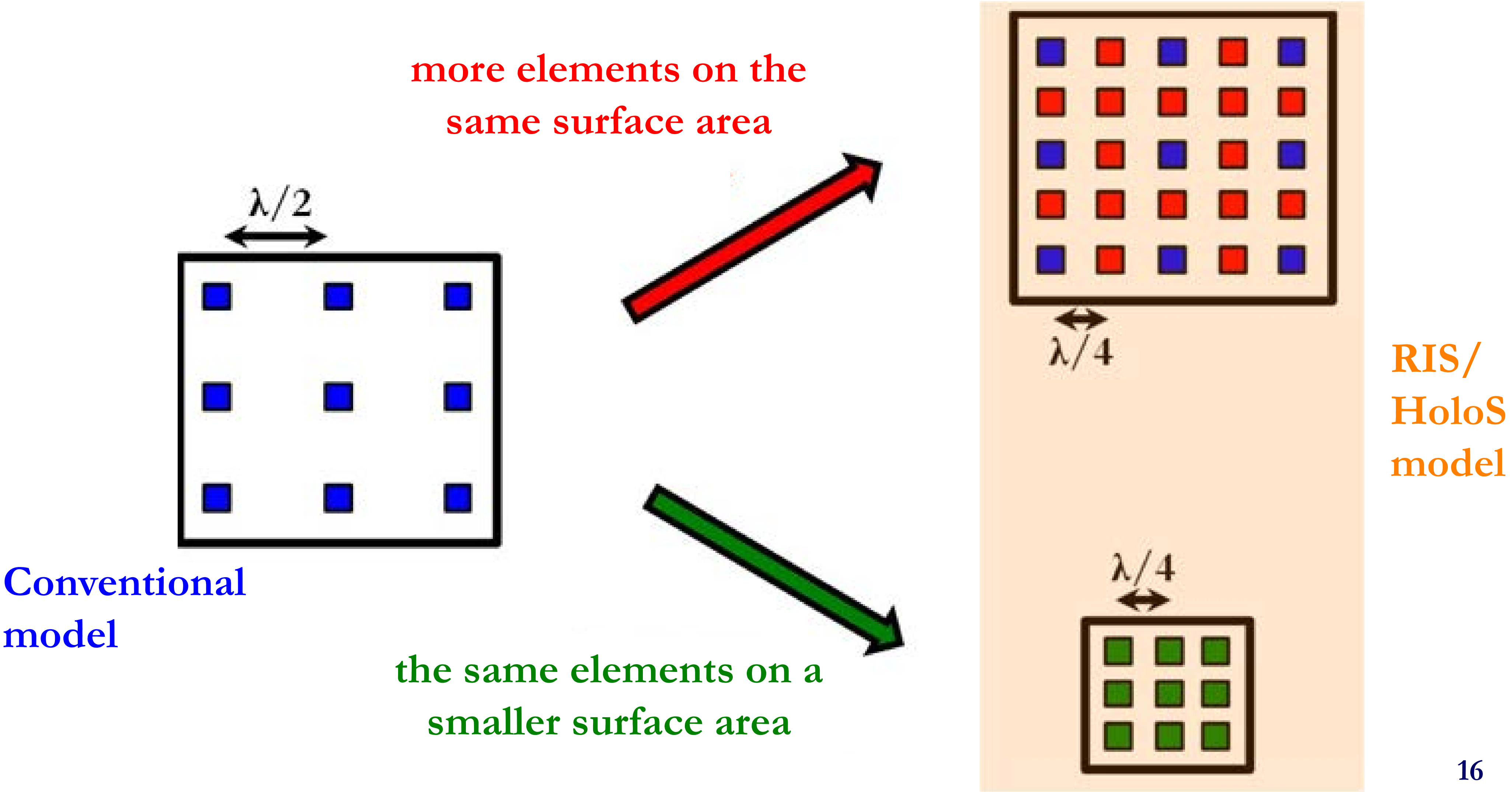

Reintroducing EM in IT/COM/SP

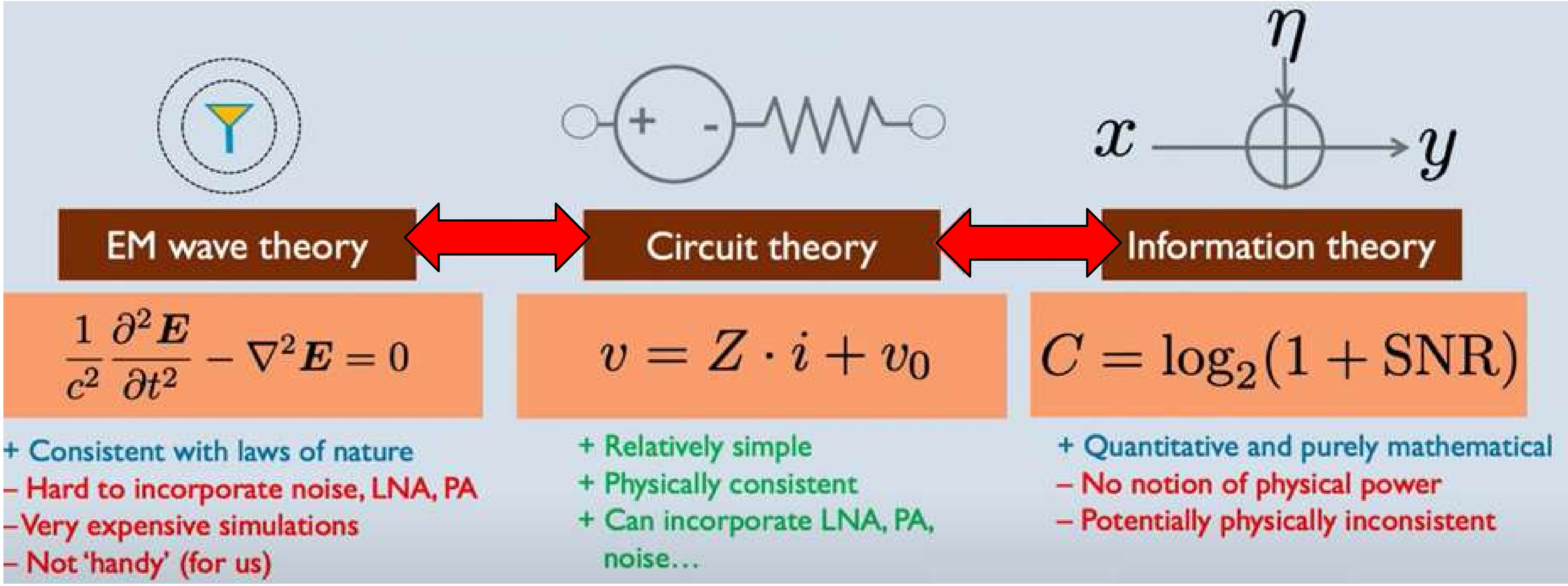

Individually, these approaches are insufficient and limited

$\downarrow$

Amalgamation of electromagnetism, metamaterials, circuits theory, and information theory

Communications: Math or Physics?

Denis Gabor (1953): "***Communication theory has up to now developed mainly on mathematical lines, taking for granted the physical significance of the quantities which figure in its formalism. But communication is the transmission of physical effects from one system to another, hence communication theory should be considered as a branch of physics. Thus, it is necessary to embody in its foundations such fundamental physical data…***".

Shannon

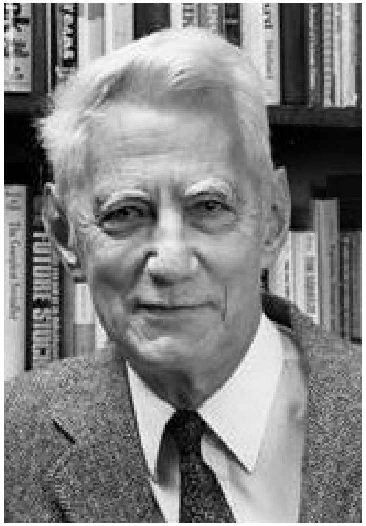

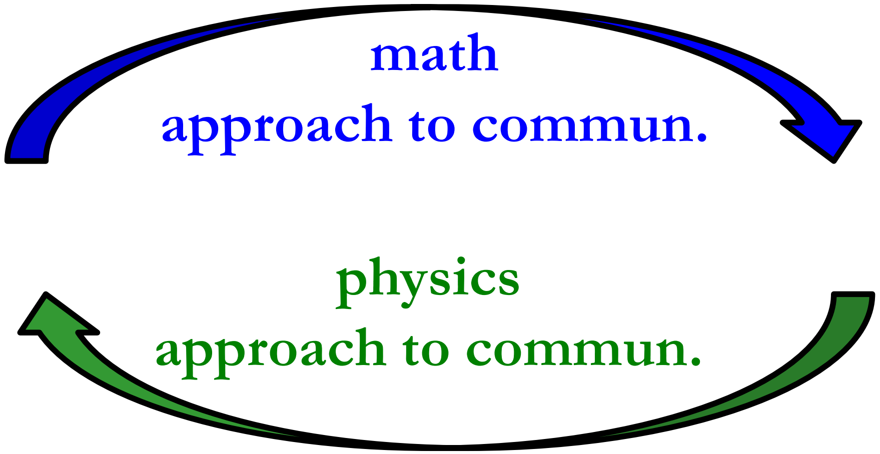

Gabor

Feature

Marco Di Renzo, Fellow, IEEE | Université Paris-Saclay, CNRS, CentraleSupélec, Laboratoire des Signaux et Systèmes, 91192 Gif-sur-Yvette, France | E-mail: marco.di-renzo@universite-paris-saclay.fr
Marco Donald Migliore, Senior Member, IEEE | DIEI, University of Cassino and Lazio Meridionale, 03043 Cassino, Italy | E-mail: mdmiglio@unicas.it

Electromagnetic Signal and Information Theory

Electromagnetically Consistent Communication Models for the Transmission and Processing of Information

Abstract—In this article, we present electromagnetic signal and information theory (ESIT). ESIT is an interdisciplinary scientific discipline, which amalgamates electromagnetic theory, signal processing theory, and information theory. ESIT is aimed at conceiving and designing physically consistent communication models and schemes for the transmission and processing of information in communication networks. In simple terms, ESIT can be defined as physics-aware information theory and signal processing for communications. We consider three relevant problems in con-

Introduction

Towards sustainable 6G networks: The radio communication division of the international telecommunication union (ITU-R) has recently drafted new recommendations for the international mobile telecommunication 2030 (IMT-2030) framework, which is referred to as the sixth generation (6G) of telecommunication standards. In the past decade, several advanced wireless technologies, including small cells, millimeter-wave communications, and massive multiple-input multiple-output (MIMO) systems, have been proposed to

Towards Machine Learning in the Wave Domain

From Digital-Domain to Wave-Domain Processing

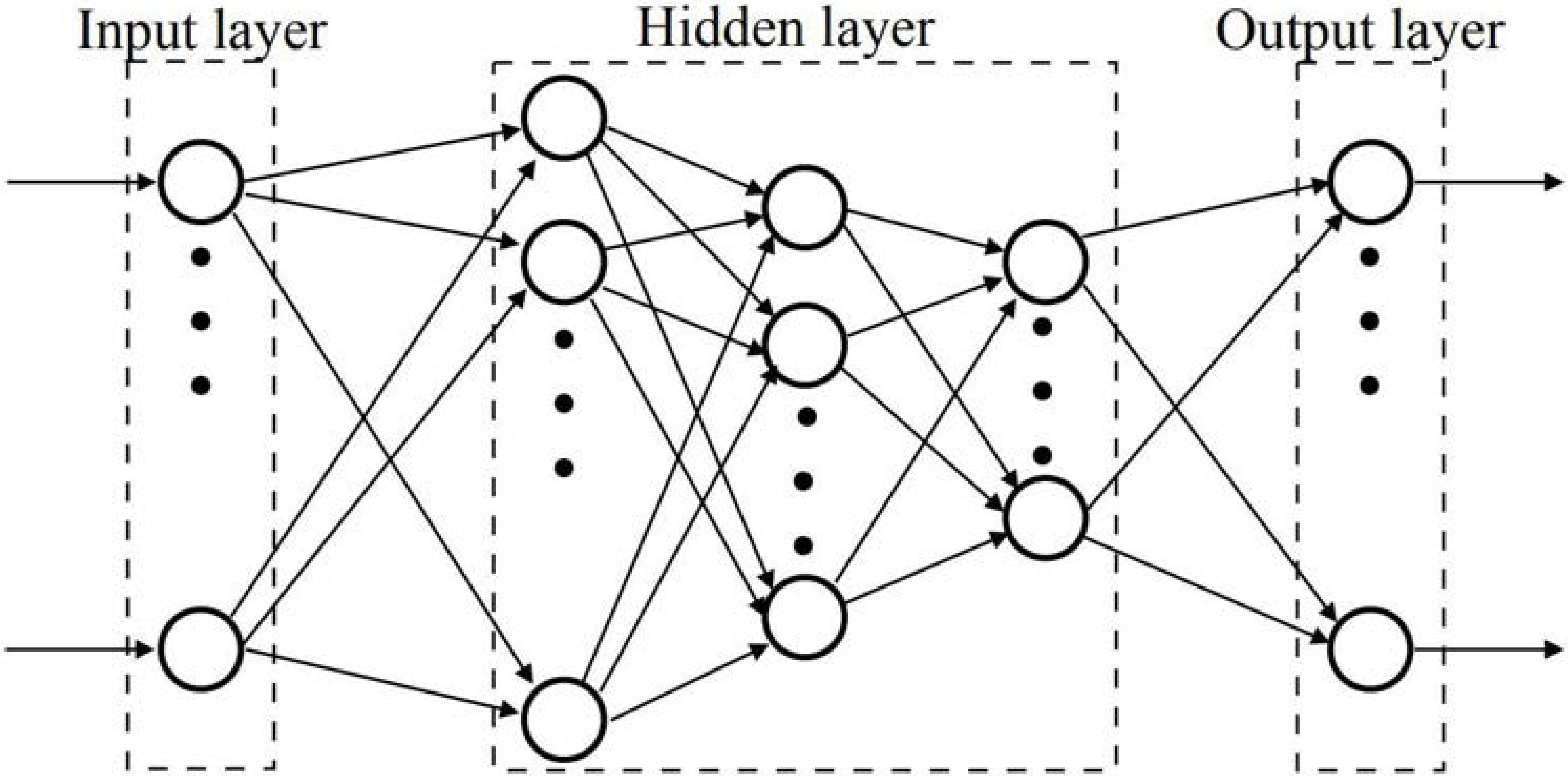

From Digital-Domain to Wave-Domain Processing

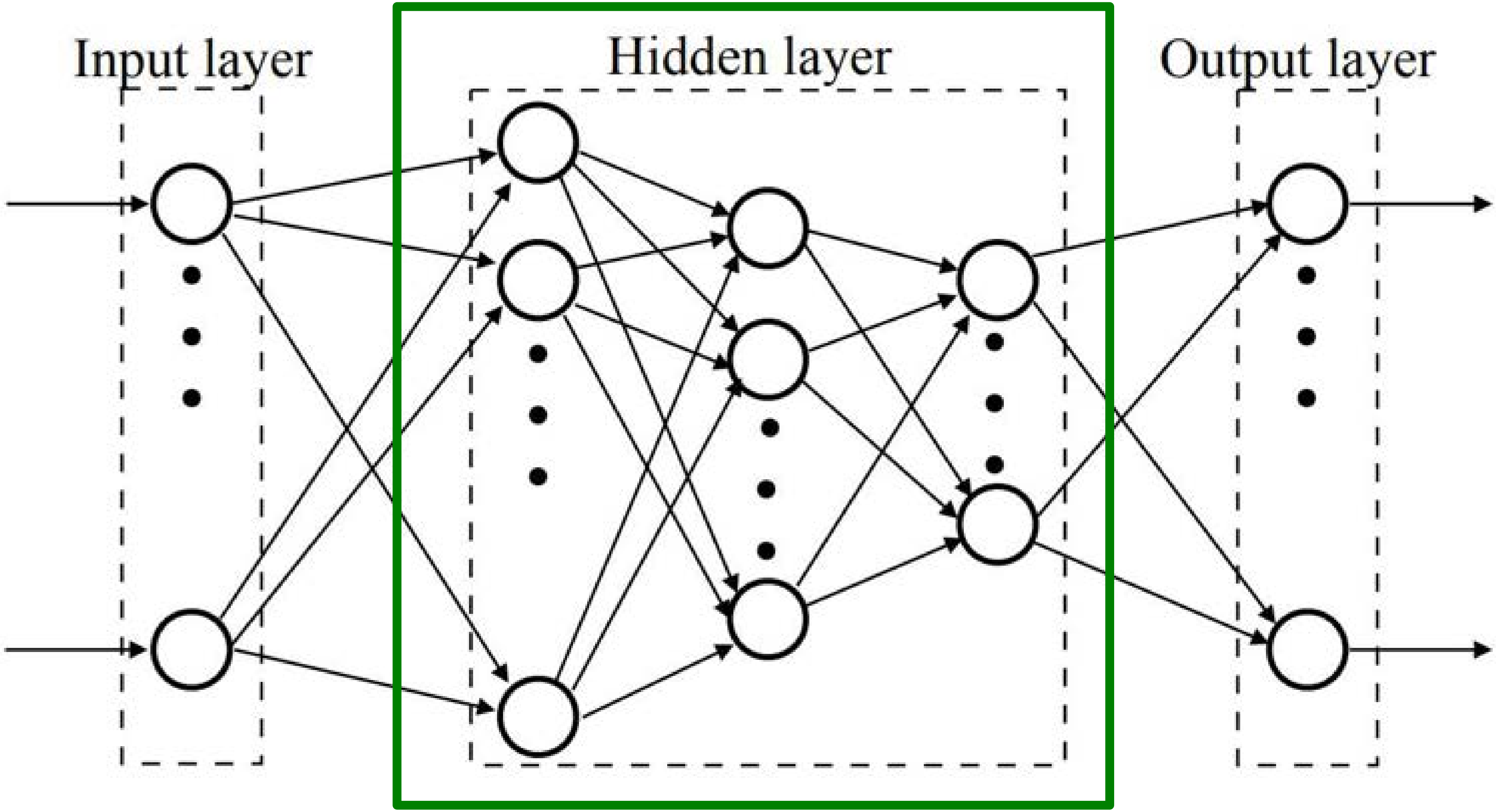

digital-domain processing

From Digital-Domain to Wave-Domain Processing

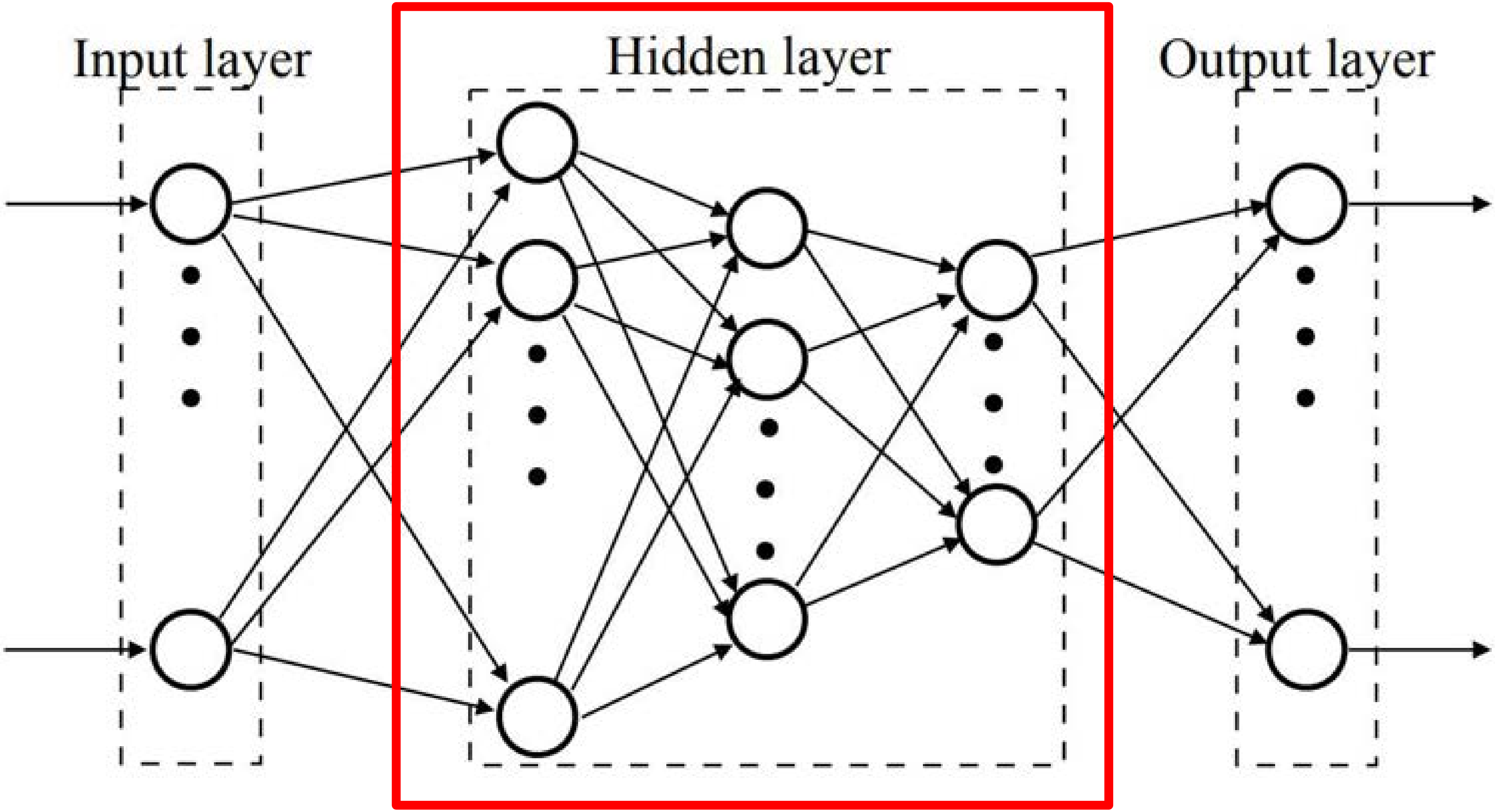

wave-domain processing

IEEE J. Solid-State Circuits. 1991

An Analog Neural Network Processor and its Application to High-Speed Character Recognition

Bernhard E. Boser, Eduard Säckinger, Jane Bromley,
Yann LeCun, Richard E. Howard, and Lawrence D. Jackel

AT&T Bell Laboratories
Crawford Corner Road, Holmdel, NJ 07733

Abstract—A high-speed programmable neural network chip and its application to character recognition are described. A network with over 130,000 connections has been implemented on a single chip and operates at a rate of over 1000 classifications per second. The chip performs up to 2000 multiplications and additions simultaneously. Its datapath is suitable particularly for the convolutional architectures that are typical in pattern classification networks, but can also be configured for fully connected or feedback topologies. Computations are performed with 6 Bits accuracy for the weights and 3 Bits for the states. The chip uses analog processing internally for higher density and reduced power dissipation, but all input/output is digital to simplify system integration.

Back to Analog Signal Processing (MWM, 2013)… ?

Analog Signal Processing

A Possible Alternative or Complement to Dominantly Digital Radio Schemes

Christophe Caloz, Shulabh Gupta, Qingfeng Zhang, and Babak Nikfal

Today's exploding demand for faster, more reliable, and ubiquitous radio systems in communication, instrumentation, radar, and sensors poses unprecedented challenges in microwave and millimeter-wave engineering. Recently, the predominant trend has been to place an increasing emphasis on digital signal processing (DSP). However, while offering device compactness microwave analog signal processing (ASP) as an alternative to DSP-based processing, with particular promise for millimeter and terahertz frequency applications.

What Is Microwave Analog Signal Processing?

Microwave ASP might be defined as the manipulation

Science 2018

Science REPORTS

Cite as: X. Lin *et al.*, *Science* 10.1126/science.aat8084 (2018).

All-optical machine learning using diffractive deep neural networks

Xing Lin[1,2,3]*, Yair Rivenson[1,2,3]*, Nezih T. Yardimci[1,3], Muhammed Veli[1,2,3], Yi Luo[1,2,3], Mona Jarrahi[1,3], Aydogan Ozcan[1,2,3,4]†

[1]Electrical and Computer Engineering Department, University of California, Los Angeles, CA, 90095, USA. [2]Bioengineering Department, University of California, Los Angeles, CA, 90095, USA. [3]California NanoSystems Institute (CNSI), University of California, Los Angeles, CA, 90095, USA. [4]Department of Surgery, David Geffen School of Medicine, University of California, Los Angeles, CA, 90095, USA.

*These authors contributed equally to this work.

†Corresponding author. Email: ozcan@ucla.edu

Deep learning has been transforming our ability to execute advanced inference tasks using computers. We introduce a physical mechanism to perform machine learning by demonstrating an all-optical Diffractive Deep Neural Network (D^2NN) architecture that can implement various functions following the deep learning-based design of passive diffractive layers that work collectively. We create 3D-printed D^2NNs that implement classification of images of handwritten digits and fashion products as well as the function of an imaging lens at terahertz spectrum. Our all-optical deep learning framework can perform, at the speed of light, various complex functions that computer-based neural networks can implement, and will find applications in all-optical image analysis, feature detection and object classification, also enabling new camera designs and optical components that perform unique tasks using D^2NNs.

Metamaterials 2018

12^{th} *International Congress on Artificial Materials for Novel Wave Phenomena - Metamaterials 2018*
Espoo, Finland, Aug. 27^{th} - Sept. 1^{th} 2018

Stacked Metasurface Slab

Nima Chamanara, Yousef Vahabzadeh and Christophe Caloz

Polytechnique Montréal, H3T 1J4, Montreal, QC, Canada
nima.chamanara@polymtl.ca

Abstract **– This paper presents *stacked metasurface slabs*, stacked array of cascaded metasurfaces synthesized using a GSTC-based algorithm that circumvent fabrication difficulties in metasurfaces involving sharply varying field transformations. The specified transformation is subdivided into several smoother transformations and shared between cascaded bianisotropic metasurfaces. This algorithm relaxes the fabrication requirements dramatically.**

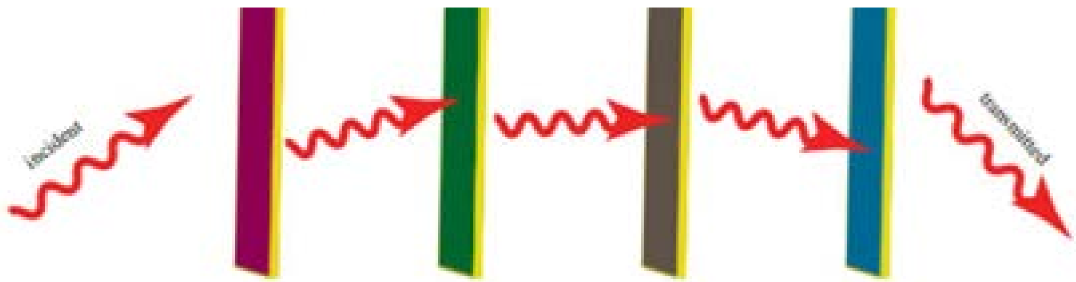

Fig. 1: Perfect negative refraction metasurface array. Negative refraction is performed by an array of metasurfaces where each metasurface performs partial rotation.

Nature Electronics 2022

Programmable AI Machine (PAIM)

nature electronics

ARTICLES

https://doi.org/10.1038/s41928-022-00719-9

Check for updates

A programmable diffractive deep neural network based on a digital-coding metasurface array

Che Liu[1,2,3,6], Qian Ma[1,2,3,6], Zhang Jie Luo[1,2,3], Qiao Ru Hong[1,2], Qiang Xiao[1,2,3], Hao Chi Zhang[1,2,3], Long Miao[3,4], Wen Ming Yu[1,2,4], Qiang Cheng[1,2,3], Lianlin Li[3,5] and Tie Jun Cui[1,2,3] ✉

The development of artificial intelligence is typically focused on computer algorithms and integrated circuits. Recently, all-optical diffractive deep neural networks have been created that are based on passive structures and can perform complicated functions designed by computer-based neural networks. However, once a passive diffractive deep neural network architecture is fabricated, its function is fixed. Here we report a programmable diffractive deep neural network that is based on a multi-layer digital-coding metasurface array. Each meta-atom on the metasurfaces is integrated with two amplifier chips and acts an active artificial neuron, providing a dynamic modulation range of 35 dB (from −22 dB to 13 dB). We show that the system, which we term a programmable artificial intelligence machine, can handle various deep learning tasks for wave sensing, including image classification, mobile communication coding–decoding and real-time multi-beam focusing. We also develop a reinforcement learning algorithm for on-site learning and a discrete optimization algorithm for digital coding.

Nature Electronics 2022

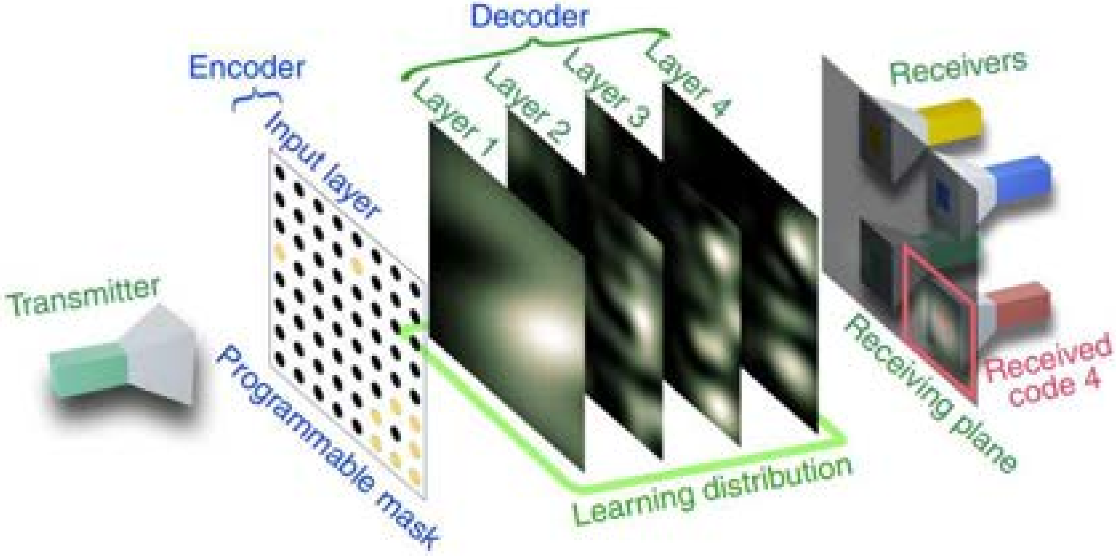

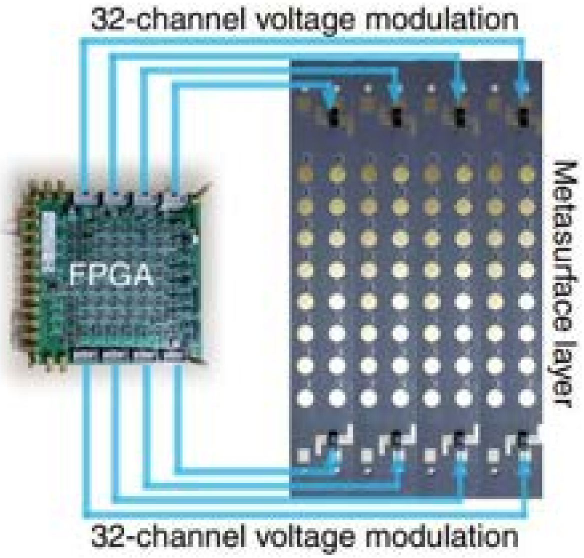

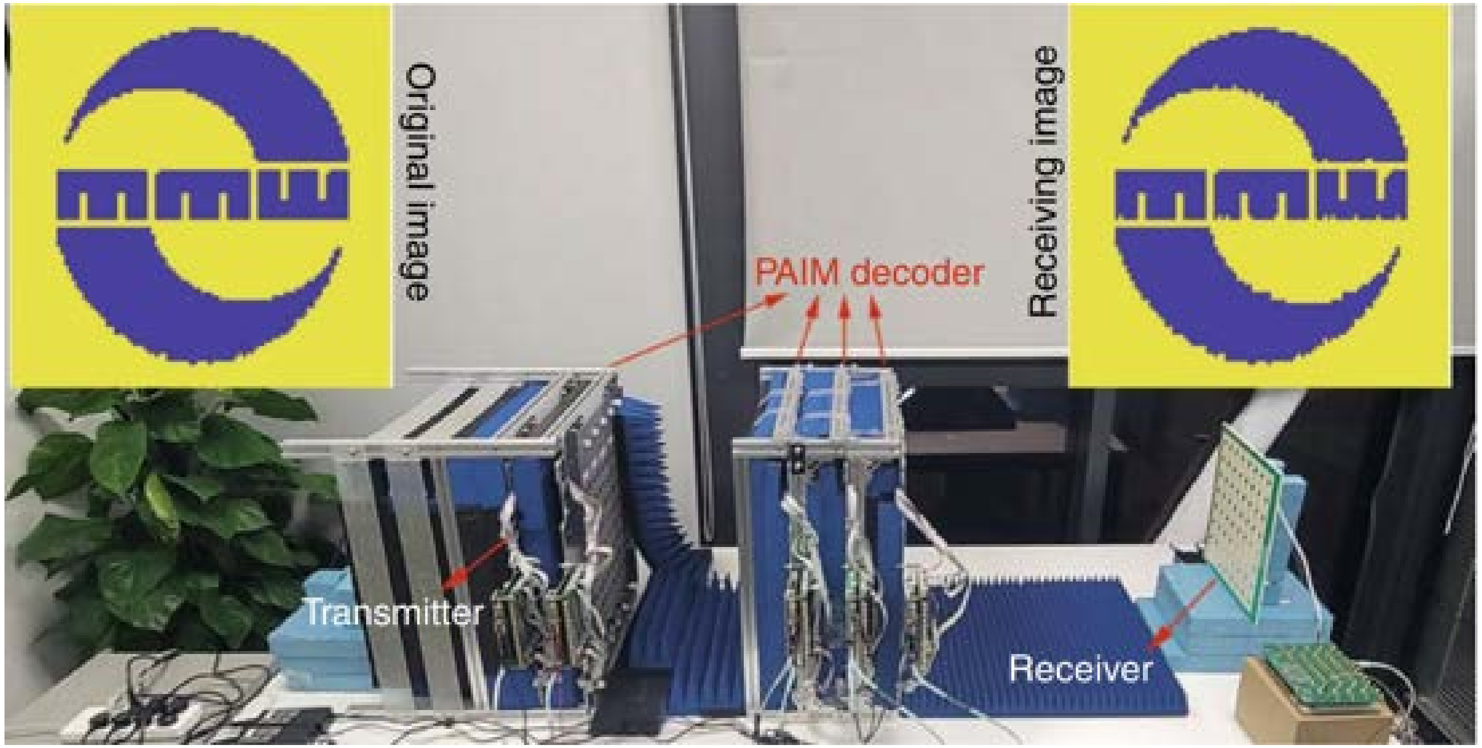

Latest Developments in 2024: Optical Computing

nature reviews physics

https://doi.org/10.1038/s42254-023-00645-5

Perspective

Check for updates

The physics of optical computing

Peter L. McMahon

Abstract

There has been a resurgence of interest in optical computing since the early 2010s, both in academia and in industry, with much of the excitement centred around special-purpose optical computers for neural-network processing. Optical computing has been a topic of periodic study since the 1960s, including for neural networks in the 1980s and early 1990s, and a wide variety of optical-computing schemes and architectures have been proposed. In this Perspective article, we provide a systematic explanation of why and how optics might be able to give speed or energy-efficiency benefits over electronics for computing, enumerating 11 features of optics that can be harnessed when designing an optical computer. One often-mentioned motivation for optical computing – that the speed of light is fast – is emphatically not a key differentiating physical property of optics for computing; understanding where an advantage could come from is more subtle. We discuss how gaining an advantage over state-of-the-art electronic processors will likely only be achievable by careful design that harnesses more than 1 of the 11 features, while avoiding a number of pitfalls that we describe.

Sections

School of Applied and Engineering Physics, Cornell University, Ithaca, NY, USA. e-mail: pmcmahon@cornell.edu

Comment

https://doi.org/10.1038/s43588-024-00657-w

Exploring the role of metamaterials in achieving advantage in optical computing

Yandong Li & Francesco Monticone

Check for updates

Optical and wave-based computing is attracting renewed interest, motivated by the need for new platforms for resource-intensive special-purpose processing tasks. Here, we discuss whether, why, and how metamaterials and metasurfaces could contribute to achieving an 'optical advantage' in computing.

Although physical intuition and historical experience suggest that the properties of electrons are well-suited for information processing, whereas photons are better for information transmission, the dream of using light for ultra-fast and ultra-efficient computing has reemerged several times over the past decades. Interest in this idea has surged recently, largely motivated by the need for alternative platforms for extremely resource-intensive processing tasks, especially in the field of artificial intelligence. Certain characteristics of optics and wave physics, which will be explored in this Comment, along with the notable advancements in photonic hardware and computational design techniques over the past two to three decades, highlight the potential of photonic platforms to meet this need. At the same time, the field of metamaterials – engineered materials based on subwavelength structuring in two/three dimensions (and, more recently, in four dimensions by including time) – has greatly expanded the design flexibility, and the range of accessible properties, of wave-based platforms.

In this Comment, we will discuss whether, why, and how metamaterials could contribute to achieving an 'optical advantage' in computing compared to electronic processors.

General aspects of optical computing

First, we briefly review what general aspects of optics and wave physics are particularly promising to deliver this advantage, following the insightful discussion of optical computing in the recent survey by P. L. McMahon[1]. We focus on analog and special-purpose computing, for tasks such as neural-network inference and image processing, where noisy computations with low precisions are acceptable. No clear avenue currently exists to replicate general-purpose digital processors with optics, primarily because of unresolved challenges in developing an optical transistor that meets the necessary quantitative requirements[1]. We also focus on linear optical systems, as the implementation of nonlinear functions all-optically remains an open challenge due to the weakness of nonlinear optical effects. In the following, we consider a few key performance metrics in computing and discuss how the unique features of optical and wave-based systems can impact them.

Energy efficiency. Optical systems can perform linear operations (notably, Fourier transforms, convolutions, and matrix–vector multiplications) passively through propagation/scattering, with virtually no energy loss, and transmit information with much lower dissipation than in electrical wires. These features are particularly appealing if the input signals to process are already optical, as in image processing and machine vision tasks. Instead, if signals need to be converted from the electronic to the optical domain and back, the energy cost of these transductions would be substantial and the efficiency of a linear optical module may lead to an overall advantage only if the size of the input is sufficiently large[1,2,3].

Throughput (operations per second). Optical systems can harness: (1) a large number of spatial modes (for example, in megapixel-scale commercial spatial light modulators) that can be used in parallel without 'cross-talk', as photons don't interact with each other in free space, and only weakly, and indirectly, in matter; and (2) a very large number of frequency modes over a broad THz-scale bandwidth. Fully harnessing the parallelism enabled by spatial- or frequency-multiplexing, and especially a combination of the two, may lead to optical systems with higher performance, especially in terms of throughput, than electronic processors. Indeed, although electronic processors can have massive component densities, they usually have much smaller bandwidth, and their actual operational parallelism is constrained by dissipation.

Speed, latency and size. We echo the argument by McMahon[1] that the high speed of light, per se, is not a key differentiating factor of optical computers compared to electronic ones, where lower-frequency electrical signals also travel, in wires, at a large percentage of the speed of light. Propagation delays are comparable in the two domains. However, operation delays in digital electronics are related to the bandwidth- and dissipation-limited clock rate, and additional delays due to analog–digital conversion may be involved. Conversely, if a certain operation can be performed directly on an input electromagnetic signal, passively and analogically, then the propagation delay is the total delay, and substantial reductions in latency are possible by making the analog system (optical or electronic) perform a complex operation in the smallest possible volume.

Metamaterials and computing

Metamaterials can offer the following further advantages compared to more standard optical architectures (Fig. 1a). (1) Metamaterials offer higher design flexibility, and allow accessing and manipulating a broader range of optical degrees of freedom (often simultaneously), for example, amplitude, phase, polarization, linear/angular momentum, and wavevector. Metamaterial-based systems can therefore perform, at least in principle, substantially more complex operations passively on the hardware layer, and hence with high efficiency and lower latency. In this context, 2D dielectric metasurfaces and meta-gratings with minimized absorption, reflections, and unwanted scattering are promising for highly efficient free-space computing architectures, whereas 3D

Latest Developments in 2023: SIM

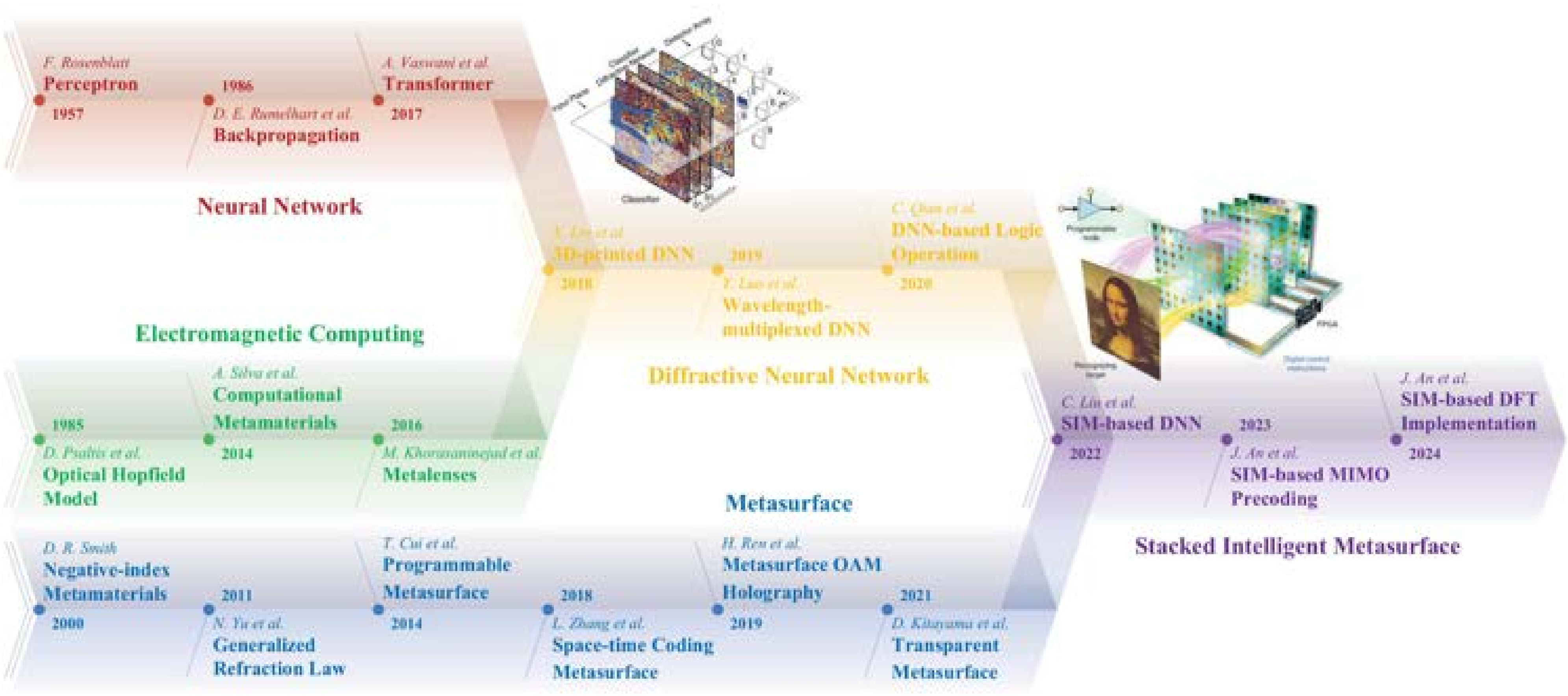

Jiancheng An, Marco Di Renzo, Mérouane Debbah, Chau Yuen:
Stacked Intelligent Metasurfaces for Multiuser Beamforming in the Wave Domain. ICC 2023: 2834-2839 (Best Paper Award)

This Talk

- Stacked intelligent metasurface (SIM)
  - What's SIM?
  - Why SIM?
  - SIM as a wave-domain base station design
  - SIM as a wave-domain fully-connected refracting node
  - SIM as a wave-domain processor / computing device

- World's first prototype of SIM for communication and sensing
  - SIM for communication, sensing and their integration

What's SIM ?

SIM: The General Concept

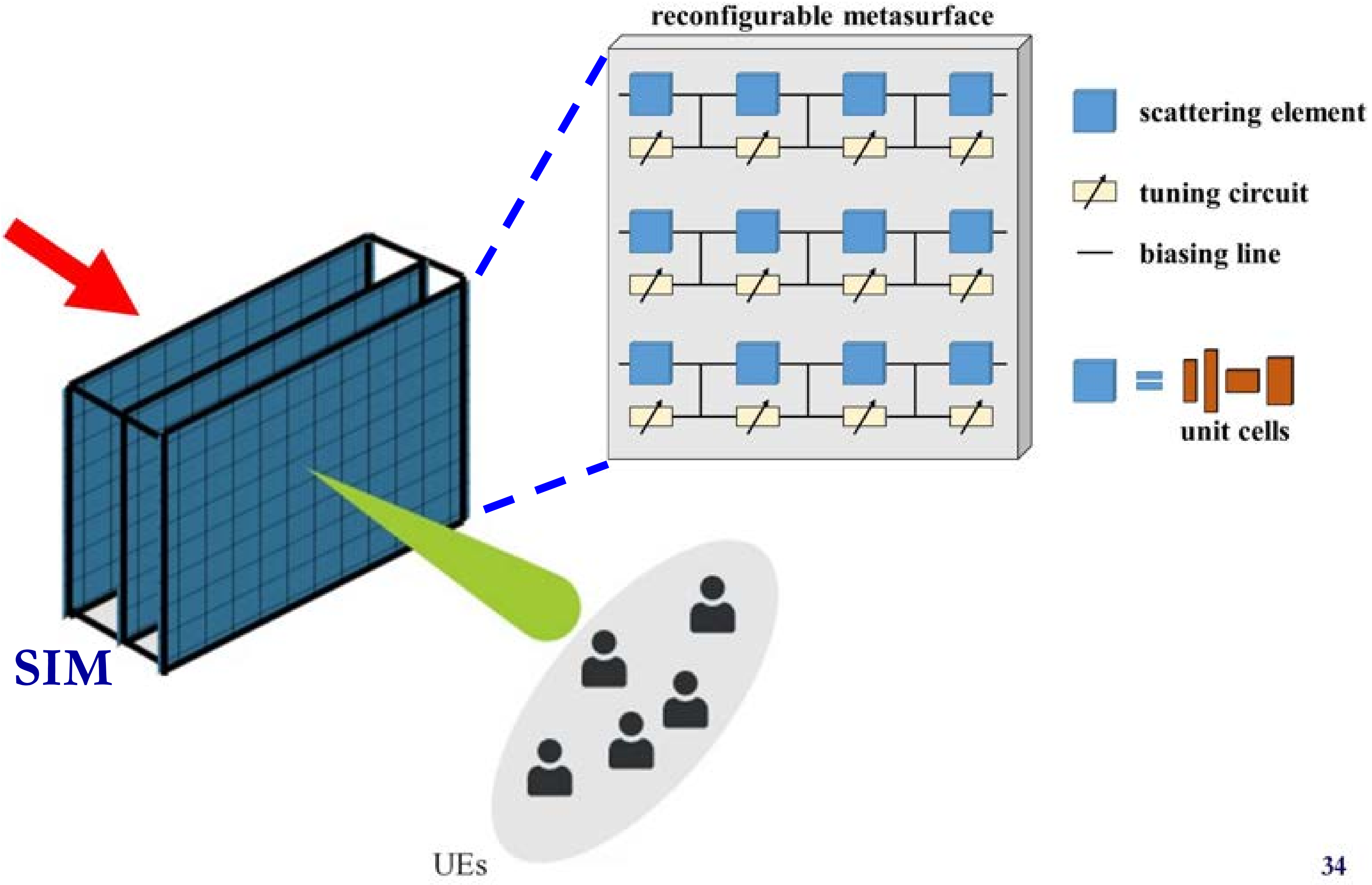

SIM: The General Concept

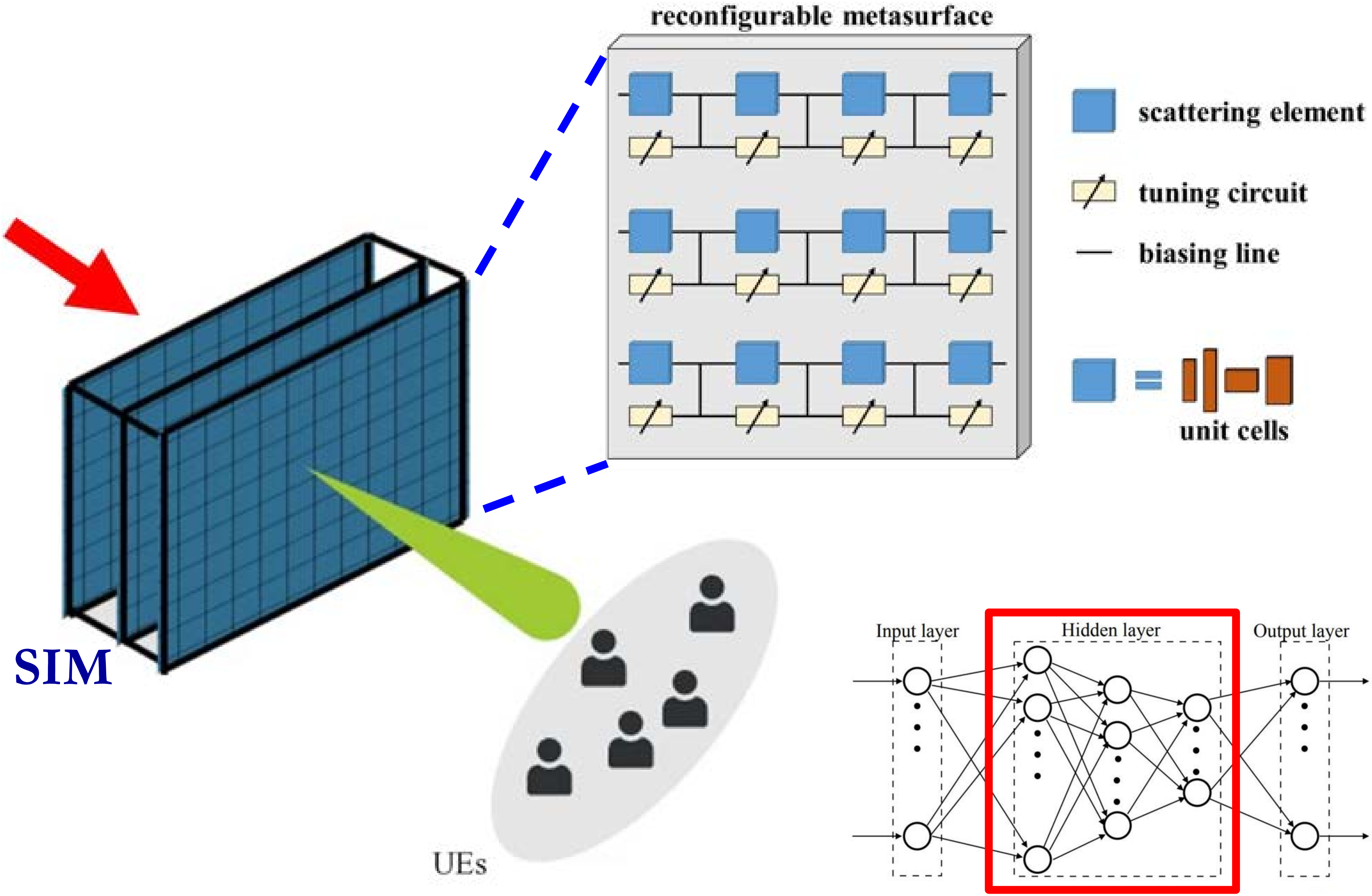

SIM: The General Concept

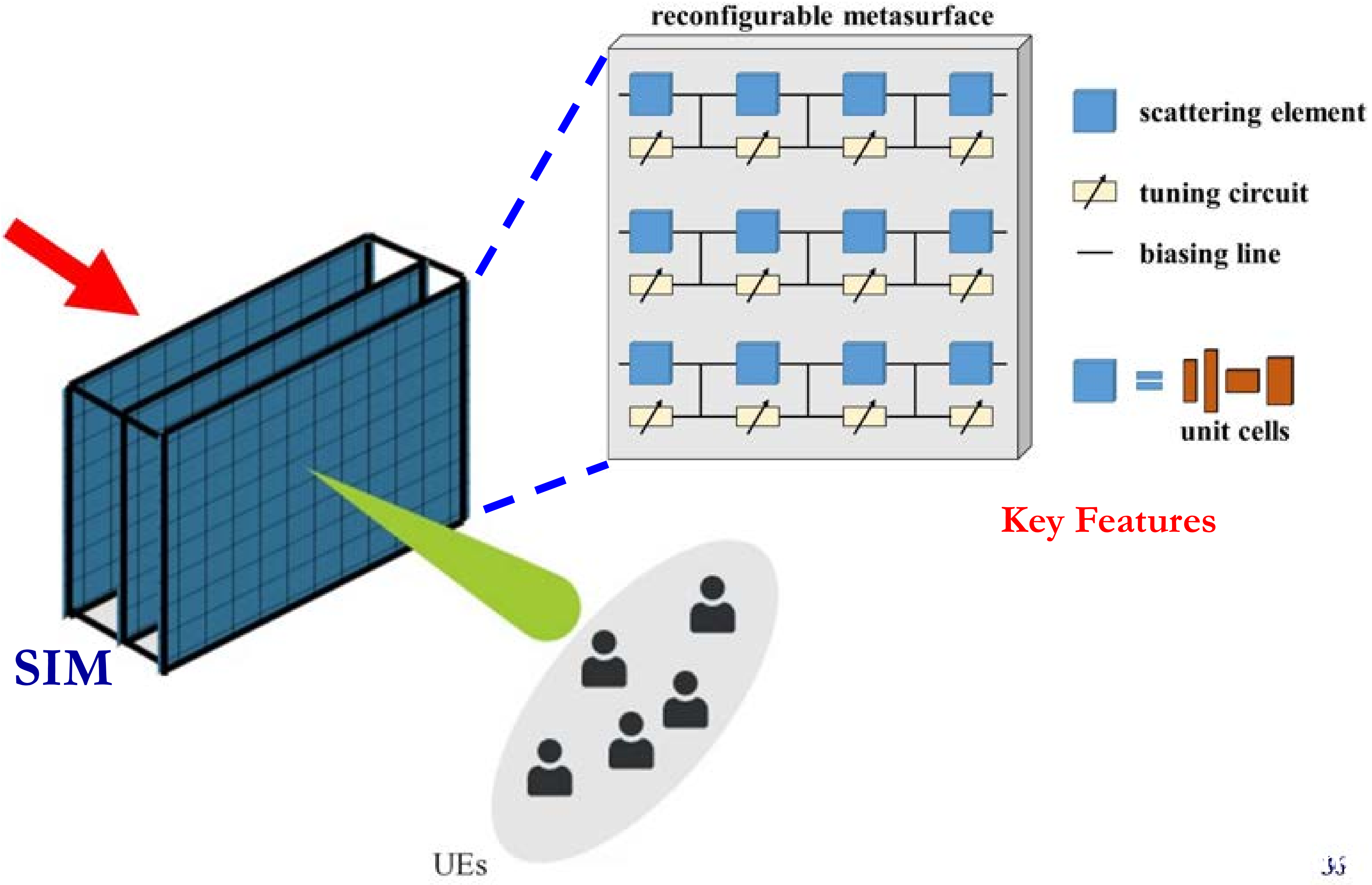

Key Features

SIM: The General Concept

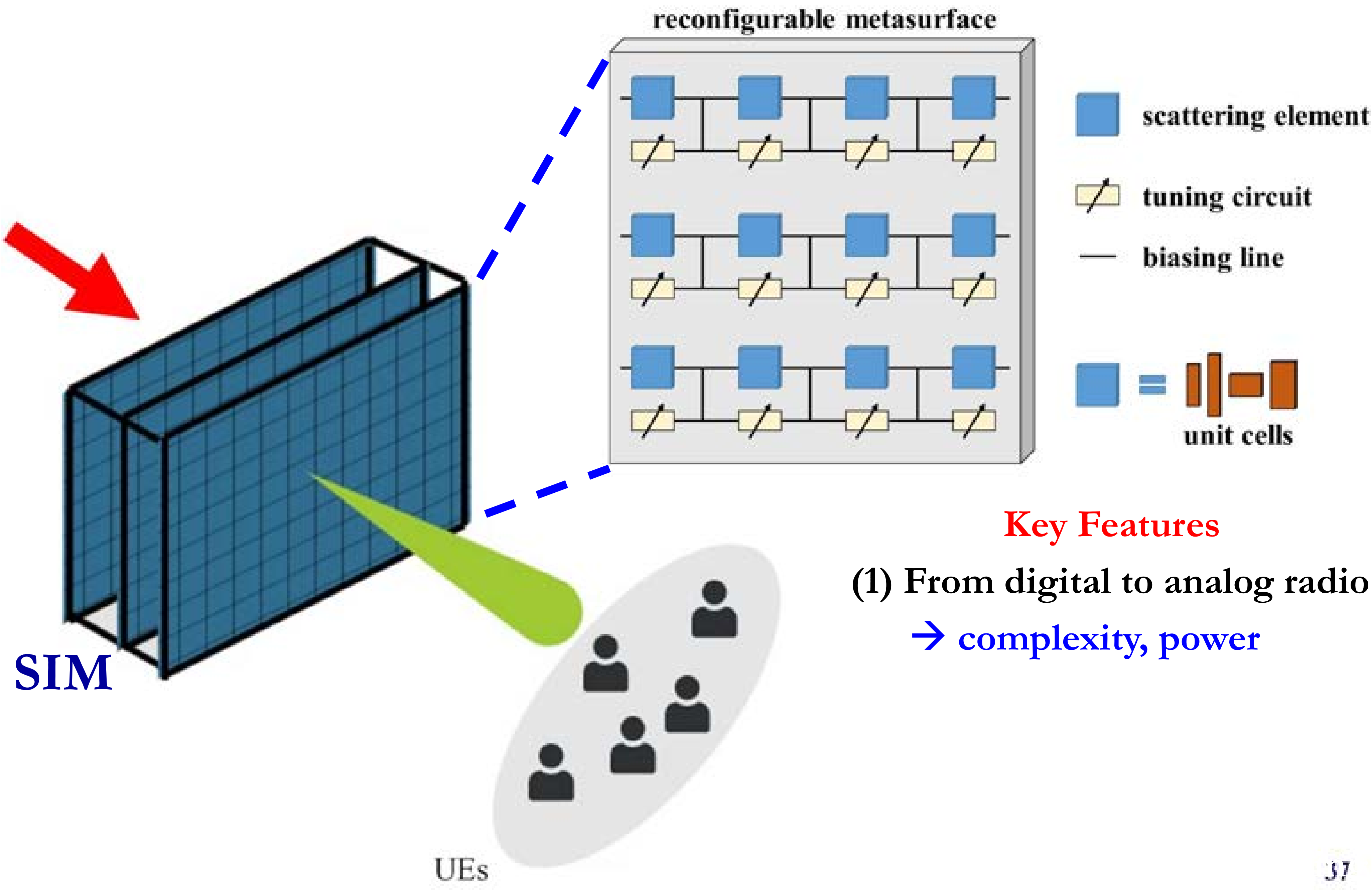

Key Features

(1) From digital to analog radio

→ complexity, power

SIM: The General Concept

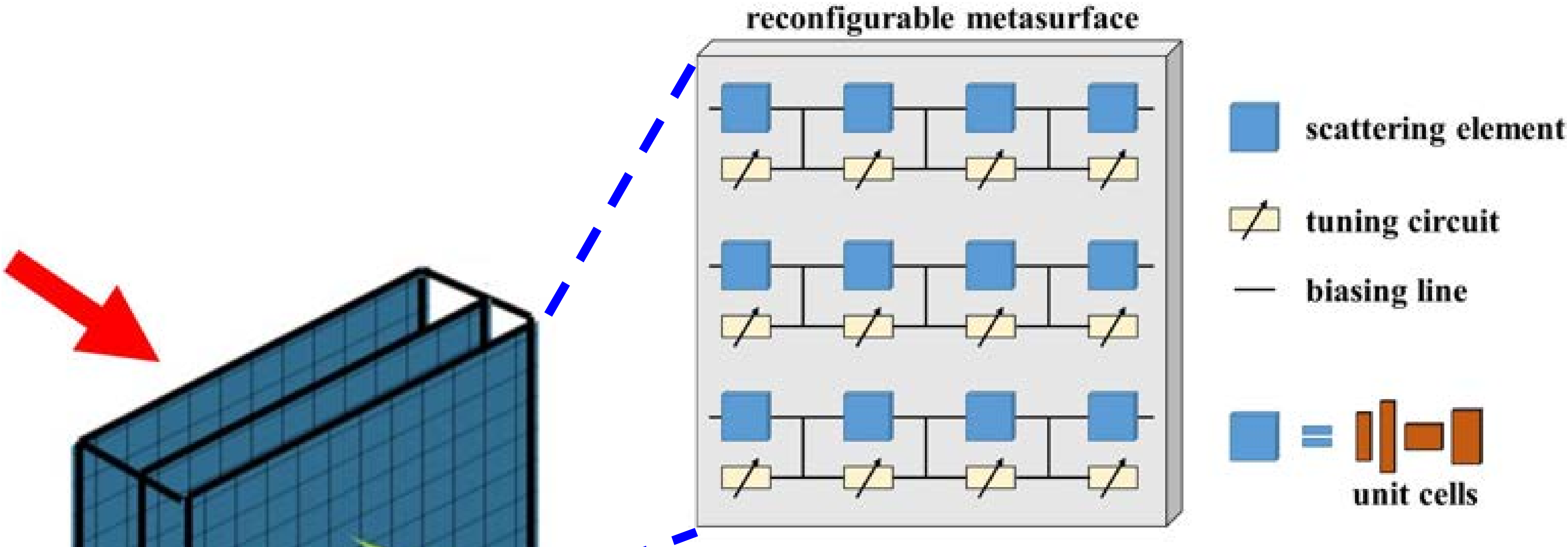

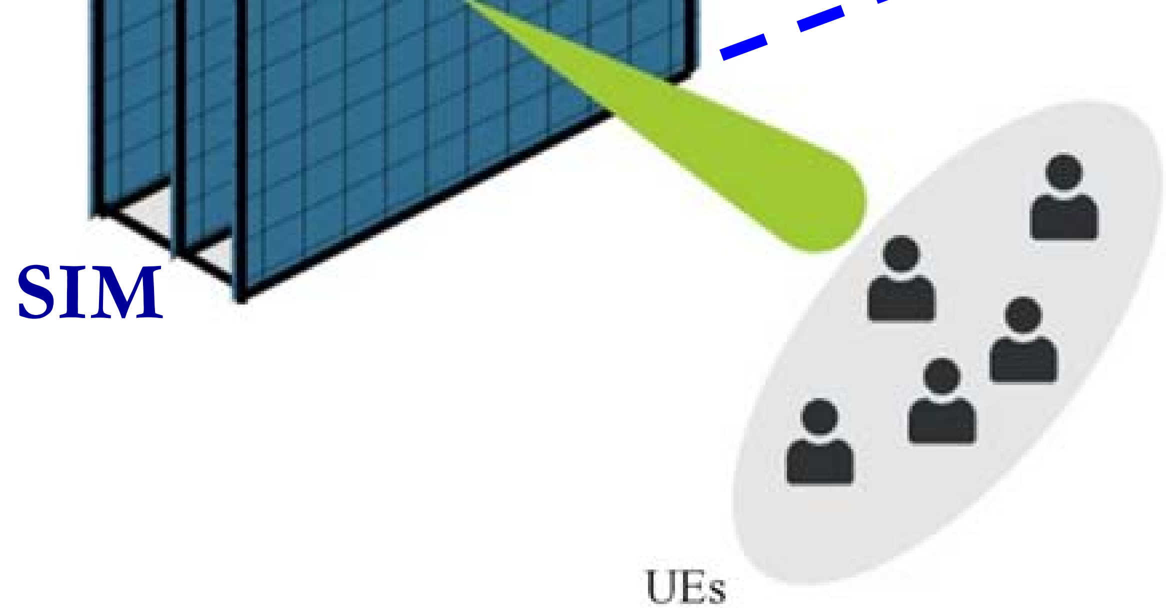

Key Features

(1) From digital to analog radio

→ complexity, power

(2) AI-based power processing

→ massive computing

SIM: The General Concept

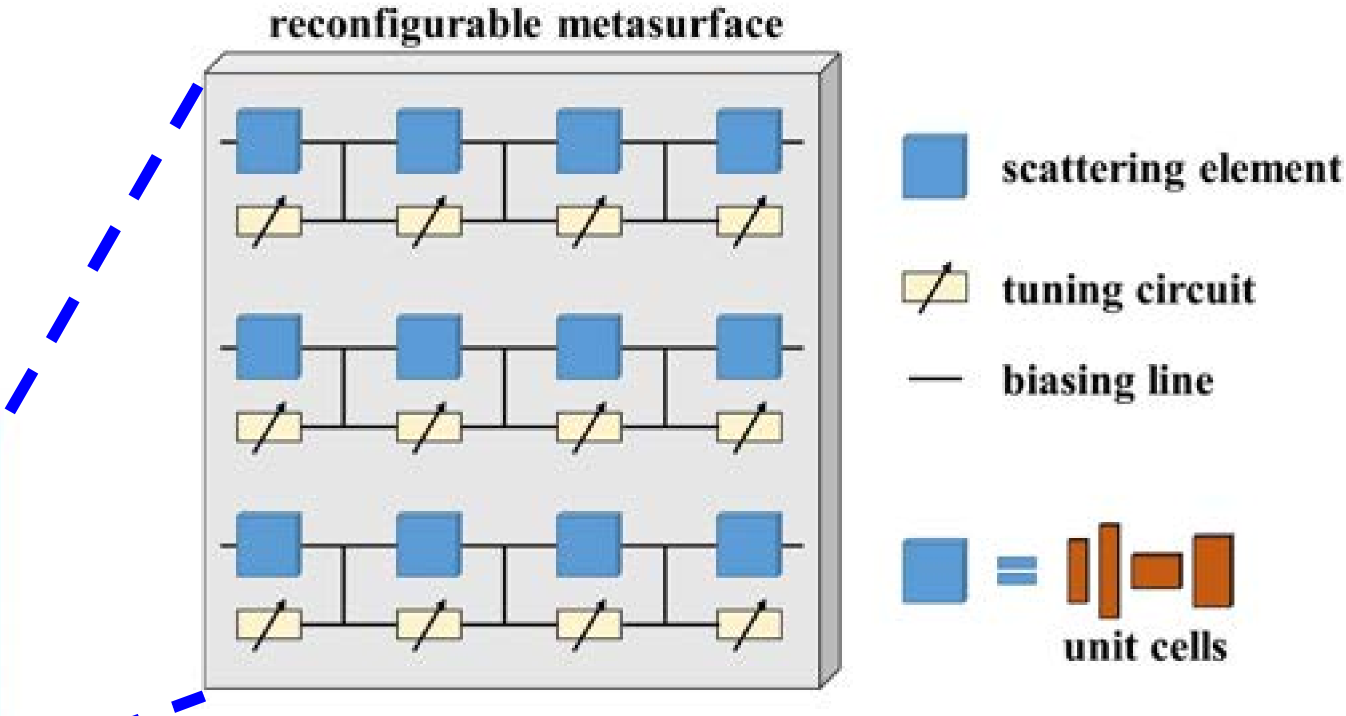

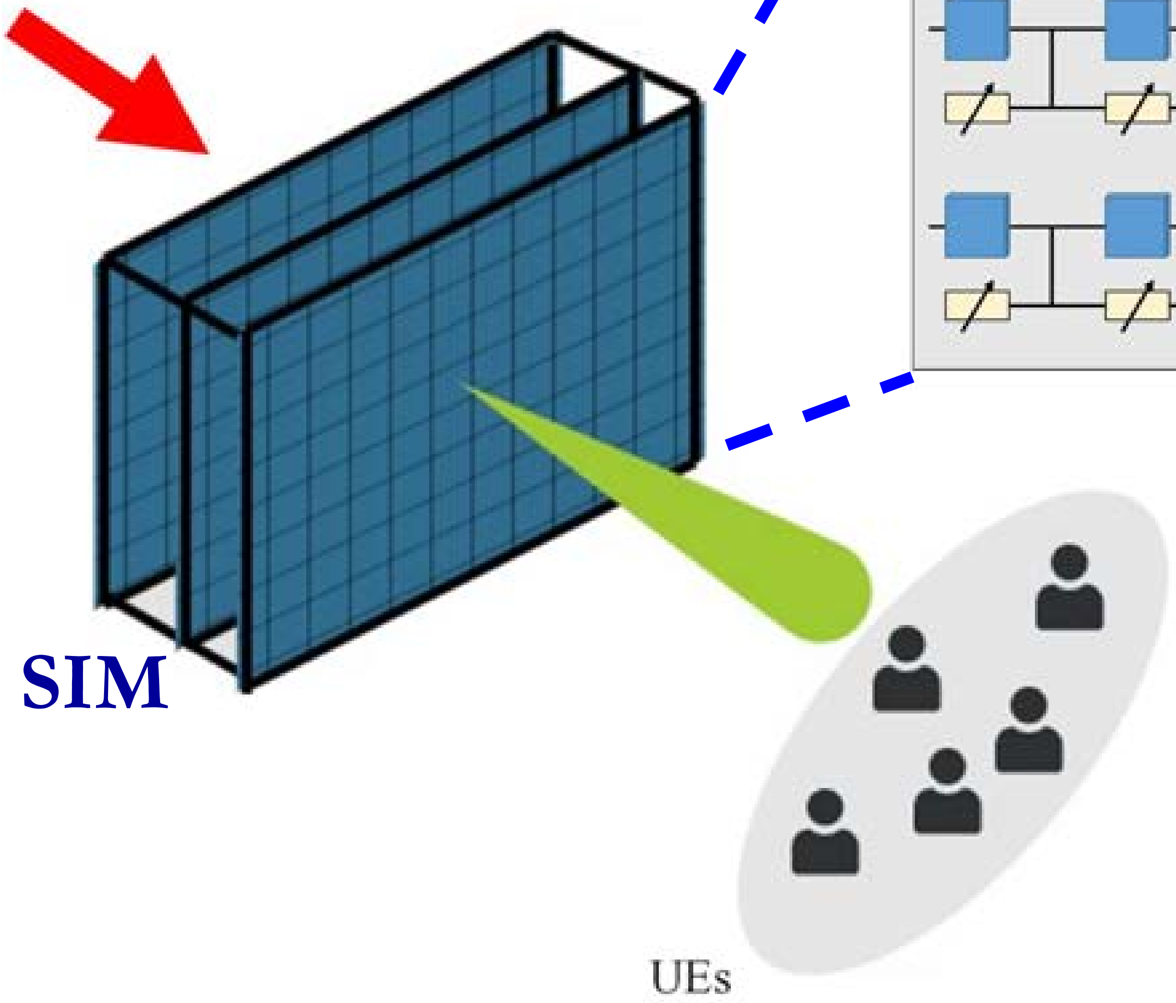

Key Features

(1) From digital to analog radio

→ complexity, power

(2) AI-based power processing

→ massive computing

(3) Multifunction

→ communication, sensing

Why SIM ?

Why SIM ?

(SIM as a multi-layer Holographic MIMO)

SIM as a Multi-Layer Holographic MIMO

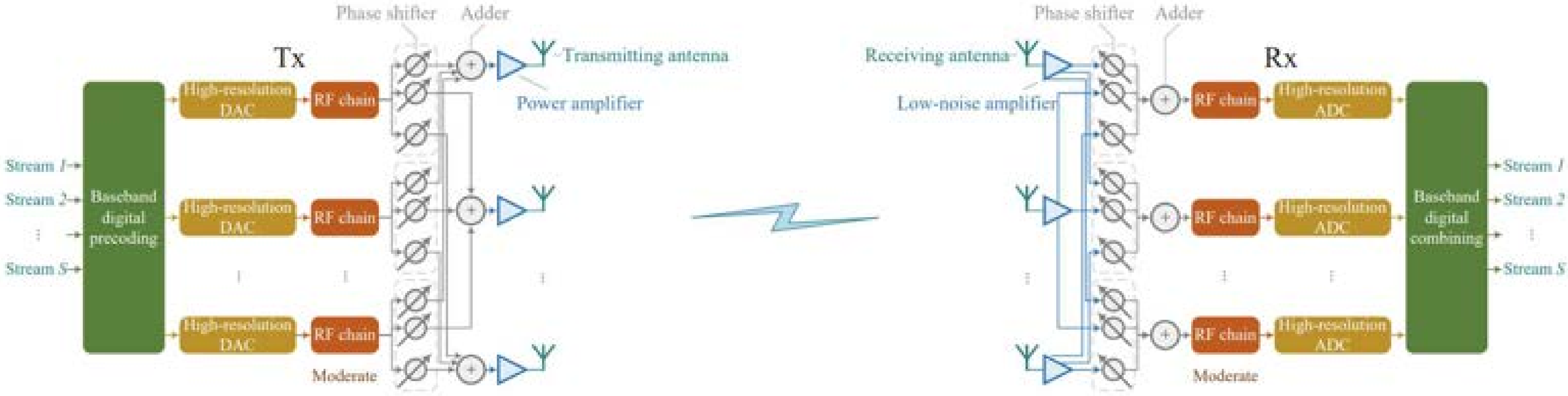

SIM as a Multi-Layer Holographic MIMO

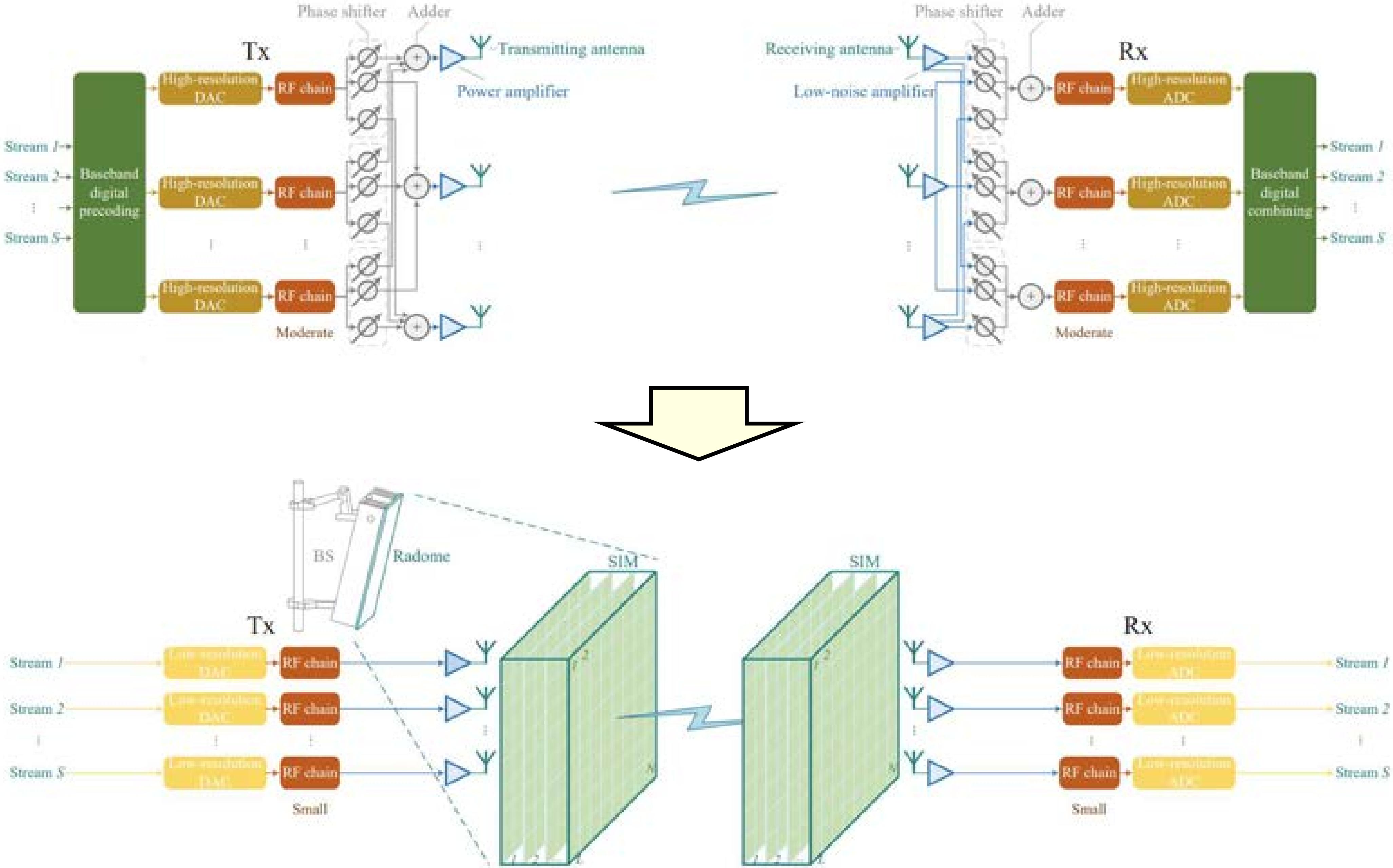

SIM as a Multi-Layer Holographic MIMO

Comparison of SIM with other MIMO technologies

MIMO technologies	Number of RF chains	ADC/DAC resolutions	Hardware cost	Energy efficiency	Digital precoder	Hardware implementation
Fully digital	Large	High	High	Low	✓	Driving each antenna with an individual RF chain.
Hybrid digital & analog	Moderate	Moderate	Moderate	Moderate	✓	Integrating phase shifters or metasurfaces with transceivers to reduce the number of RF chains.
Hybrid active & passive	Moderate	Moderate	Low	High	✓	Deploying RISs in the environment to improve the wireless link quality.
Proposed wave-based	Small	Low	Very low	Very high	✗	Leveraging multi-layer SIM to realize precoding and combining in the wave domain.

"… *the power consumption of analog-to-digital converters grows linearly with the bandwidth and exponentially with the number of bits* …" [arXiv:2109.04390]

$$\text{Power} \approx \text{Bandwidth} \cdot \text{const}^{\#\text{bits}}$$

Why SIM ?
(SIM as a multi-layer Refracting Surface)

SIM as a Multi-Layer Refracting RIS

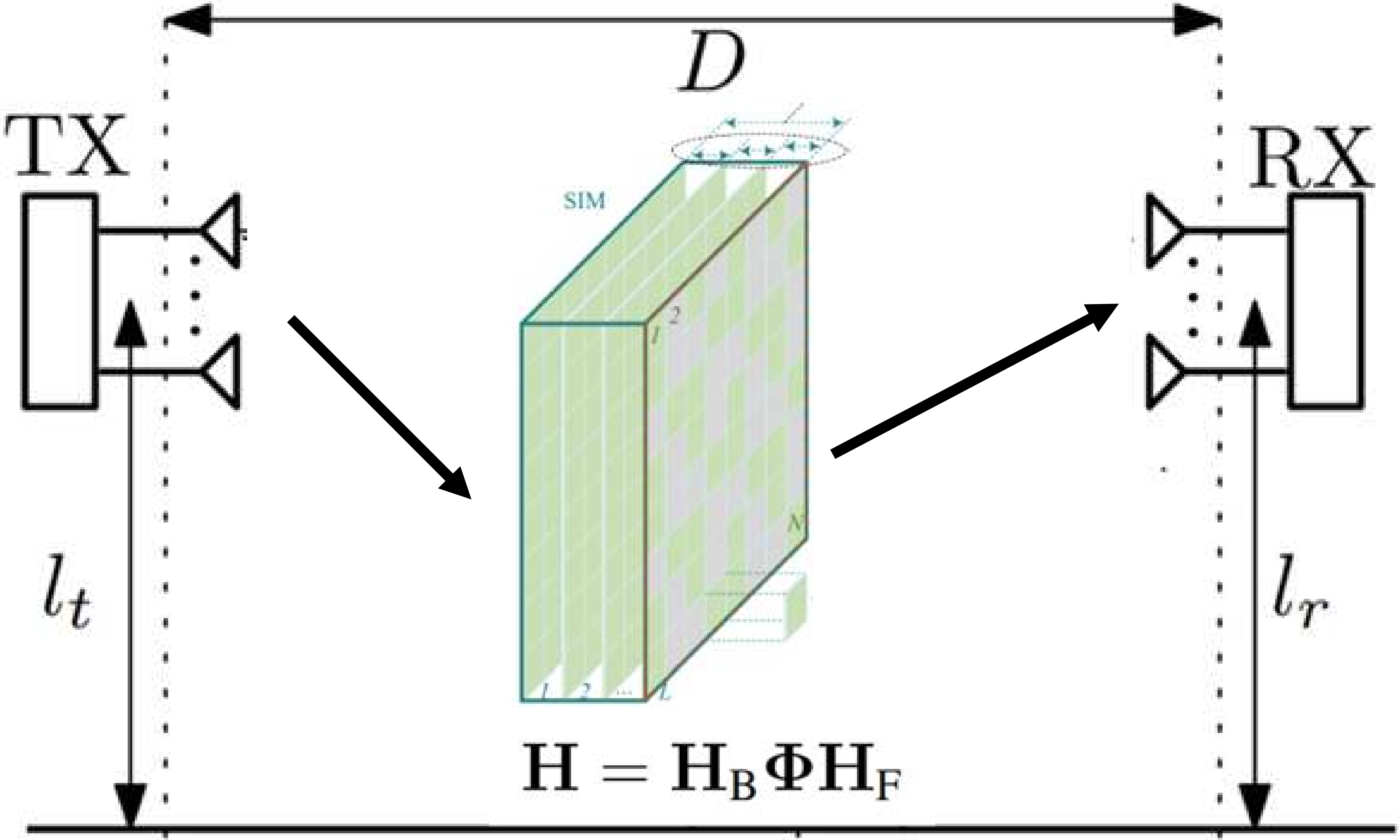

$$\mathbf{H} = \mathbf{H}_{\mathrm{B}} \mathbf{\Phi} \mathbf{H}_{\mathrm{F}}$$

Intelligent Metasurfaces

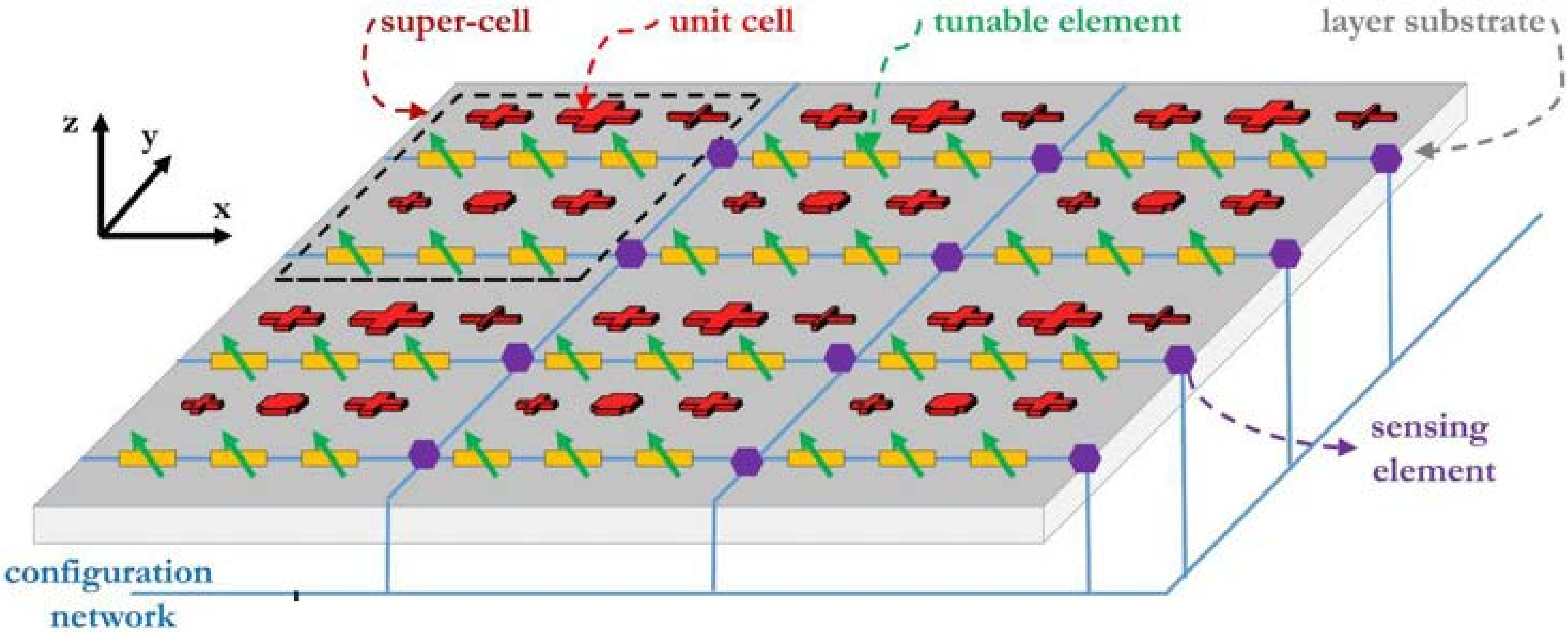

Intelligent Metasurfaces (typical design)

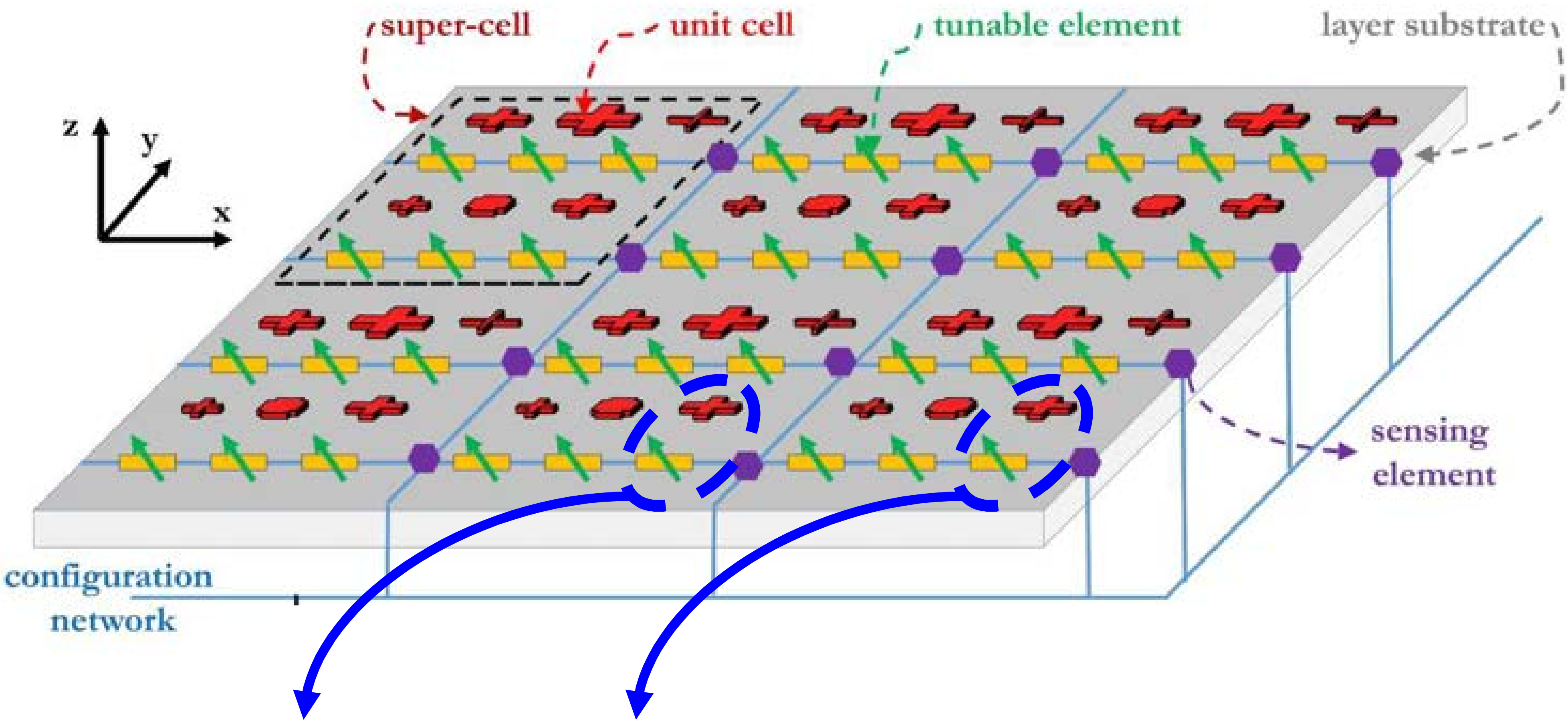

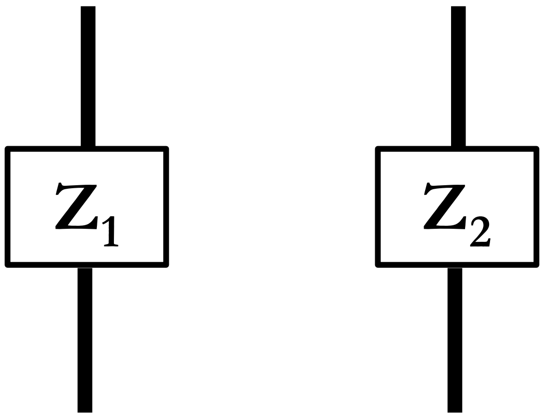

$$\mathbf{\Phi} = \begin{bmatrix} \theta_1 & 0 \\ 0 & \theta_2 \end{bmatrix}$$

Diagonal Design

Intelligent Metasurfaces (IT-optimal design)

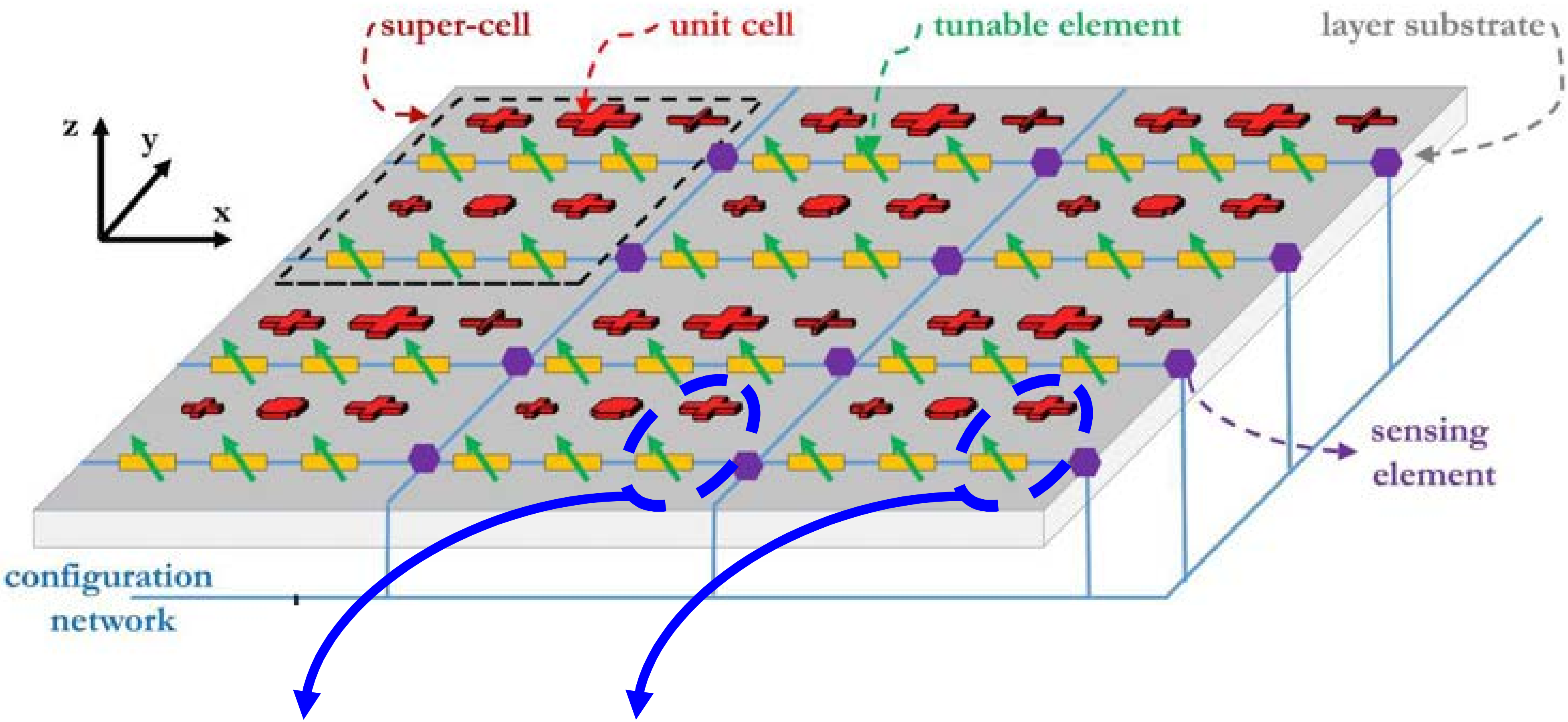

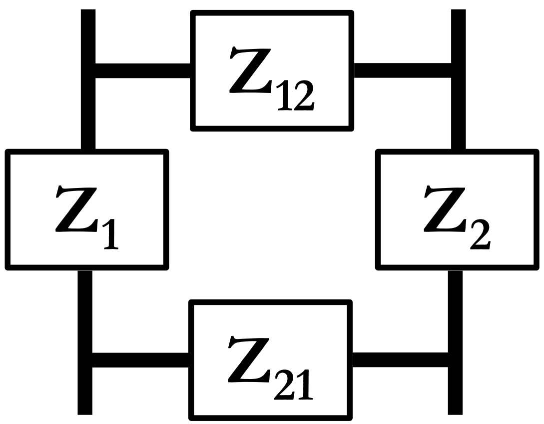

$$\Phi = \begin{bmatrix} \theta_1 & \theta_{12} \\ \theta_{21} & \theta_2 \end{bmatrix}$$

Non-Diagonal Design

SIM as a Multi-Layer Refracting RIS

Received: 21 December 2022 | Revised: 7 February 2023 | Accepted: 13 February 2023

DOI: 10.1049/sil2.12195

IET Signal Processing

The Institution of Engineering and Technology WILEY

ORIGINAL RESEARCH

Spatial multiplexing in near field MIMO channels with reconfigurable intelligent surfaces

Giulio Bartoli[1] | Andrea Abrardo[1] | Nicolo Decarli[2] | Davide Dardari[3] | Marco Di Renzo[4]

[1]University of Siena, Siena, Italy

[2]Italian Research Council, Bologna, Italy

[3]University of Bologna, Bologna, Italy

[4]Universite Paris-Saclay, CNRS, CentraleSupelec, Laboratoire des Signaux et Systèmes, Gif-sur-Yvette, France

Correspondence

Marco Di Renzo.
Email: marco.di-renzo@universite-paris-saclay.fr

Funding information

Theory Lab, Central Research Institute, 2012 Labs, Huawei Technologies Co., Ltd.; The European Commission through the HE TIMES project, Grant/Award Number: 101096307; The European Commission through the H2020 ARIADNE project, Grant/Award Number: 871464; The European Commission through the H2020 RISE-6G project, Grant/Award Number: 101017011; The Fulbright Foundation

Abstract

We consider a multiple-input multiple-output (MIMO) channel in the presence of a reconfigurable intelligent surface (RIS). Specifically, our focus is on analysing the spatial multiplexing gains in line-of-sight and low-scattering MIMO channels in the near field. We prove that the channel capacity is achieved by diagonalising the end-to-end transmitter-RIS-receiver channel, and applying the water-filling power allocation to the ordered product of the singular values of the transmitter-RIS and RIS-receiver channels. The obtained capacity-achieving solution requires an RIS with a non-diagonal matrix of reflection coefficients. Under the assumption of nearly-passive RIS, that is, no power amplification is needed at the RIS, the water-filling power allocation is necessary only at the transmitter. We refer to this design of RIS as a linear, nearly-passive, reconfigurable electromagnetic object (EMO). In addition, we introduce a closed-form and low-complexity design for RIS, whose matrix of reflection coefficients is diagonal with unit-modulus entries. The reflection coefficients are given by the product of two focusing functions: one steering the RIS-aided signal towards the mid-point of the MIMO transmitter and one steering the RIS-aided signal towards the mid-point of the MIMO receiver. We prove that this solution is exact in line-of-sight channels under the paraxial setup. With the aid of extensive numerical simulations in line-of-sight (free-space) channels, we show that the proposed approach offers performance (rate and degrees of freedom) close to that obtained by numerically solving non-convex optimization problems at a high computational complexity. Also, we show that it provides performance close to that achieved by the EMO (non-diagonal RIS) in most of the considered case studies.

SIM as a Multi-Layer Refracting RIS

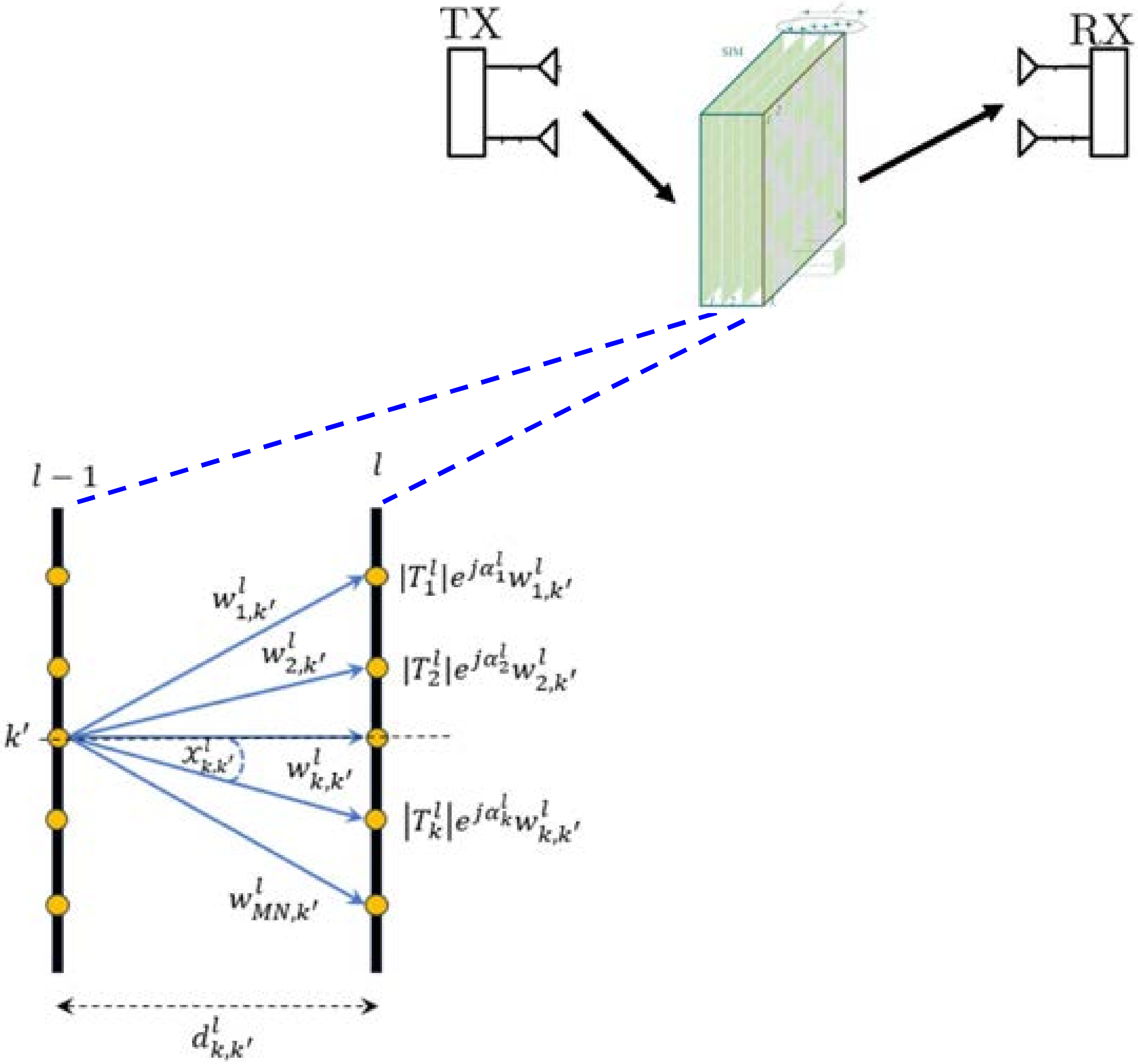

SIM as a Multi-Layer Refracting RIS

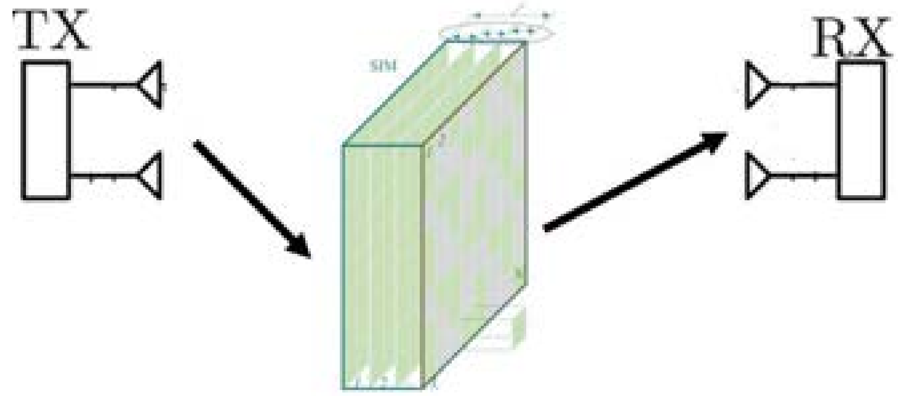

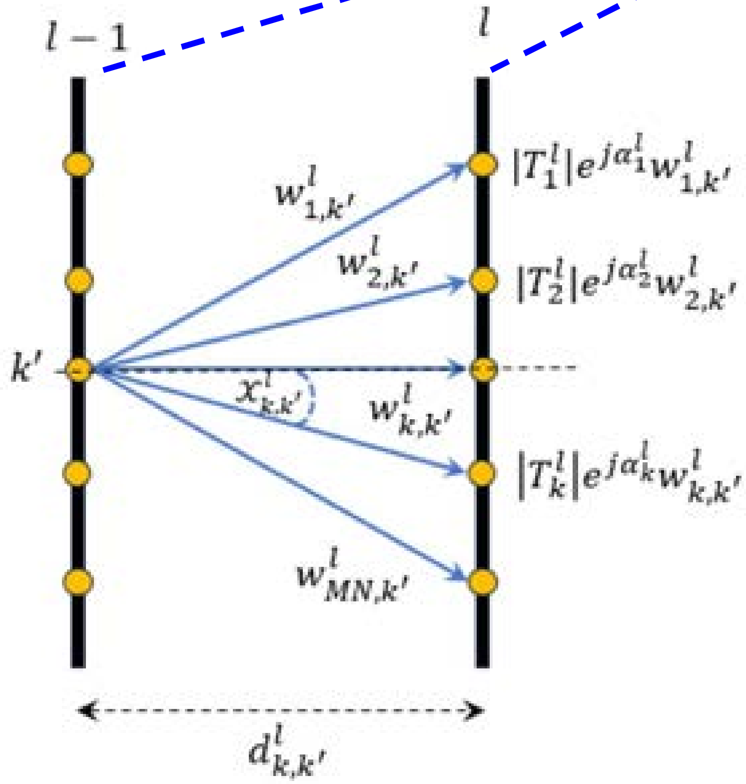

$$\mathbf{W}^{\mathrm{SIM}} = \left(\mathbf{T}^L\mathbf{W}^L\right)\left(\mathbf{T}^{L-1}\mathbf{W}^{L-1}\right)\ldots\left(\mathbf{T}^2\mathbf{W}^2\right)\left(\mathbf{T}^1\mathbf{W}^1\right)$$

SIM as a Multi-Layer Refracting RIS

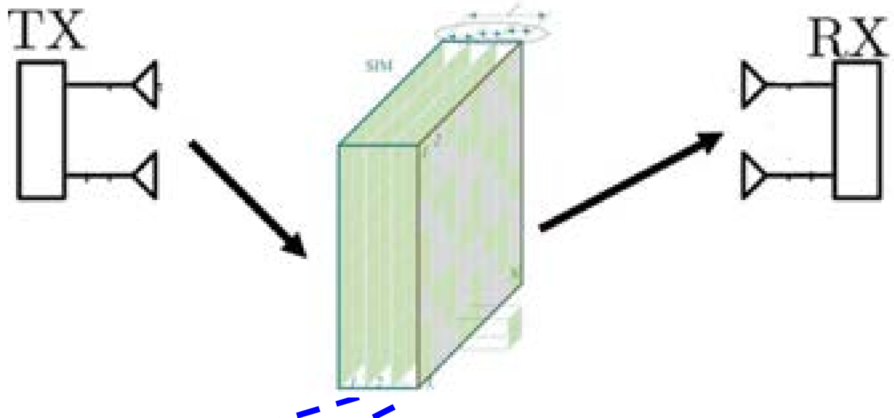

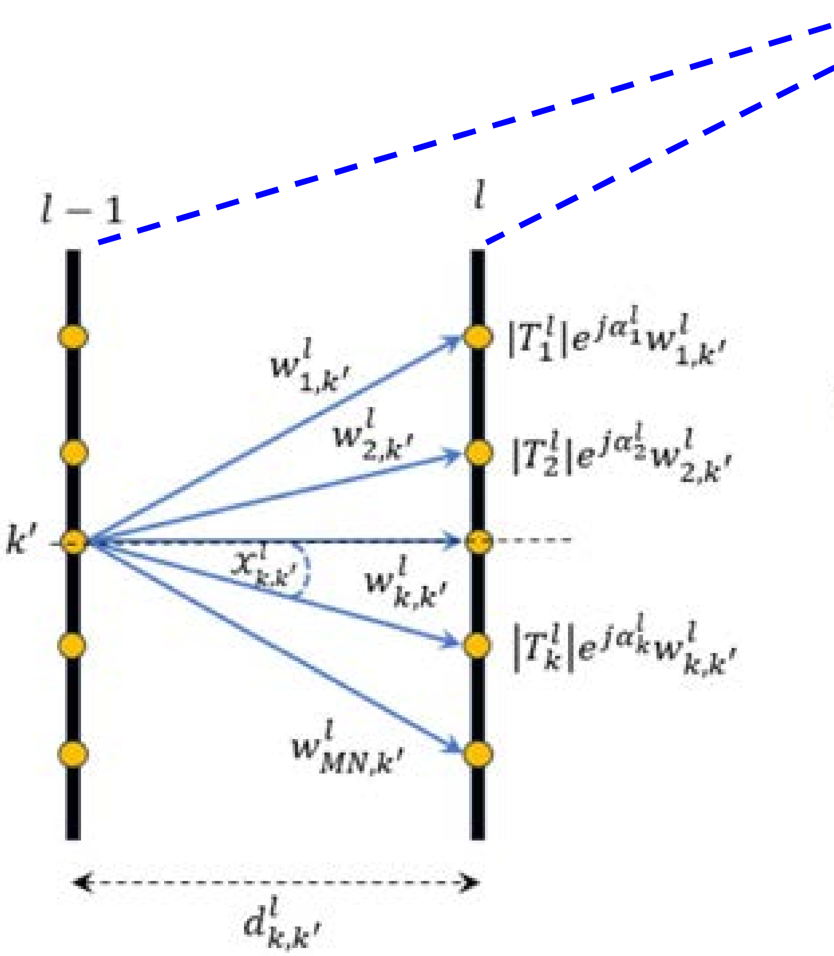

$$\mathbf{W}^{\mathrm{SIM}} = \left(\mathbf{T}^L\mathbf{W}^L\right)\left(\mathbf{T}^{L-1}\mathbf{W}^{L-1}\right)\ldots\left(\mathbf{T}^2\mathbf{W}^2\right)\left(\mathbf{T}^1\mathbf{W}^1\right)$$

$\mathbf{T}^l$: <u>Diagonal</u> matrices of metasurface transmission coefficients

SIM as a Multi-Layer Refracting RIS

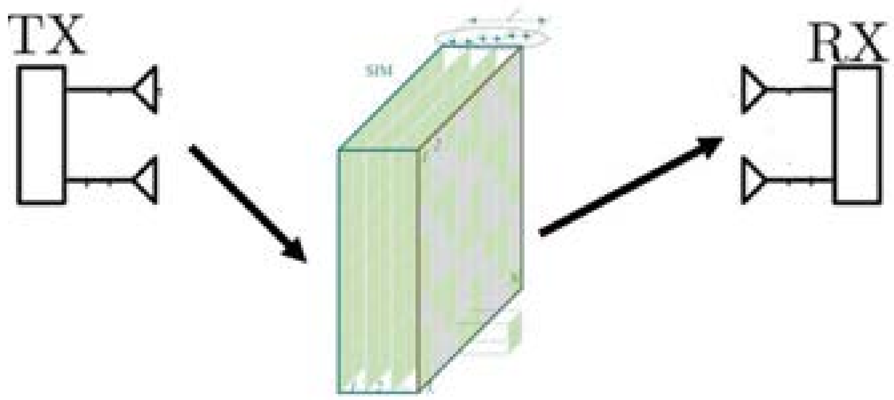

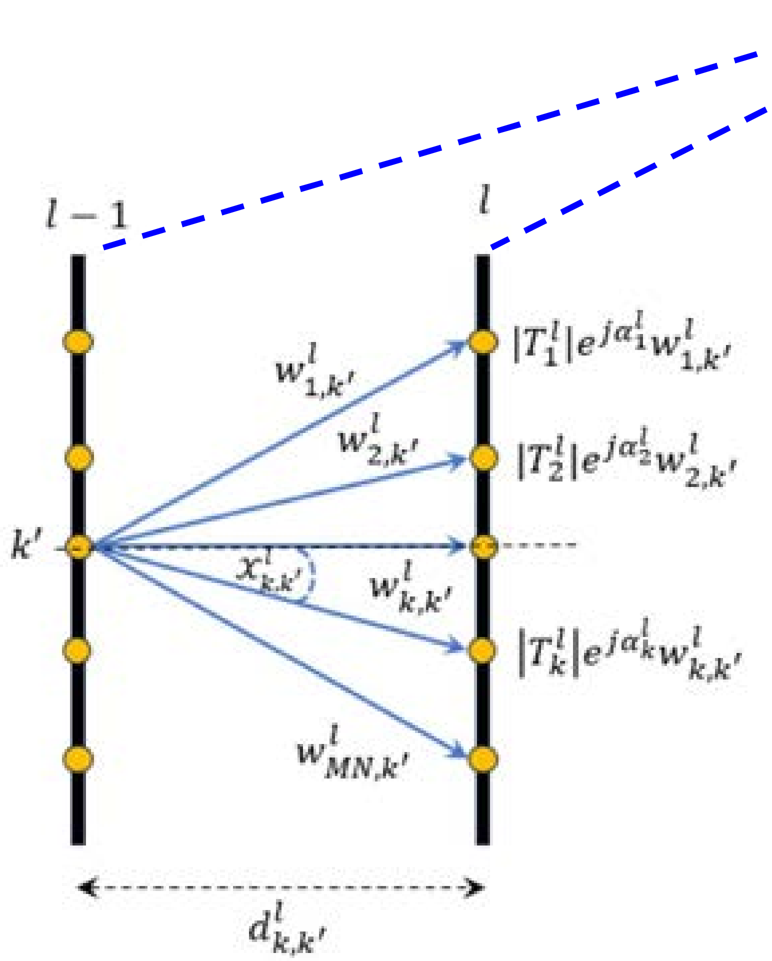

$$\mathbf{W}^{\mathrm{SIM}} = \left(\mathbf{T}^L\mathbf{W}^L\right)\left(\mathbf{T}^{L-1}\mathbf{W}^{L-1}\right)\ldots\left(\mathbf{T}^2\mathbf{W}^2\right)\left(\mathbf{T}^1\mathbf{W}^1\right)$$

$\mathbf{T}^l$: Diagonal matrices of metasurface transmission coefficients

$\mathbf{W}^l$: Non-diagonal matrices of inter-layer propagation coefficients

SIM as a Multi-Layer Refracting RIS

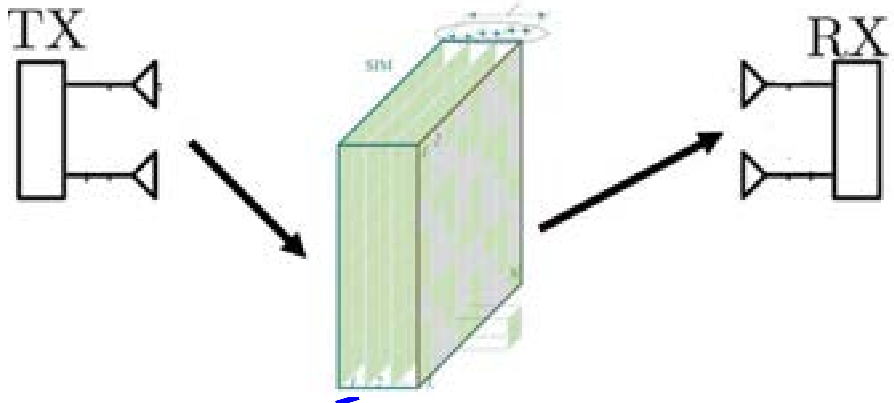

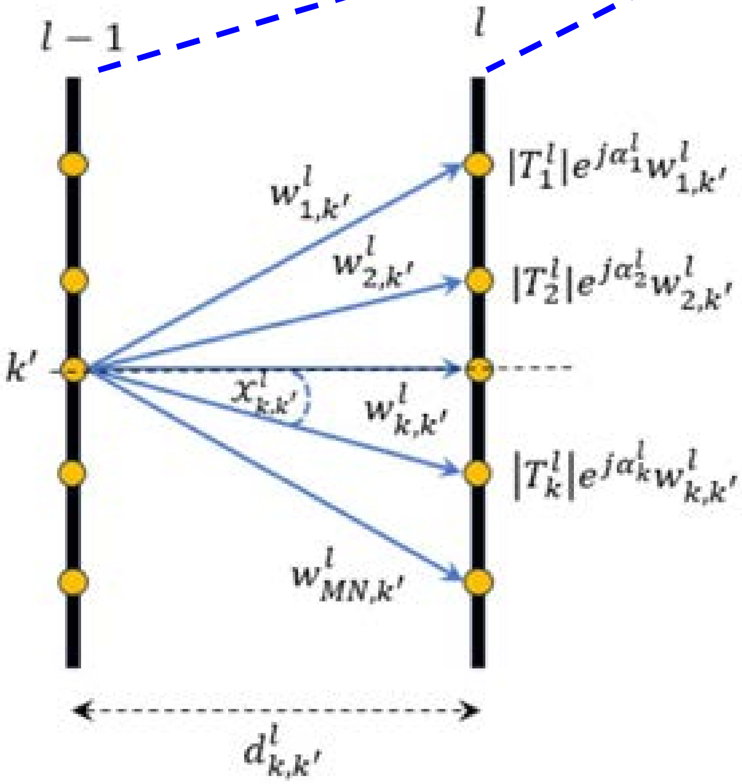

"non-diagonal" structure

$$\mathbf{W}^{\mathrm{SIM}} = \left(\mathbf{T}^L\mathbf{W}^L\right)\left(\mathbf{T}^{L-1}\mathbf{W}^{L-1}\right)\ldots\left(\mathbf{T}^2\mathbf{W}^2\right)\left(\mathbf{T}^1\mathbf{W}^1\right)$$

$\mathbf{T}^l$: <u>Diagonal</u> matrices of metasurface transmission coefficients

$\mathbf{W}^l$: <u>Non-diagonal</u> matrices of inter-layer propagation coefficients

Why SIM ?

(SIM as a Wave-Domain Computing Platform)

Wave-Domain Signal Processing (Computing)

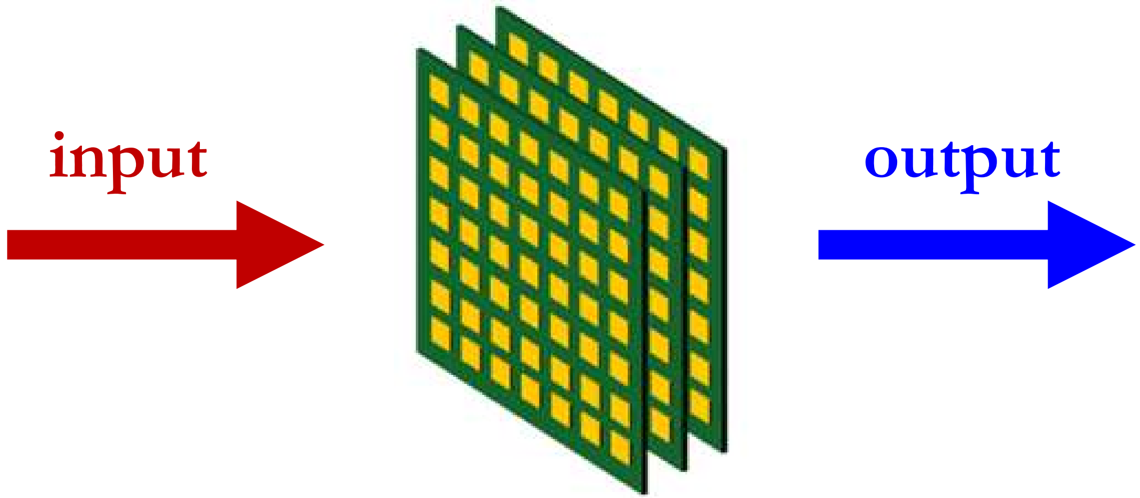

Wave-Domain Signal Processing (Computing)

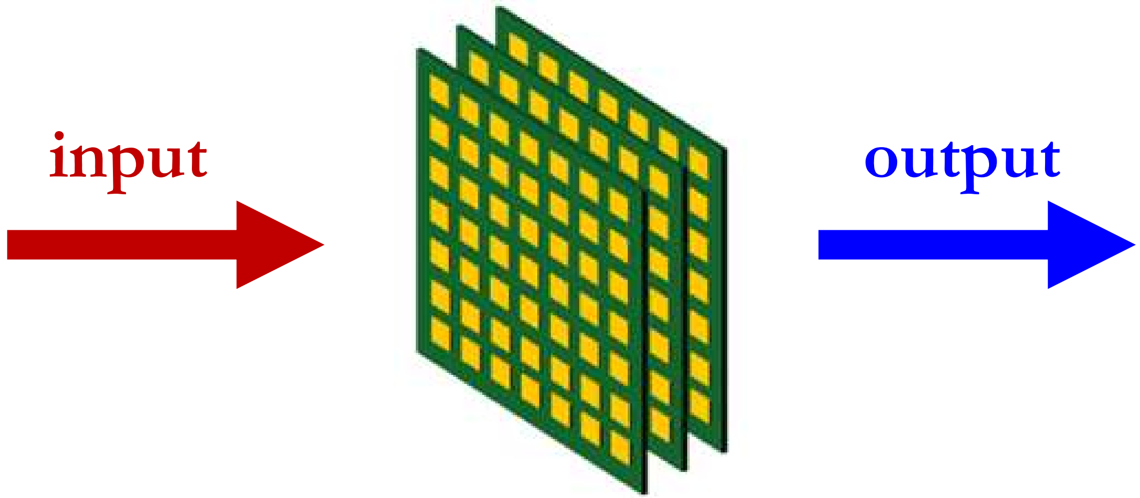

Science

Performing Mathematical Operations with Metamaterials

Alexandre Silva,[1]* Francesco Monticone,[2]* Giuseppe Castaldi,[3] Vincenzo Galdi,[3]
Andrea Alù,[2] Nader Engheta[1]†

We introduce the concept of metamaterial analog computing, based on suitably designed metamaterial blocks that can perform mathematical operations (such as spatial differentiation, integration, or convolution) on the profile of an impinging wave as it propagates through these blocks. Two approaches are presented to achieve such functionality: (i) subwavelength structured metascreens combined with graded-index waveguides and (ii) multilayered slabs designed to achieve a desired spatial Green's function. Both techniques offer the possibility of miniaturized, potentially integrable, wave-based computing systems that are thinner than conventional lens-based optical signal and data processors by several orders of magnitude.

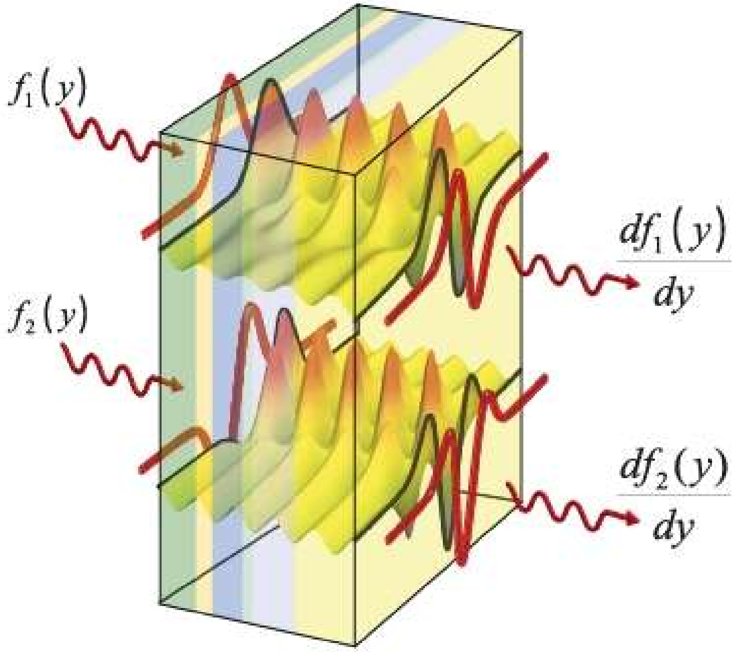

Wave-Domain Signal Processing Example: 2D DFT

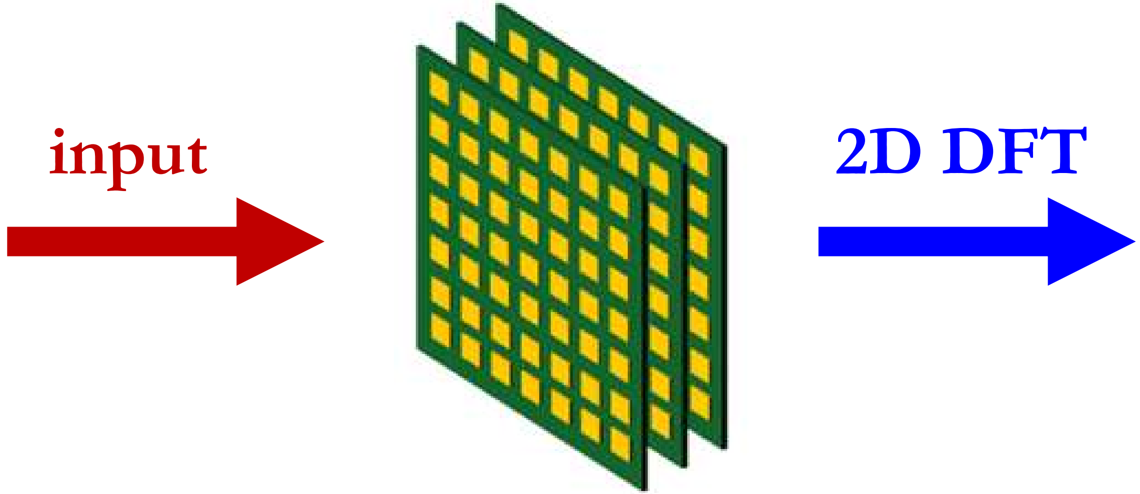

DFT $$f_{n,\breve{n}} = [\boldsymbol{F}]_{n,\breve{n}} \triangleq e^{-j2\pi\frac{(n_{\mathrm{x}}-1)(\breve{n}_{\mathrm{x}}-1)}{N_{\mathrm{x}}}} e^{-j2\pi\frac{(n_{\mathrm{y}}-1)(\breve{n}_{\mathrm{y}}-1)}{N_{\mathrm{y}}}}$$

Wave-Domain Signal Processing Example: 2D DFT

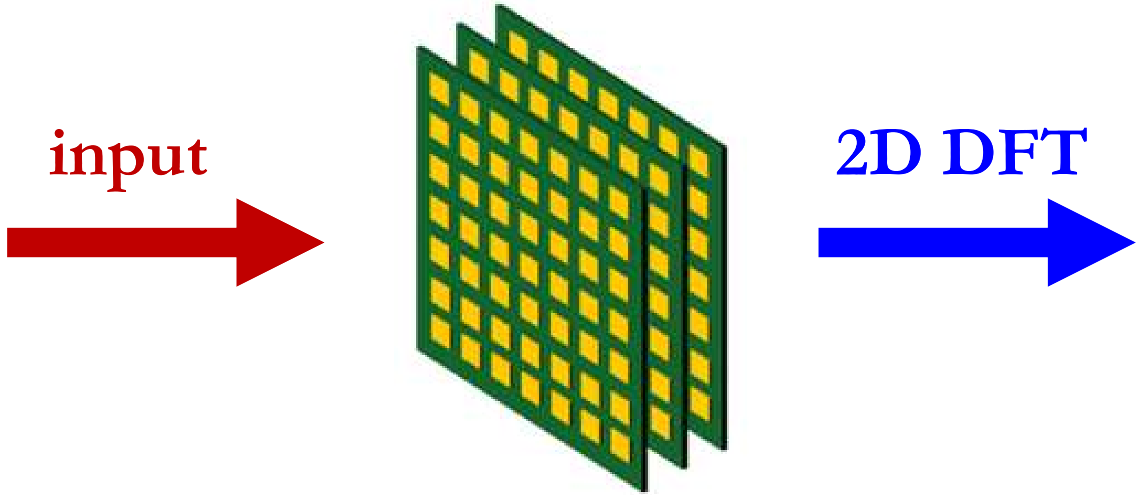

DFT $$f_{n,\breve{n}} = [\boldsymbol{F}]_{n,\breve{n}} \triangleq e^{-j2\pi\frac{(n_{\mathrm{x}}-1)(\breve{n}_{\mathrm{x}}-1)}{N_{\mathrm{x}}}} e^{-j2\pi\frac{(n_{\mathrm{y}}-1)(\breve{n}_{\mathrm{y}}-1)}{N_{\mathrm{y}}}}$$

SIM

$$\boldsymbol{G} = \boldsymbol{W}_L \boldsymbol{\Upsilon}_L \boldsymbol{W}_{L-1} \cdots \boldsymbol{W}_2 \boldsymbol{\Upsilon}_2 \boldsymbol{W}_1 \boldsymbol{\Upsilon}_1 \boldsymbol{W}_0$$
$$\boldsymbol{r} = \sqrt{\varrho}\boldsymbol{G}\boldsymbol{\Upsilon}_0 \boldsymbol{x}$$

Wave-Domain Signal Processing Example: 2D DFT

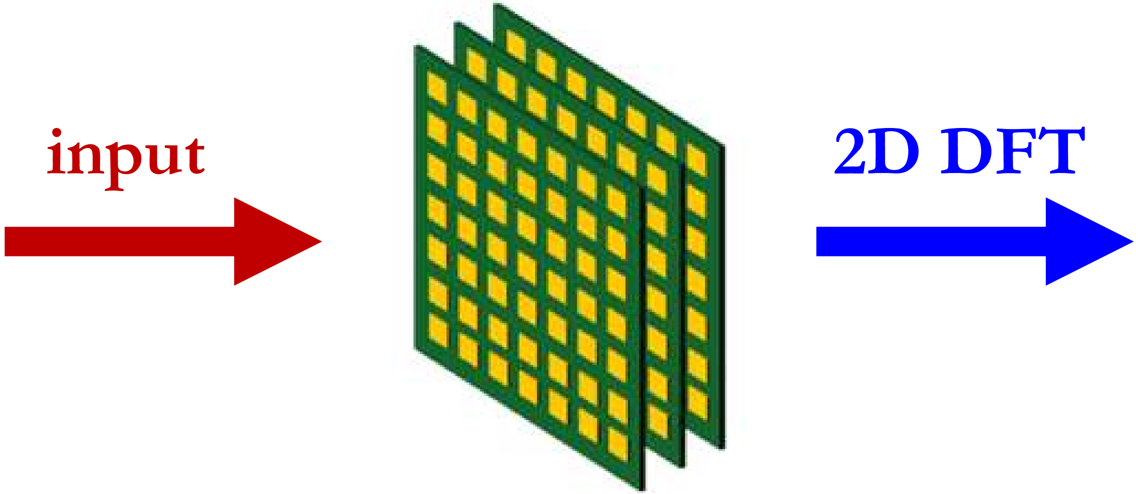

DFT

$$f_{n,\breve{n}} = [\boldsymbol{F}]_{n,\breve{n}} \triangleq e^{-j2\pi\frac{(n_{\mathrm{x}}-1)(\breve{n}_{\mathrm{x}}-1)}{N_{\mathrm{x}}}} e^{-j2\pi\frac{(n_{\mathrm{y}}-1)(\breve{n}_{\mathrm{y}}-1)}{N_{\mathrm{y}}}}$$

SIM

$$\boldsymbol{G} = \boldsymbol{W}_L \boldsymbol{\Upsilon}_L \boldsymbol{W}_{L-1} \cdots \boldsymbol{W}_2 \boldsymbol{\Upsilon}_2 \boldsymbol{W}_1 \boldsymbol{\Upsilon}_1 \boldsymbol{W}_0$$

$$\boldsymbol{r} = \sqrt{\varrho}\boldsymbol{G}\boldsymbol{\Upsilon}_0 \boldsymbol{x}$$

Wave-Domain Signal Processing Example: 2D DFT

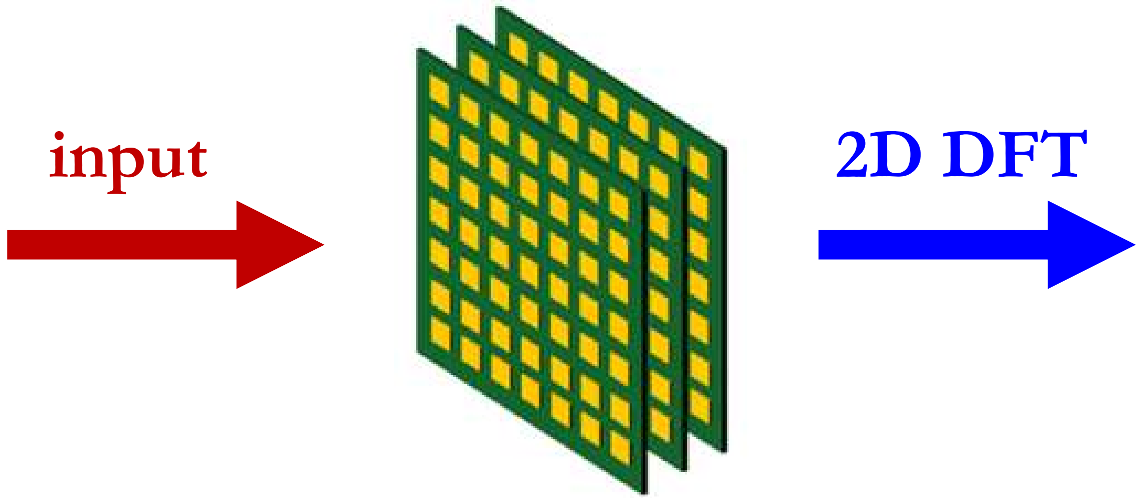

DFT $$f_{n,\breve{n}} = [\boldsymbol{F}]_{n,\breve{n}} \triangleq e^{-j2\pi \frac{(n_{\mathrm{x}}-1)(\breve{n}_{\mathrm{x}}-1)}{N_{\mathrm{x}}}} e^{-j2\pi \frac{(n_{\mathrm{y}}-1)(\breve{n}_{\mathrm{y}}-1)}{N_{\mathrm{y}}}}$$

$$\begin{aligned} \min_{\{\xi_{l,m}\}} \quad & \mathcal{L} = \|\beta \boldsymbol{G} - \boldsymbol{F}\|_F^2 \\ \text{s.t.} \quad & \boldsymbol{G} = \boldsymbol{W}_L \boldsymbol{\Upsilon}_L \boldsymbol{W}_{L-1} \cdots \boldsymbol{W}_2 \boldsymbol{\Upsilon}_2 \boldsymbol{W}_1 \boldsymbol{\Upsilon}_1 \boldsymbol{W}_0, \\ & \boldsymbol{\Upsilon}_l = \operatorname{diag}\left(\left[e^{j\xi_{l,1}}, e^{j\xi_{l,2}}, \cdots, e^{j\xi_{l,M}}\right]^T\right), \end{aligned}$$

SIM
$$\boldsymbol{G} = \boldsymbol{W}_L \boldsymbol{\Upsilon}_L \boldsymbol{W}_{L-1} \cdots \boldsymbol{W}_2 \boldsymbol{\Upsilon}_2 \boldsymbol{W}_1 \boldsymbol{\Upsilon}_1 \boldsymbol{W}_0$$
$$\boldsymbol{r} = \sqrt{\varrho} \boldsymbol{G} \boldsymbol{\Upsilon}_0 \boldsymbol{x}$$

2D DFT: Direction of Arrival Estimation

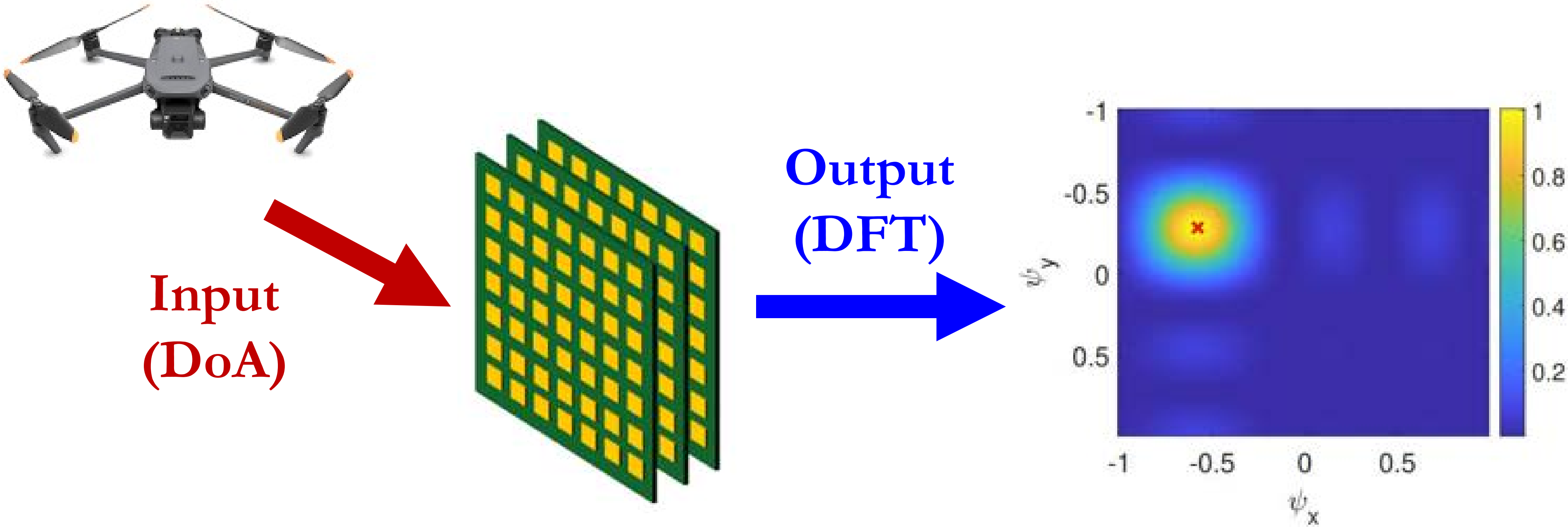

The 2D index of the peak

Received signal

$$[\hat{n}, \hat{t}] = \arg \max_{\substack{n=1,\cdots,N,\\ t=1,\cdots,T}} |r_{n,t}|^2$$

Antenna Snapshot

The estimated electrical angles

$$\hat{\psi}_{\mathrm{x}} = \mathrm{mod}\left[2\left(\frac{\hat{n}_{\mathrm{x}}-1}{N_{\mathrm{x}}} + \frac{\hat{t}_{\mathrm{x}}-1}{N_{\mathrm{x}}T_{\mathrm{x}}}\right)+1, 2\right]-1$$

$$\hat{\psi}_{\mathrm{y}} = \mathrm{mod}\left[2\left(\frac{\hat{n}_{\mathrm{y}}-1}{N_{\mathrm{y}}} + \frac{\hat{t}_{\mathrm{y}}-1}{N_{\mathrm{y}}T_{\mathrm{y}}}\right)+1, 2\right]-1$$

The estimated azimuth and elevation angles

$$\hat{\varphi} = \arctan\left(\frac{\hat{\psi}_{\mathrm{y}} d_{\mathrm{x}}}{\hat{\psi}_{\mathrm{x}} d_{\mathrm{y}}}\right),$$

$$\hat{\vartheta} = \arcsin\left(\frac{1}{\kappa}\sqrt{\frac{\hat{\psi}_{\mathrm{x}}^2}{d_{\mathrm{x}}^2} + \frac{\hat{\psi}_{\mathrm{y}}^2}{d_{\mathrm{y}}^2}}\right)$$

Numerical Examples

Numerical Examples
(wave-domain base station)

Wave-Domain Base Station

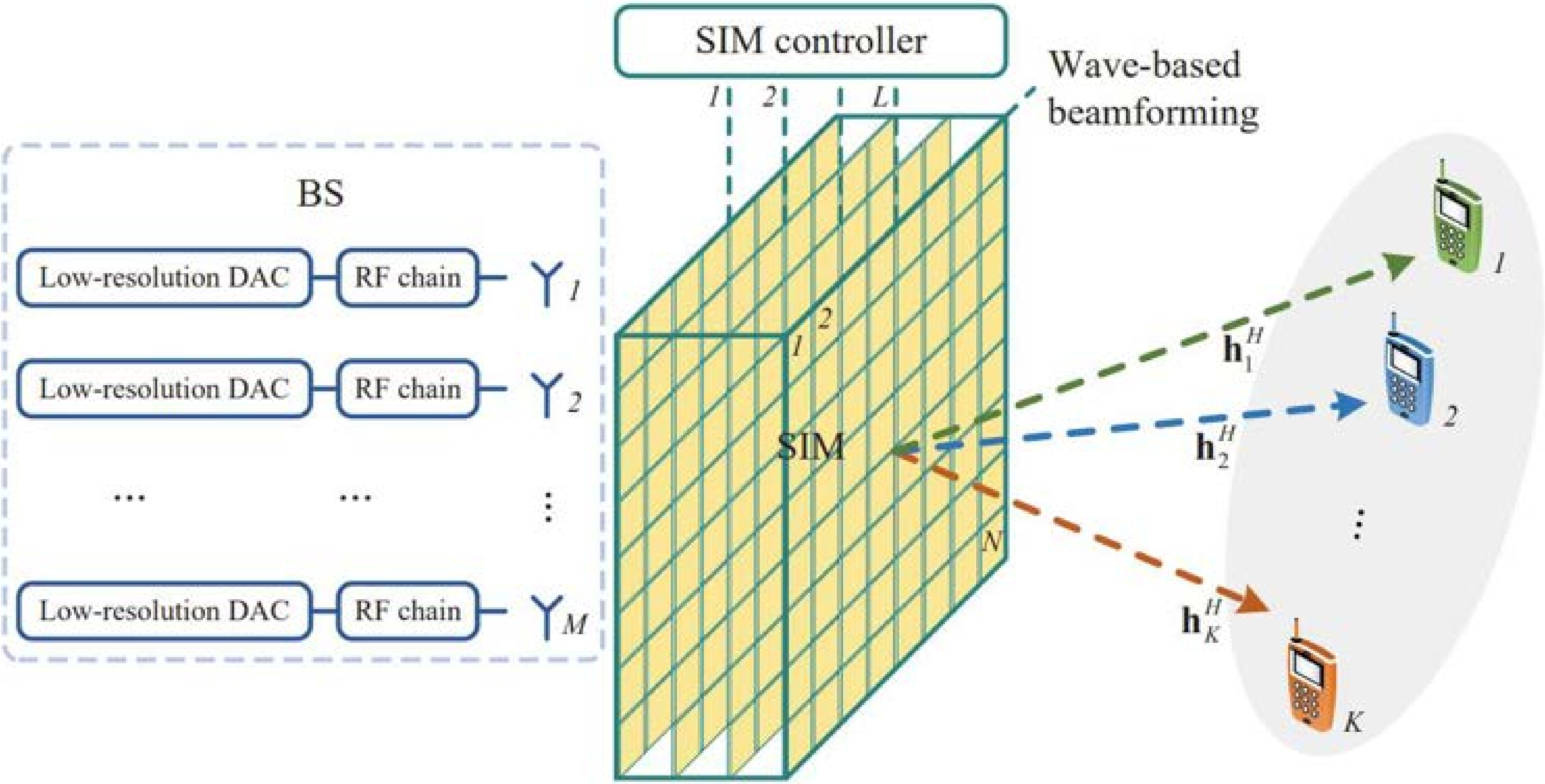

SIM Model: Rayleigh-Sommerfield Diffraction

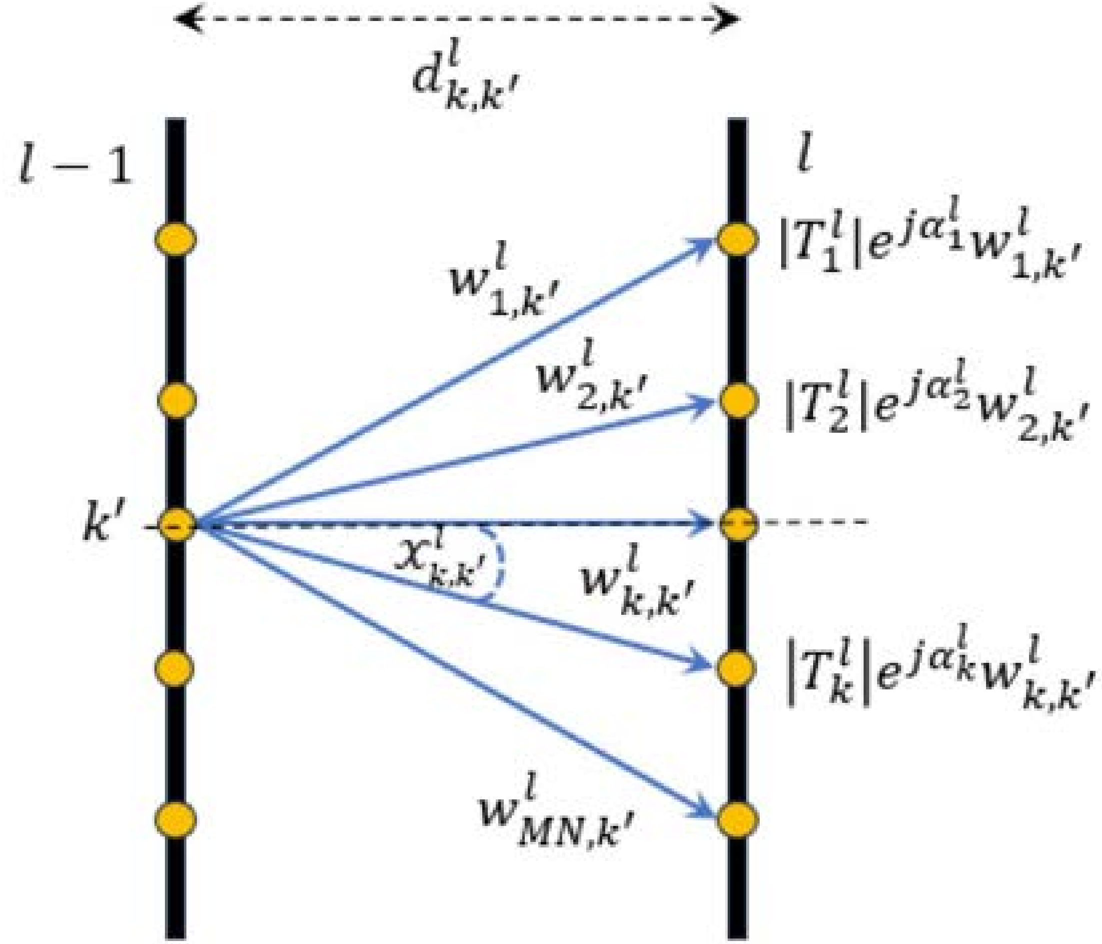

$$w^l_{k,k'} = \frac{A_u \cos \mathcal{X}^l_{k,k'}}{d^l_{k,k'}} \left(\frac{1}{2\pi d^l_{k,k'}} - j\frac{1}{\lambda} \right) e^{j2\pi d^l_{k,k'}/\lambda}$$

Problem Formulation

$$(\mathcal{P}_{\mathcal{A}}):\ \max_{\mathbf{p},\,\boldsymbol{\vartheta}}\ R=\sum\nolimits_{k=1}^{K}\log_2\left(1+\gamma_k\right)$$

$$\text{s.t.}\quad \gamma_k=\frac{\left|\mathbf{h}_k^{\mathrm{H}}\mathbf{G}\mathbf{w}_k^1\right|^2 p_k}{\sum\nolimits_{k'\neq k}^{K}\left|\mathbf{h}_k^{\mathrm{H}}\mathbf{G}\mathbf{w}_{k'}^1\right|^2 p_{k'}+\sigma_k^2},\ \forall k,$$

$$\mathbf{G}=\boldsymbol{\Phi}^L\mathbf{W}^L\boldsymbol{\Phi}^{L-1}\cdots\boldsymbol{\Phi}^2\mathbf{W}^2\boldsymbol{\Phi}^1,$$

$$\boldsymbol{\Phi}^l=\mathrm{diag}\left(e^{j\theta_1^l},e^{j\theta_2^l},\cdots,e^{j\theta_N^l}\right),\ \forall l,$$

$$\theta_n^l\in\mathcal{B},\ \forall n\in\mathcal{N},\ \forall l\in\mathcal{L},$$

$$\sum\nolimits_{k=1}^{K}p_k\le P_{\mathrm{T}},$$

$$p_k\ge 0,\ \forall k\in\mathcal{K}.$$

Wave-Domain Base Station (7 layers)

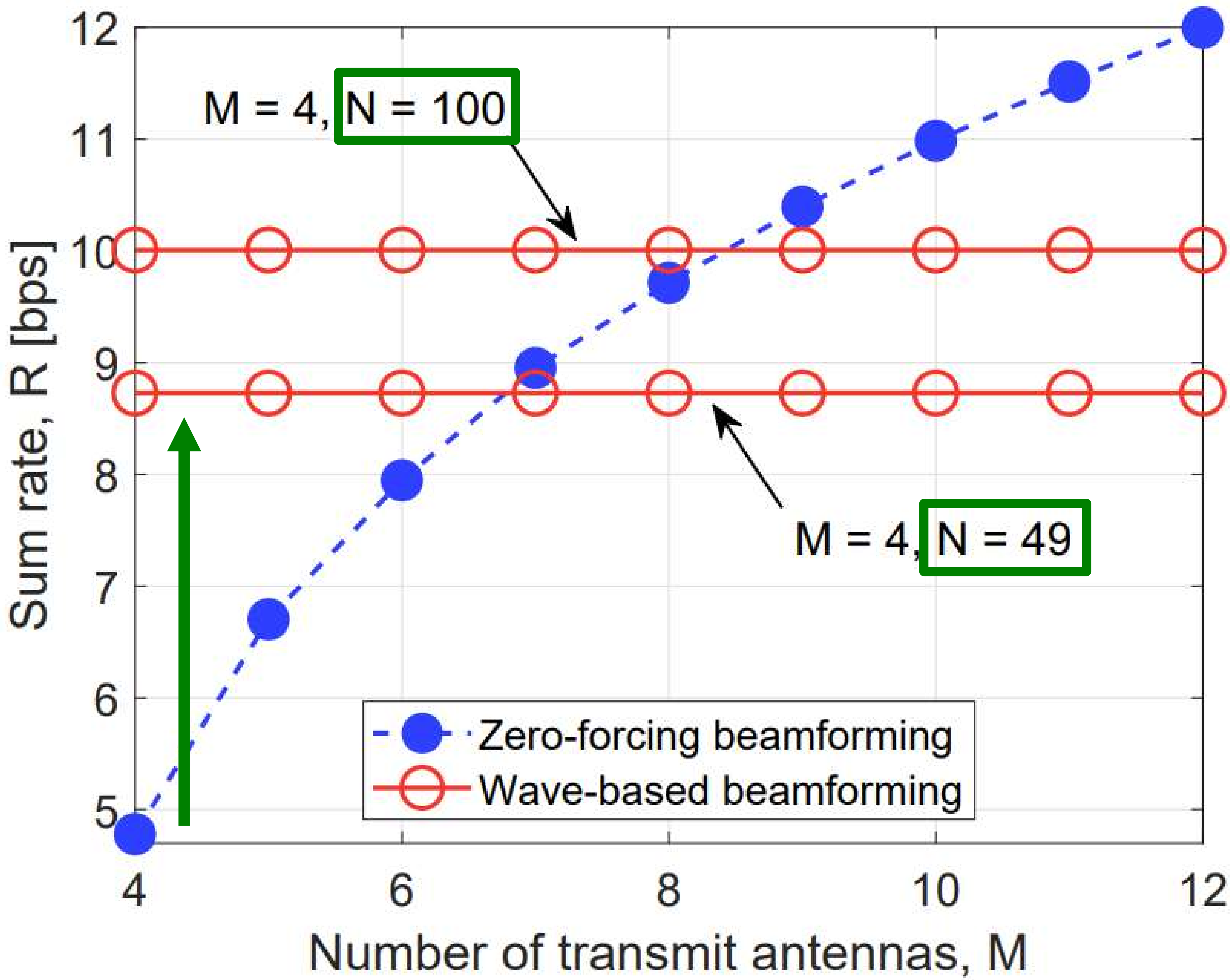

Numerical Examples
(radiation pattern shaping)

Radiation Pattern Shaping

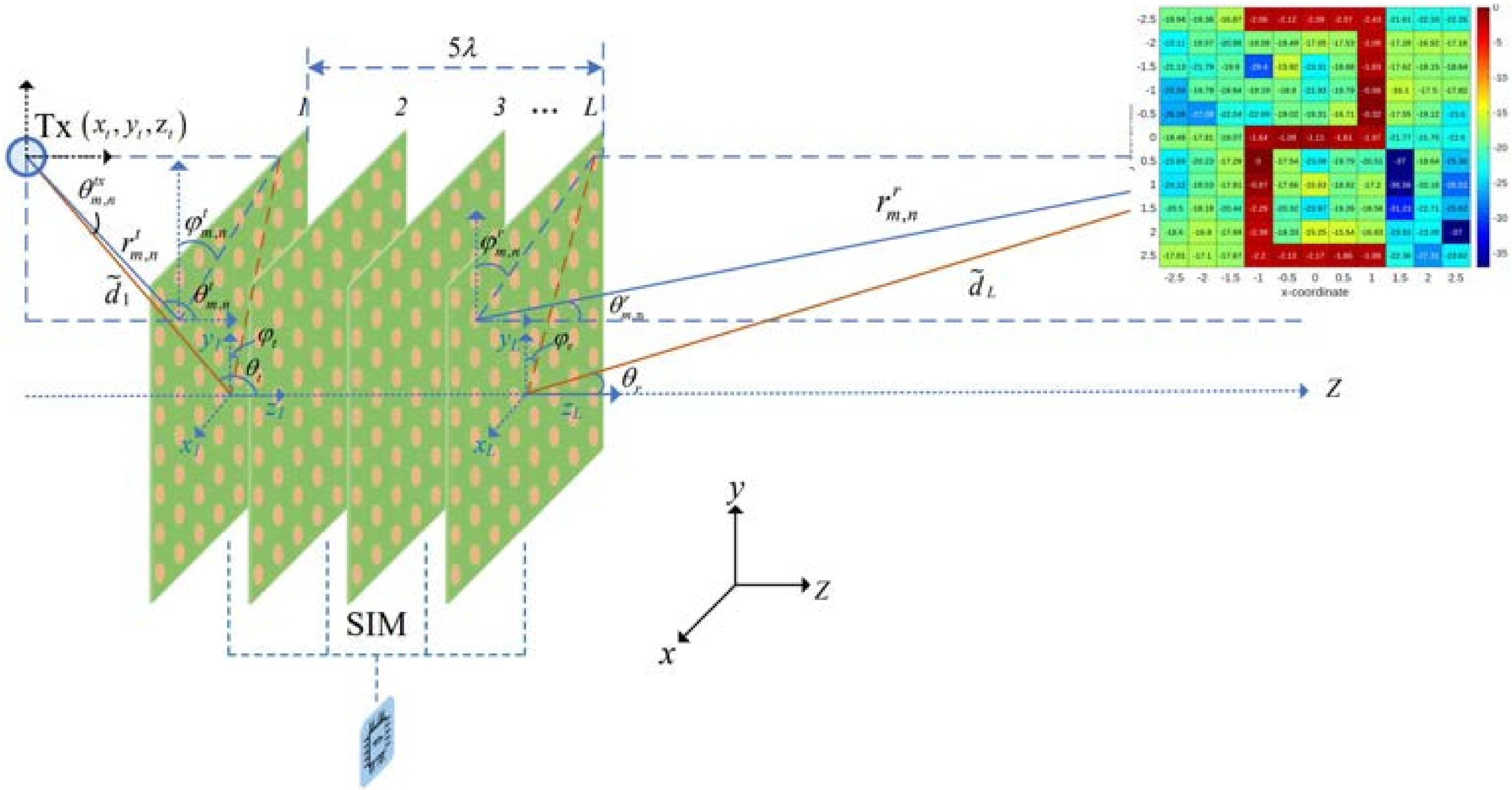

Problem Formulation

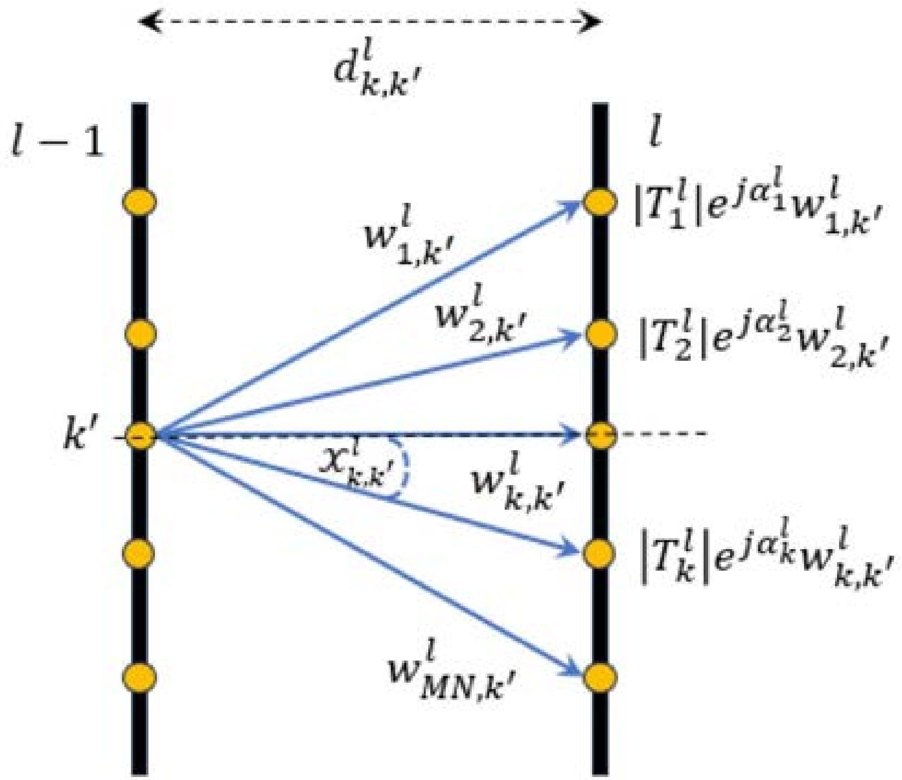

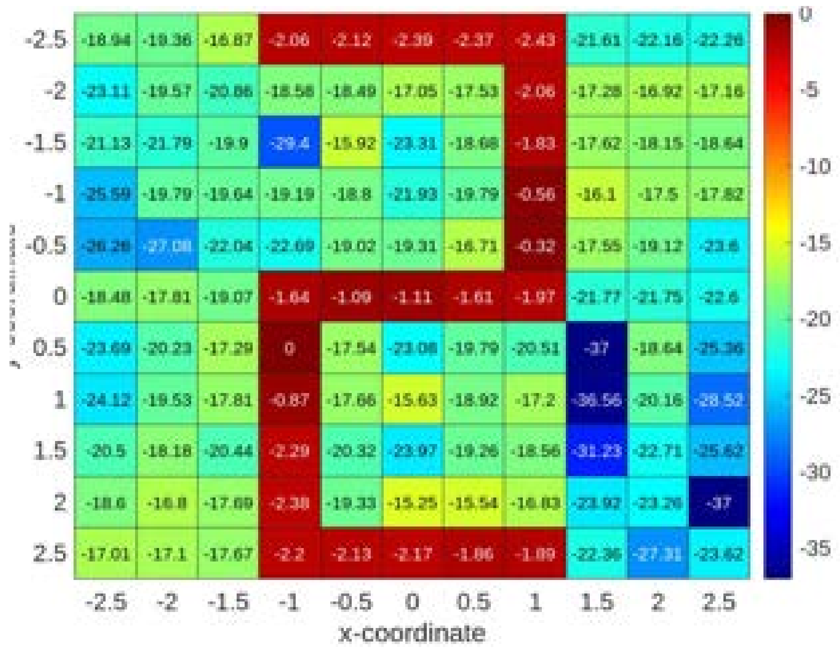

$$\min_{\alpha^l_k} \ \mathcal{J} = \frac{1}{M_p N_p} \sum_{i=1}^{M_p} \sum_{j=1}^{N_p} \left(P_{i,j} - P^{\text{tg}}_{i,j} \right)^2$$

$$\text{subject to } \alpha^l_k \in [0, 2\pi), \quad \forall k, l.$$

Radiation Pattern Shaping

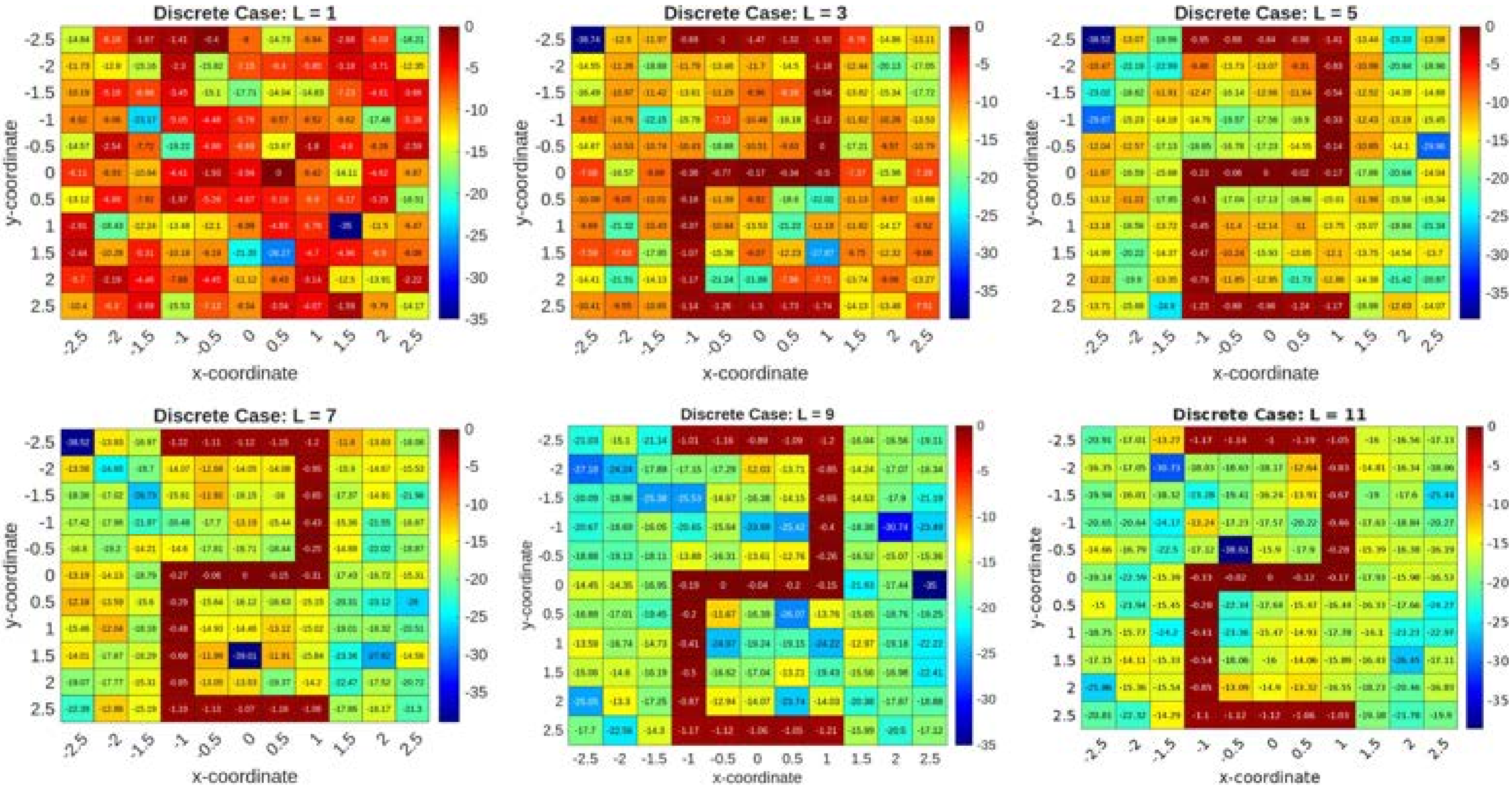

Numerical Examples
(sensing: direction of arrival estimation)

Direction of Arrival Estimation

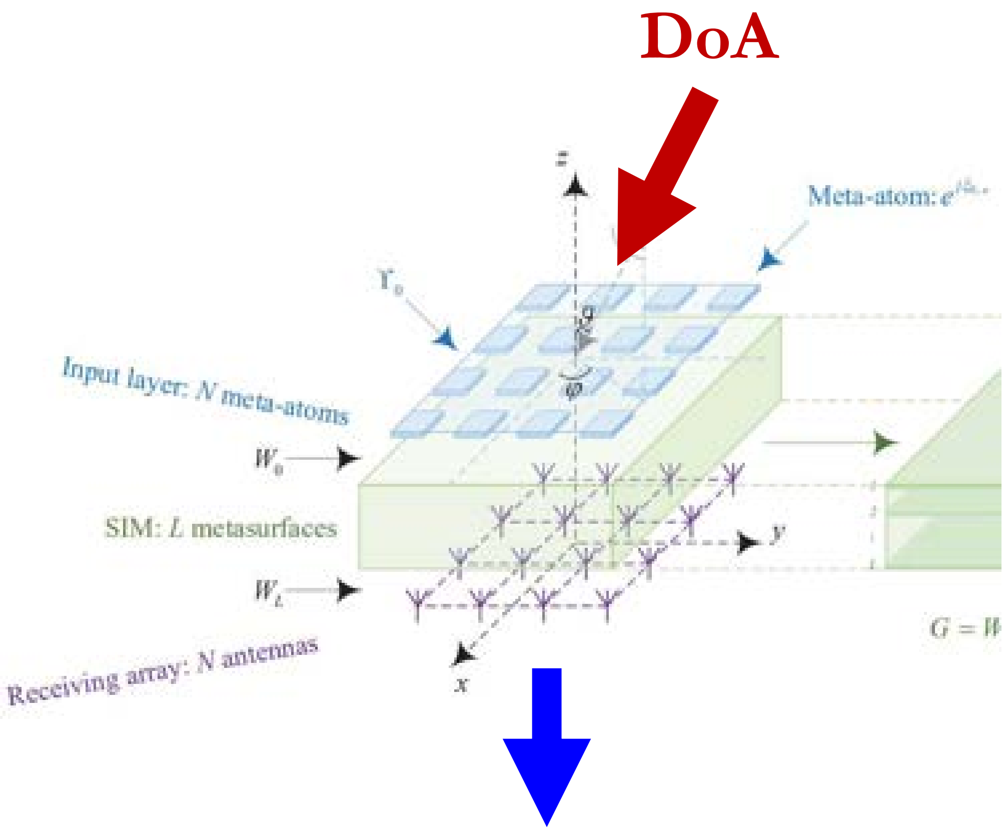

2D DFT → Angular Spectrum → Estimated DoA

Operating Principle

- The electrical angles in the x- and y-directions are

$$\psi_{\mathrm{x}} = \kappa d_{\mathrm{x}} \sin(\vartheta) \cos(\varphi)$$
$$\psi_{\mathrm{y}} = \kappa d_{\mathrm{y}} \sin(\vartheta) \sin(\varphi)$$

- The steering vector *w.r.t.* the input layer of the SIM

$$\boldsymbol{a}(\psi_{\mathrm{x}}, \psi_{\mathrm{y}}) = \boldsymbol{a}_{\mathrm{y}}(\psi_{\mathrm{y}}) \otimes \boldsymbol{a}_{\mathrm{x}}(\psi_{\mathrm{x}})$$

$$[\boldsymbol{a}_{\mathrm{x}}(\psi_{\mathrm{x}})]_{n_{\mathrm{x}}} \triangleq e^{j\psi_{\mathrm{x}}(n_{\mathrm{x}}-1)}$$
$$[\boldsymbol{a}_{\mathrm{y}}(\psi_{\mathrm{y}})]_{n_{\mathrm{y}}} \triangleq e^{j\psi_{\mathrm{y}}(n_{\mathrm{y}}-1)}$$

- The signal being incident upon the input layer is

$$\boldsymbol{x} = \boldsymbol{a}(\psi_{\mathrm{x}}, \psi_{\mathrm{y}})\, s$$

  - A single source
  - Continuous phase tunning

- The inter-layer propagation coefficient is

$$[\boldsymbol{W}_l]_{m,\tilde{m}} = \frac{A_{\text{meta-atom}} \cos \epsilon_{m,\tilde{m}}}{2\pi d_{m,\tilde{m}}^2} (1 - j\kappa d_{m,\tilde{m}})\, e^{j\kappa d_{m,\tilde{m}}}$$

- The transfer function matrix of the SIM is

$$\boldsymbol{G} = \boldsymbol{W}_L \underbrace{\boldsymbol{\Upsilon}_L}_{\text{Transmission coefficient matrix}} \boldsymbol{W}_{L-1} \cdots \boldsymbol{W}_2 \boldsymbol{\Upsilon}_2 \boldsymbol{W}_1 \boldsymbol{\Upsilon}_1 \boldsymbol{W}_0$$

- The complex signal received at the array is

$$\boldsymbol{r} = \sqrt{\underbrace{\varrho}_{\text{SNR}}}\, \boldsymbol{G} \boldsymbol{\Upsilon}_0 \boldsymbol{x} + \underbrace{\boldsymbol{u}}_{\text{Normalized noise}} = \sqrt{\varrho}\, \boldsymbol{G} \boldsymbol{\Upsilon}_0 \boldsymbol{a}(\psi_{\mathrm{x}}, \psi_{\mathrm{y}})\, s + \boldsymbol{u}$$

Direction of Arrival Estimation

Operating Principle

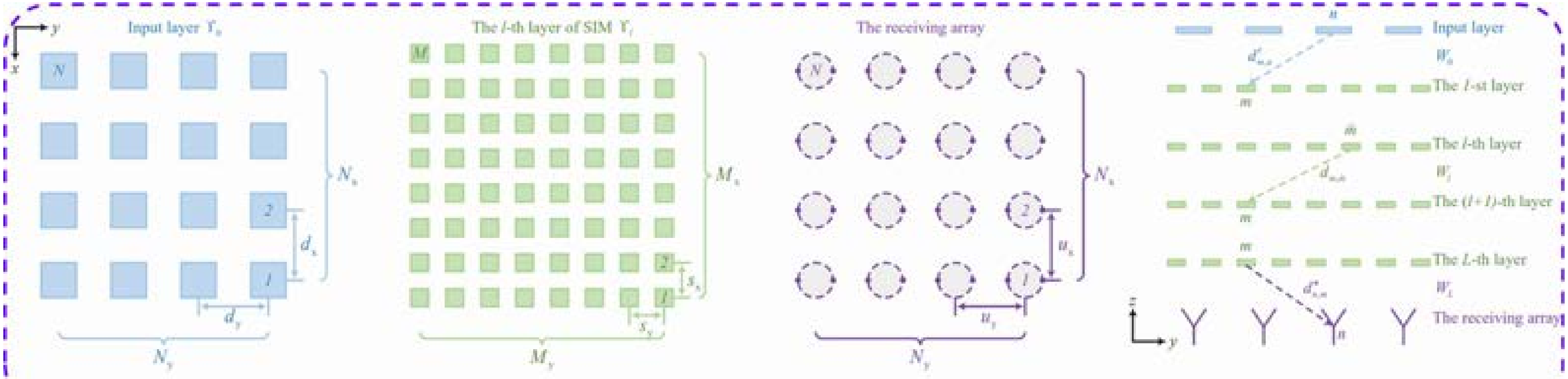

(a) The top view. (b) The front view.

The 2D index of the peak

Received signal

$$[\hat{n}, \hat{t}] = \arg \max_{\substack{n=1,\cdots,N,\\ t=1,\cdots,T}} |r_{n,t}|^2$$

Antenna Snapshot

The estimated electrical angles

$$\hat{\psi}_x = \mathrm{mod}\left[2\left(\frac{\hat{n}_x - 1}{N_x} + \frac{\hat{t}_x - 1}{N_x T_x}\right) + 1, 2\right] - 1$$

$$\hat{\psi}_y = \mathrm{mod}\left[2\left(\frac{\hat{n}_y - 1}{N_y} + \frac{\hat{t}_y - 1}{N_y T_y}\right) + 1, 2\right] - 1$$

The estimated azimuth and elevation angles

$$\hat{\varphi} = \arctan\left(\frac{\hat{\psi}_y d_x}{\hat{\psi}_x d_y}\right),$$

$$\hat{\vartheta} = \arcsin\left(\frac{1}{\kappa}\sqrt{\frac{\hat{\psi}_x^2}{d_x^2} + \frac{\hat{\psi}_y^2}{d_y^2}}\right)$$

Observed on a 4x4 Receiver

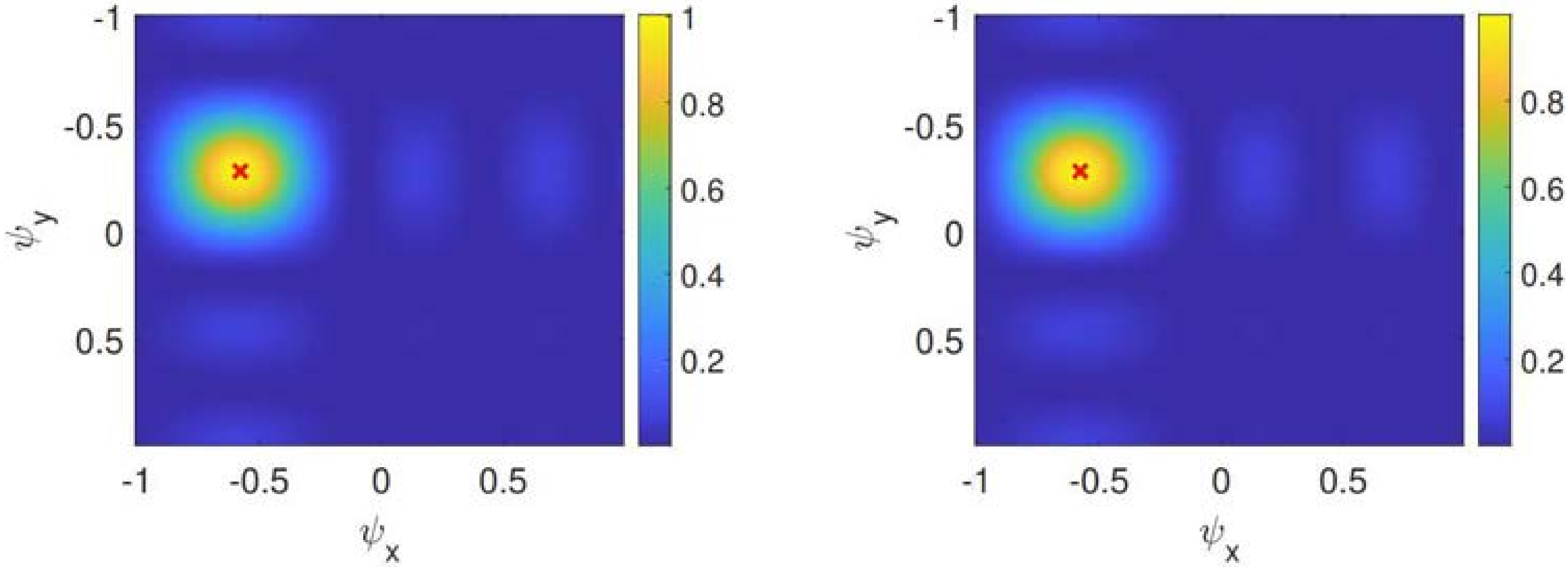

(a) 2D DFT in the wave domain; (b) 2D DFT in the digital domain.

$$\bar{\psi}_\mathrm{x} = -0.58 \text{ and } \bar{\psi}_\mathrm{y} = -0.28$$

Numerical Examples (communication and sensing)

Wave-Domain Signal Processing (Computing)

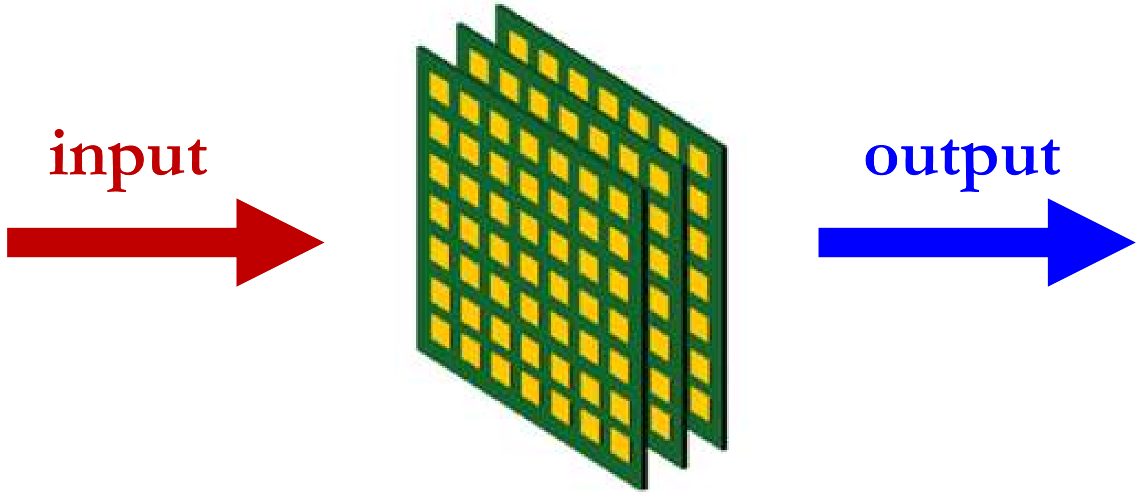

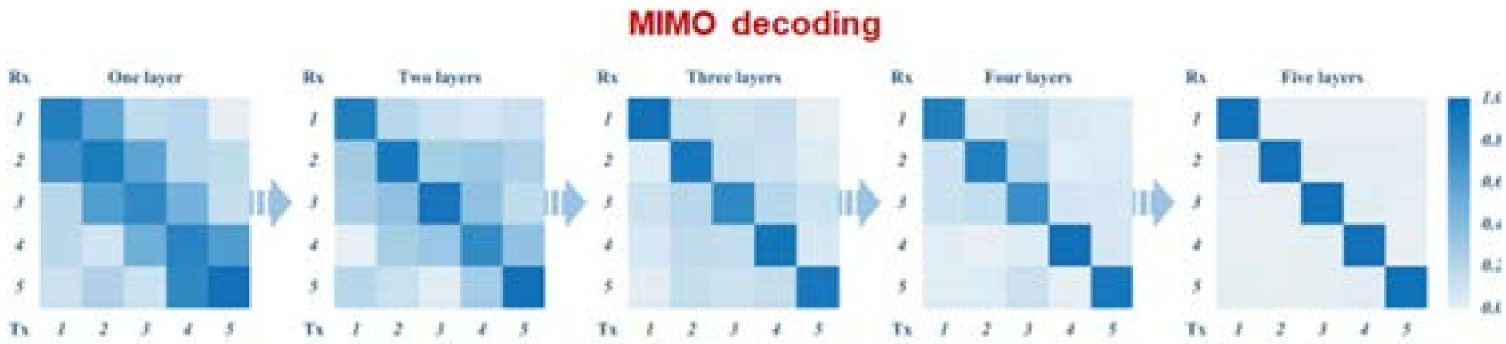

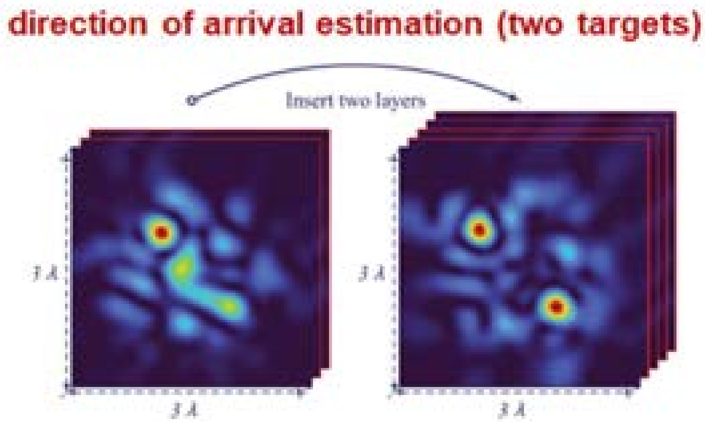

SIM Testbed Platform

A Prototype of SIM (communication & sensing)

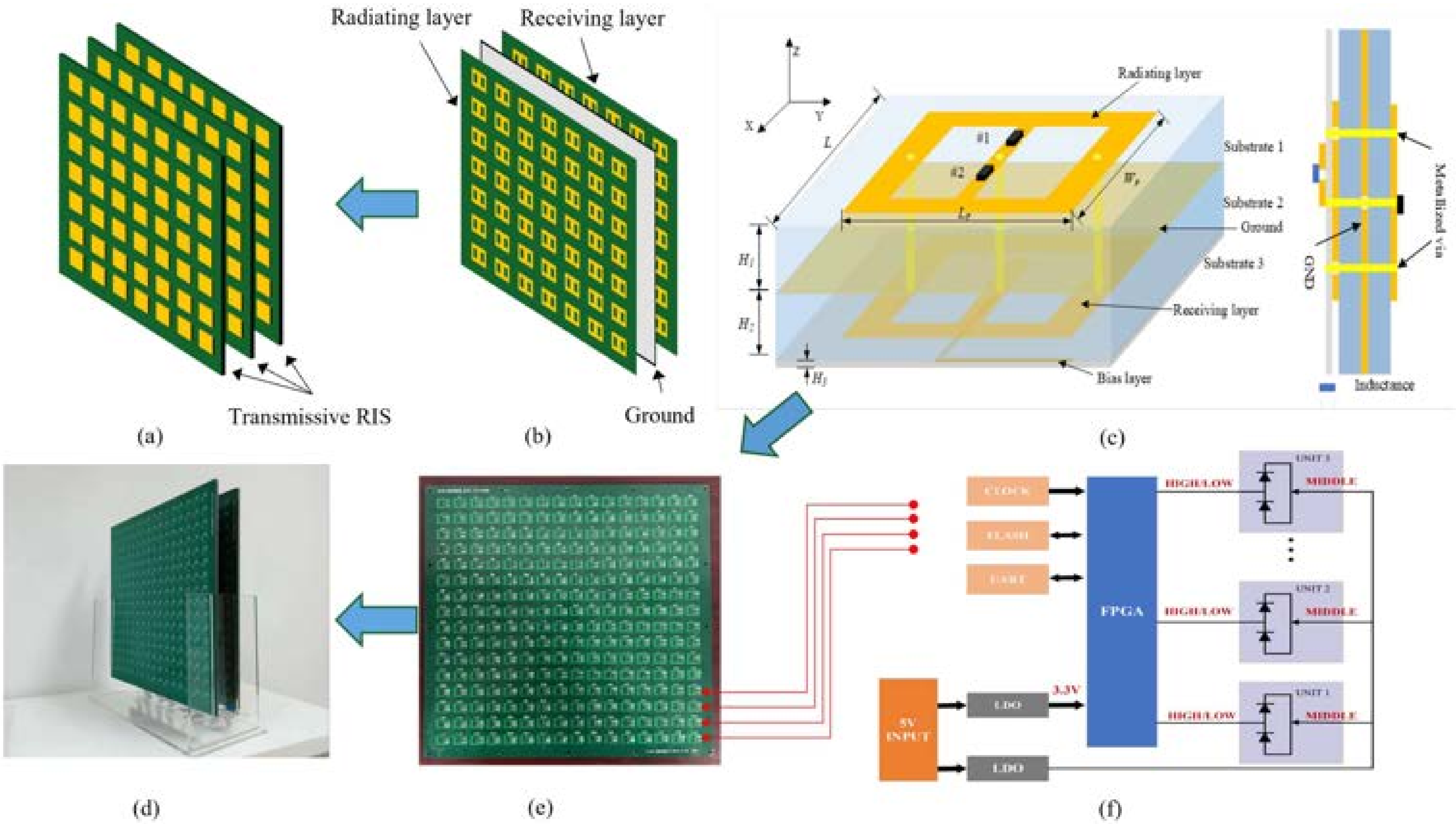

joint with

Huazhong University of Science and Technology (China)

A Prototype of SIM (communication & sensing)

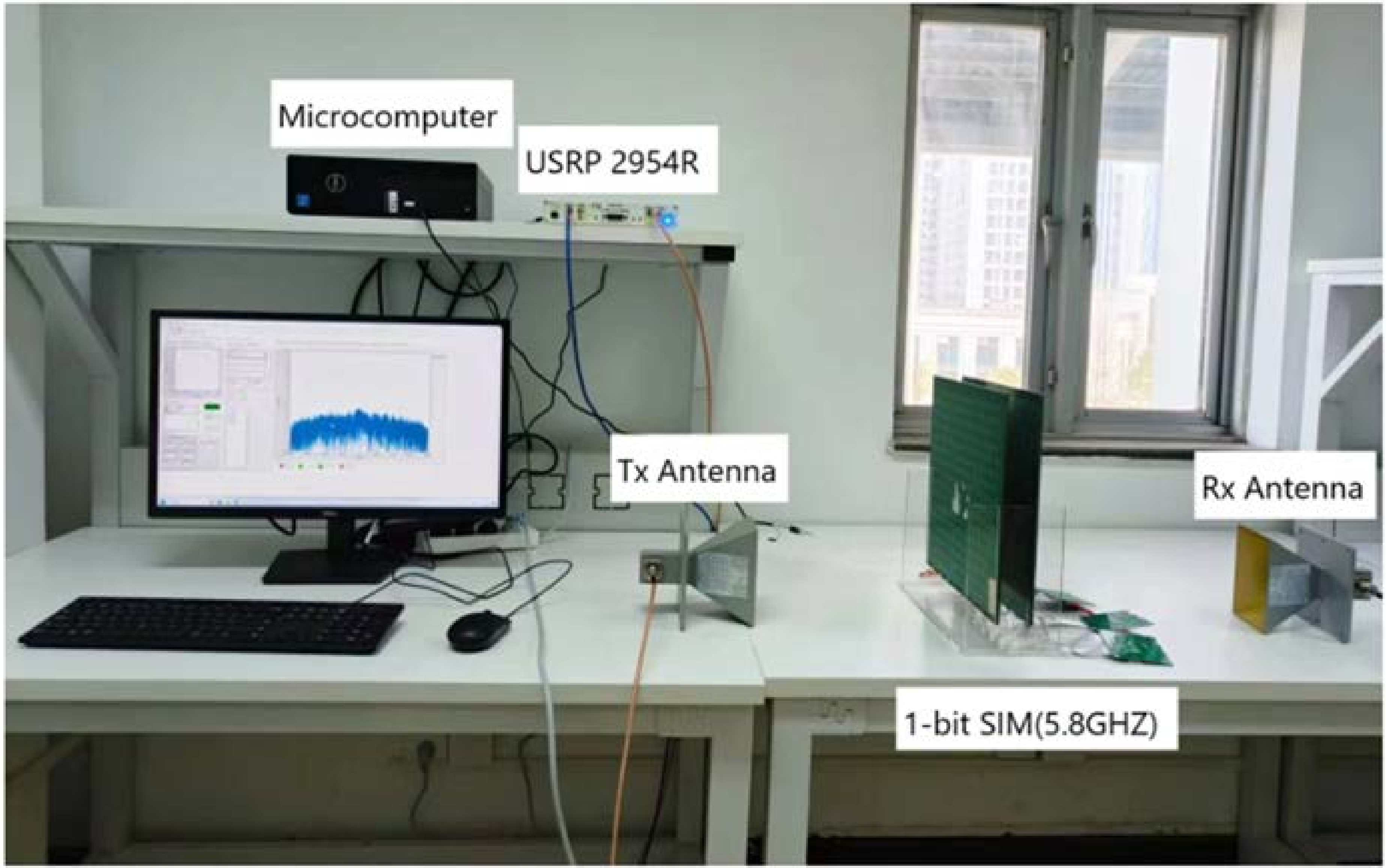

A Prototype of SIM (communication & sensing)

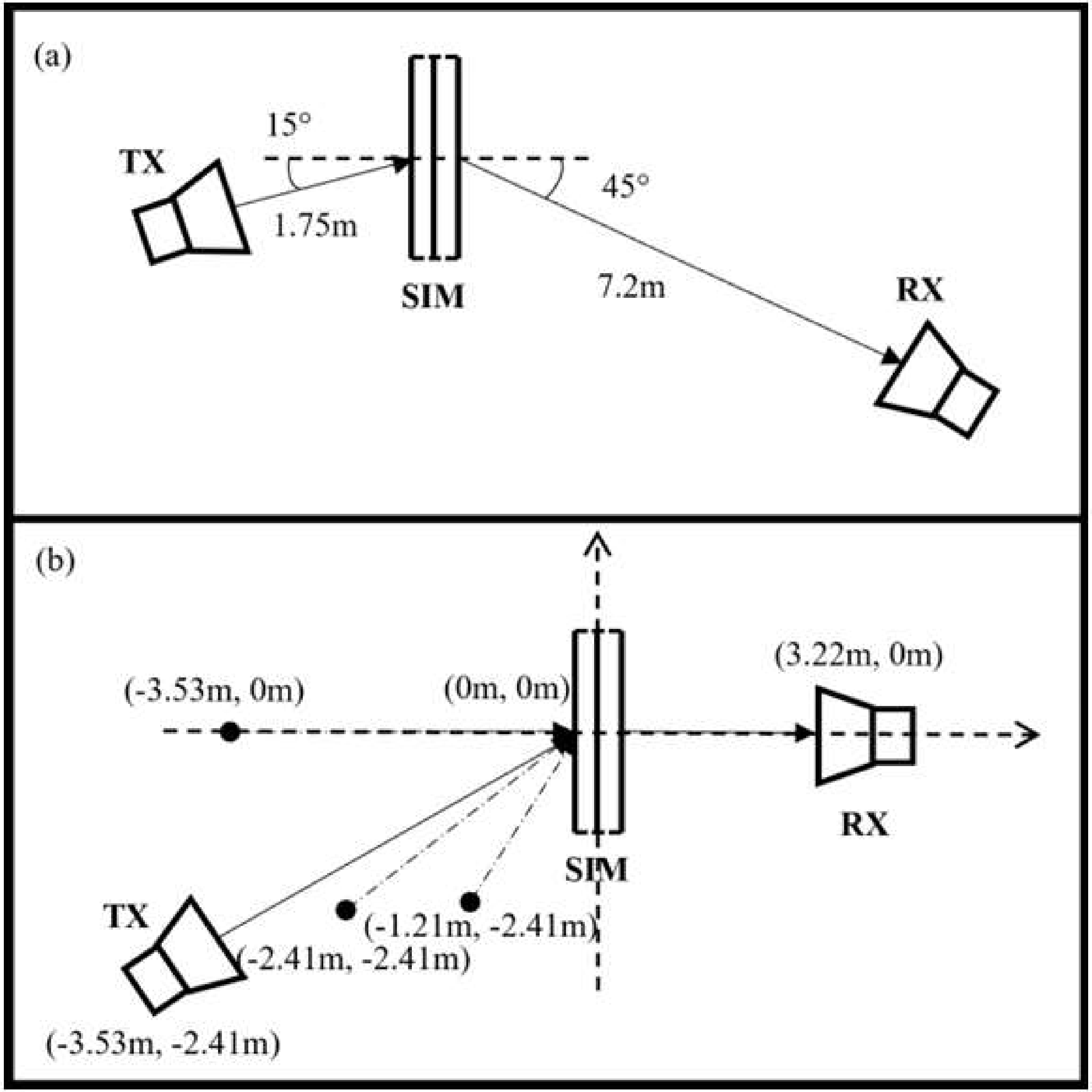

A Prototype of SIM (communication & sensing)

Communications (power)

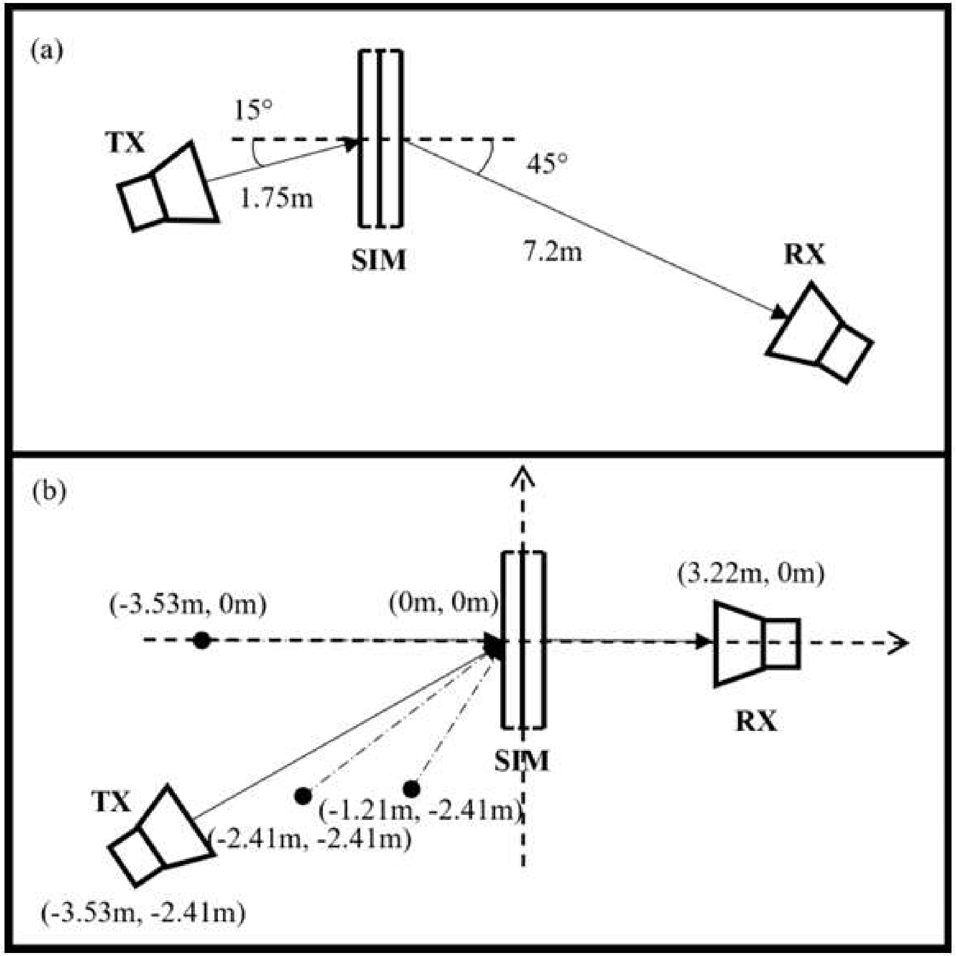

Sensing (DoA)

Num of layers	$\lambda/4$	$\lambda/2$
1-layer	-53dBm	-53dBm
2-layer	-49dBm	-50dBm
3-layer	-46dBm	-49dBm

Coordinates of TX	1-layer	2-layer	3-layer
(-3.53m, 0.00m)	4.00°	3.00°	2.50°
(-3.53m, -2.41m)	2.71°	1.79°	1.29°
(-2.41m, -2.41m)	3.50°	1.50°	1.50°
(-1.22m, -2.41m)	1.93°	0.93°	0.43°
Average error	3.572°	1.488°	1.388°

Interested in SIM ?

Recent Papers

- Jiancheng An, Marco Di Renzo, Mérouane Debbah, Chau Yuen: Stacked Intelligent Metasurfaces for Multiuser Beamforming in the Wave Domain. ICC 2023: 2834-2839 (Best Paper Award).
- Jiancheng An, Marco Di Renzo, Mérouane Debbah, H. Vincent Poor, Chau Yuen: Stacked Intelligent Metasurfaces for Multiuser Downlink Beamforming in the Wave Domain. CoRR abs/2309.02687 (2023)
- Jiancheng An, Chau Yuen, Chao Xu, Hongbin Li, Derrick Wing Kwan Ng, Marco Di Renzo, Mérouane Debbah, Lajos Hanzo: Stacked Intelligent Metasurface-Aided MIMO Transceiver Design. CoRR abs/2311.09814 (2023).
- Naveed Ul Hassan, Jiancheng An, Marco Di Renzo, Mérouane Debbah, Chau Yuen: Efficient Beamforming and Radiation Pattern Control Using Stacked Intelligent Metasurfaces. IEEE Open J. Commun. Soc. 5: 599-611 (2024).
- Jiancheng An, Chau Yuen, Marco Di Renzo, Mérouane Debbah, H. Vincent Poor, Lajos Hanzo: Stacked Intelligent Metasurface Performs a 2D DFT in the Wave Domain for DOA Estimation. CoRR abs/2310.09861 (2023).
- Jiancheng An, Chau Yuen, Yong Liang Guan, Marco Di Renzo, Mérouane Debbah, H. Vincent Poor, Lajos Hanzo: Two-Dimensional Direction-of-Arrival Estimation Using Stacked Intelligent Metasurfaces. CoRR abs/2402.08224 (2024).
- Xianghao Yao, Jiancheng An, Lu Gan, Marco Di Renzo, Chau Yuen: Channel Estimation for Stacked Intelligent Metasurface-Assisted Wireless Networks. CoRR abs/2403.05870 (2024).
- Changsheng You, Yunlong Cai, Yuanwei Liu, Marco Di Renzo, Tolga M. Duman, Aylin Yener, A. Lee Swindlehurst: Next Generation Advanced Transceiver Technologies for 6G. CoRR abs/2403.16458 (2024).

COMMAG & EuCAP 2025 – Overview Paper

An Overview of Stacked Intelligent Metasurfaces

Jiancheng An, *Member, IEEE*, Tie Jun Cui, *Fellow, IEEE*, Marco Di Renzo, *Fellow, IEEE*, Mérouane Debbah, *Fellow, IEEE*, and Chau Yuen, *Fellow, IEEE*

***Abstract*—Neural networks have incredible abilities to learn abstract features from data. Electromagnetic (EM) computing leverages wave propagation to perform computations. Metasurfaces, made up of subwavelength meta-atoms, are capable of engineering EM waves in unprecedented ways. What happens when combining these cutting-edge technologies? This question has sparked a surge of interest in designing neural networks using stacked intelligent metasurface (SIM) technology, with the aim of implementing various computational tasks by directly processing EM waves. SIMs open up an exciting avenue toward high-speed, massively parallel, and low-power signal processing in the EM domain. This article aims to provide an overview of SIM**

surface composed of periodically arranged subwavelength scattering meta-atoms. By tuning external stimuli, such as the mechanical deformation or the bias voltage using a field-programmable gate array (FPGA), each individual meta-atom can independently modulate the phase and/or amplitude of incident EM waves [2]. This breakthrough has opened up new possibilities for manipulating EM wavefronts at an unprecedented scale to achieve a wide range of functionalities, from planar hologram generation to the customization of communication environments.

State of the Art on Stacked Intelligent Metasurfaces

Communication, Sensing and Computing in the Wave Domain

Marco Di Renzo
Université Paris-Saclay, CNRS, CentraleSupélec
Laboratoire des Signaux et Systèmes, 91192 Gif-sur-Yvette, France
marco.di-renzo@universite-paris-saclay.fr

***Abstract*—Stacked intelligent metasurface (SIM) is an emerging technology that capitalizes on reconfigurable metasurfaces for several applications in wireless communications. SIM is considered an enabler for integrating communication, sensing and computing in a unique platform. In this paper, we offer a survey on the state of the art of SIM for wireless communications.**

***Index Terms*—Dynamic metasurfaces, reconfigurable intelligent surfaces, stacked intelligent metasurfaces.**

A. Beamforming Design

Most available research works are focused on beamforming design, with the objective of optimizing and comparing the performance of SIM against fully-digital implementations. Examples of recent contributions include [10], [15], [16], [17], [18], [19], [20], [21], [22], [23], [24], [25]. In [17], for example, several illustrations about the impact of the number of stacked layers are presented. Machine learning

What’s next ?

Conformal Metamorphic Metasurfaces

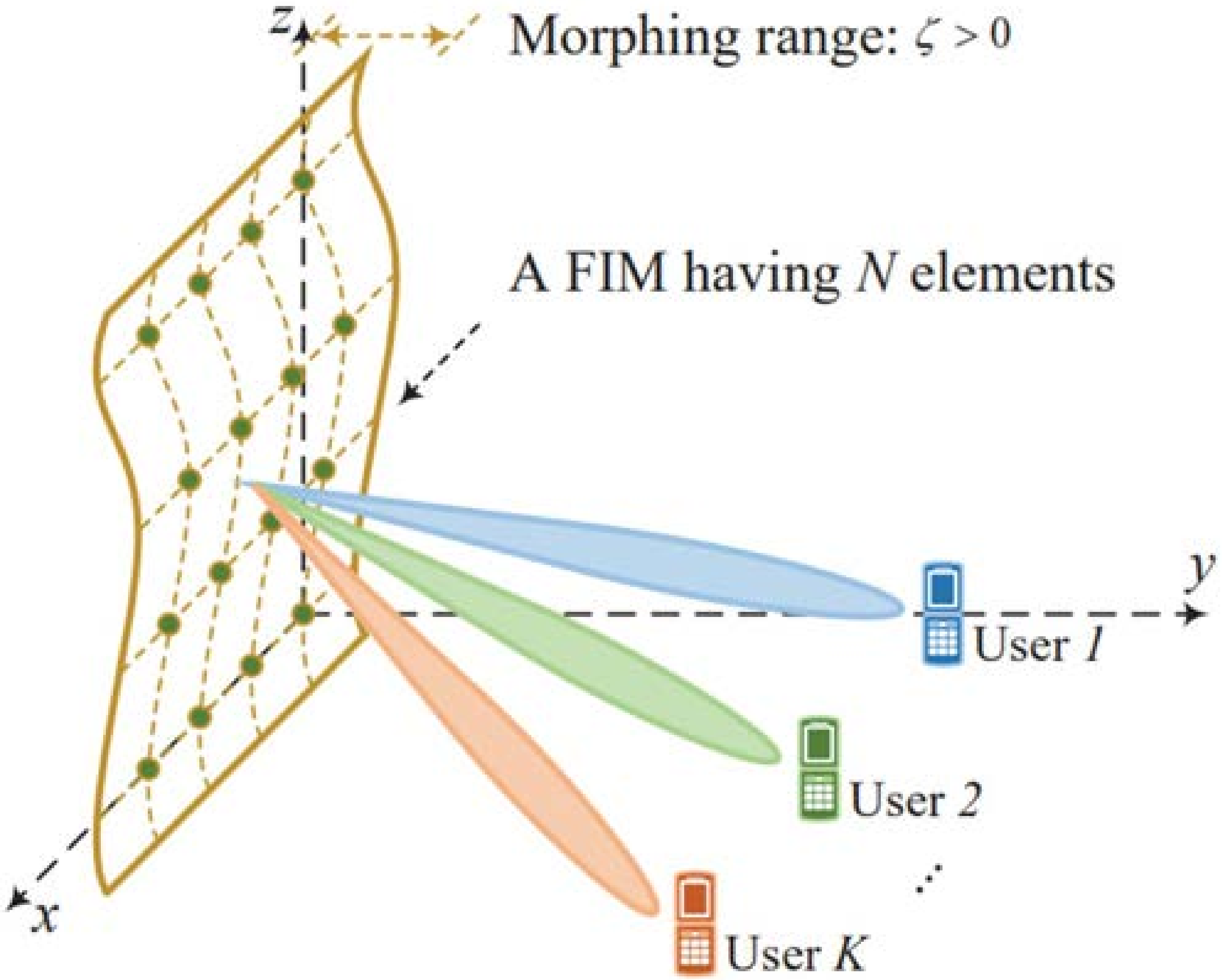

Flexible Intelligent Metasurface (FIM)

Flexible Intelligent Metasurface for Multiuser MISO Communications: Joint Transmit Beamforming and Surface-Shape Morphing

Jiancheng An, *Member, IEEE*, Chau Yuen, *Fellow, IEEE*, Marco Di Renzo, *Fellow, IEEE*, Mérouane Debbah, *Fellow, IEEE*, H. Vincent Poor, *Life Fellow, IEEE*, and Lajos Hanzo, *Life Fellow, IEEE*

***Abstract*—A flexible intelligent metasurface (FIM) shows promise in terms of enhancing the spectrum and energy efficiency of wireless networks. Specifically, it is composed of an array of low-cost radiating elements, each of which can independently radiate electromagnetic signals, while flexibly adjusting its position along the direction perpendicular to the surface. This is of particular interest for wireless communication systems operating at TeraHertz frequencies, where the deep fading generally occurs within a few millimeters. Hence, in contrast to conventional rigid 2D antenna arrays, the FIM surface-shape may be reconfigured for improving the channel quality by beneficial 3D morphing. Explicitly, we investigate the multiuser downlink, where an FIM at the base station (BS) communicates with multiple single-antenna users. We formulate a transmit optimization problem for minimizing the total transmit power at the BS by jointly optimizing the transmit beamforming and the FIM surface-shape, subject to the individual signal-to-interference-plus-noise ratio constraint of each user as well as to the maximum FIM morphing range. To solve this problem, we first consider a simple single-user scenario and show that the optimal surface-shape is achieved by independently adjusting each FIM element to the position having the strongest channel gain. However, in the realistic multiuser scenario, the FIM surface-shape morphing involves complex tradeoffs. To address this issue, an efficient alternating optimization method is conceived for iteratively updating the FIM surface-shape and the transmit beamformer for gradually reducing the transmit power. Additionally, we analyze the performance gain of the FIM, showcasing a logarithmic received power scaling law versus its maximum morphing range. Finally, our simulation results show that the FIM reduces the transmit power by about 3 dB compared to conventional rigid 2D arrays at a given data rate.**

***Index Terms*—Flexible intelligent metasurface (FIM), transmit beamforming, surface-shape morphing, MIMO, intelligent surfaces.**

I. Introduction

NEXT-GENERATION wireless networks aim for supporting many innovative applications, such as brain-computer interfaces, high-fidelity holograms, connected robotics, and autonomous vehicles [1]. However, these applications entail very stringent quality-of-service (QoS) demands, including extremely high data rates, ubiquitous and ultra-reliable connectivity, as well as ultra-low latency [2], which cannot be readily achieved by the current network infrastructure. While deploying a plethora of antennas and base stations operating at higher frequencies having ample bandwidth could meet these goals, both the energy consumption and hardware costs of these solutions would be excessive. To balance these challenging QoS requirements against energy efficiency, researchers have developed sophisticated wireless technologies over the past decade. Among them, the emerging metasurface technology is regarded as one of the most promising solutions [3]–[6].

Generally speaking, a metasurface is an artificially engineered planar surface constructed of an array of tiny meta-atoms [3]. Each meta-atom is capable of independently radiating or scattering wireless signals by beneficially ameliorating the properties of electromagnetic (EM) waves, such as their amplitude, phase, and polarization [5]. In recent years, deploying near-passive reconfigurable intelligent surfaces (RISs) in wireless networks has shown significant potential for shaping wireless propagation environments [7]. For example, in indoor scenarios, installing RISs on walls or ceilings can circumvent the blockage of the line-of-sight (LoS) propagation link between a WiFi access point and a mobile device [8], hence significantly boosting the received signal strength. Since RISs interact with the incoming signals without requiring power amplifiers and complex signal processing, they avoid the costly radio frequency (RF) hardware of conventional active transceivers [4].

While RISs promise appealing benefits, their real-world applications still face several major challenges. *Firstly*, the acquisition of channel state information (CSI) is more difficult for RIS-aided networks, since a large number of pilots are required to probe the two-hop source-RIS-destination channels [4]. *Secondly*, the RIS phase shifts have to be optimized together with the active beamformer to enhance the network performance, resulting in high computational complexity [8]. *Thirdly*, the optimized phase shifts have to be sent to the RIS controller over a dedicated feedback link, imposing additional control signaling overhead [7]. The wireless research community is actively working on practical deployments of RISs having scalable overhead and complexity, as detailed in [4], [9].

A complementary approach to the above near-passive RISs is to harness active metasurfaces as transceivers, which are known as large intelligent surfaces (LISs) [10]. Given an electrically large aperture operating in high-frequency bands,

J. An and C. Yuen are with the School of Electrical and Electronics Engineering, Nanyang Technological University, Singapore 639798 (e-mail: jiancheng.an@ntu.edu.sg, chau.yuen@ntu.edu.sg). M. Di Renzo is with Université Paris-Saclay, CNRS, CentraleSupélec, Laboratoire des Signaux et Systèmes, 3 Rue Joliot-Curie, 91192 Gif-sur-Yvette, France (e-mail: marco.di-renzo@universite-paris-saclay.fr). M. Debbah is with Khalifa University of Science and Technology, P O Box 127788, Abu Dhabi, UAE (e-mail: merouane.debbah@ku.ac.ae). H. V. Poor is with the Department of Electrical and Computer Engineering, Princeton University, Princeton, NJ 08544, USA (e-mail: poor@princeton.edu). L. Hanzo is with the School of Electronics and Computer Science, University of Southampton, Southampton SO17 1BJ, U.K. (e-mail: lh@ecs.soton.ac.uk).

T3DRIS: Advancing Conformal RIS Design through In-depth Analysis of Mutual Coupling Effects

Placido Mursia, *Member, IEEE*, Francesco Devoti, *Member, IEEE*, Marco Rossanese, *Student Member, IEEE*, Vincenzo Sciancalepore, *Senior Member, IEEE*, Gabriele Gradoni, *Senior Member, IEEE*, Marco Di Renzo, *Fellow, IEEE*, Xavier Costa-Pérez, *Senior Member, IEEE*

***Abstract*—This paper presents a theoretical and mathematical framework for the design of a conformal reconfigurable intelligent surface (RIS) that adapts to non-planar geometries, which is a critical advancement for the deployment of RIS on non-planar and irregular surfaces as envisioned in smart radio environments. Previous research focused mainly on the optimization of RISs assuming a predetermined shape, while neglecting the intricate interplay between shape optimization, phase optimization, and mutual coupling effects. Our contribution, the T3DRIS framework, addresses this fundamental problem by integrating the configuration and shape optimization of RISs into a unified model and design framework, thus facilitating the application of RIS technology to a wider spectrum of environmental objects. The mathematical core of T3DRIS is rooted in optimizing the 3D deployment of the unit cells and tuning circuits, aiming at maximizing the communication performance. Through rigorous full-wave simulations and a comprehensive set of numerical analyses, we validate the proposed approach and demonstrate its superior performance and applicability over contemporary designs. This study—the first of its kind—paves the way for a new direction in RIS research, emphasizing the importance of a theoretical and mathematical perspective in tackling the challenges of conformal RISs.**

***Index Terms*—Reconfigurable intelligent surfaces, smart radio environments, conformal metasurfaces, mutual coupling, optimization.**

I. Introduction

A. Background & Motivation

In the landscape of modern wireless communication systems, the advent of reconfigurable intelligent surface (RIS) marks a significant milestone [1], introducing the capability to dynamically manipulate the propagation of electromagnetic (EM) waves. This property, together with its flexibility in deployment and reconfiguration, low implementation cost and energy consumption, positions RIS as a primary technology candidate for the upcoming 6th generation of wireless networks (6G) [2], opening up the possibility of optimizing the communication channel to best serve different use cases that 6G will support [3], [4]. Conventional implementations have

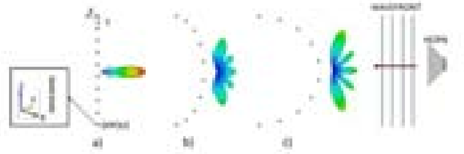

Fig. 1. Reflection properties of curved surfaces (a) planar, (b) cylindrical and (c) super-cylindrical).

predominantly explored planar RIS architectures, which, while effective, encounter limitations in adaptability and versatility, particularly when confronted with the complexity of non-planar deployment scenarios [5].

Fig. 1 shows an interesting experiment: a wave from a signal source (on the right) hits three different surfaces made of dipoles spaced evenly apart. When the wave hits the flat surface (sub-figure (*a*)), it acts like a mirror, bouncing the wave back in a tight, focused beam. However, when the surface is curved (sub-figures (*b*) and (*c*)), an insightful behavior can be observed: several beams are spreading out over a larger area. This prompts an exploration into how the design of an EM surface shape can influence the way it interacts with incoming waves, giving rise to the burgeoning field of conformal or three dimensional (3D) RIS,[1] sculpted to the unique topography of their hosting environments [6].

Notwithstanding the progress in advanced printing techniques that facilitate the fabrication of irregular electronic boards, the precision placement and orientation of unit cells on 3D surfaces present formidable technical challenges [7]. These include not only the physical constraints of inter-element spacing, alignment, and orientation in 3D, but also the intricate mathematical modeling necessary for effective dynamic control of such systems [8], [9]. The fidelity of models based on infinite planar arrays falters when confronted with the finite size and curvature of real-world structures, leading to discrepancies between theoretical predictions and empirical observations. Therefore, the optimization of the 3D RIS layout and its corresponding configuration demands sophisticated algorithms tuned to complex environmental dynamics and EM interactions.

Recently, impedance-based models have been proposed to advance the optimization and efficient design of RISs [10].

P. Mursia, F. Devoti, M. Rossanese and V. Sciancalepore, are with NEC Laboratories Europe, 69115 Heidelberg, Germany (email: name.surname@neclab.eu).
G. Gradoni is with University of Surrey, Stag Hill, University Campus, Guildford GU2 7XH, UK (email: g.gradoni@surrey.ac.uk).
M. Di Renzo is with Université Paris-Saclay, CNRS, CentraleSupélec, Laboratoire des Signaux et Systèmes, 91190 Gif-sur-Yvette, France (email: marco.di-renzo@universite-paris-saclay.fr).
X. Costa-Pérez is with i2cat, ICREA, 08034 Barcelona, Spain and NEC Laboratories Europe (email: xavier.costa@neclab.eu).
Email of the corresponding author: placido.mursia@neclab.eu

[1] We use the terms 3D RIS and conformal RIS interchangeably throughout the paper.

Conformal Metamorphic Metasurfaces

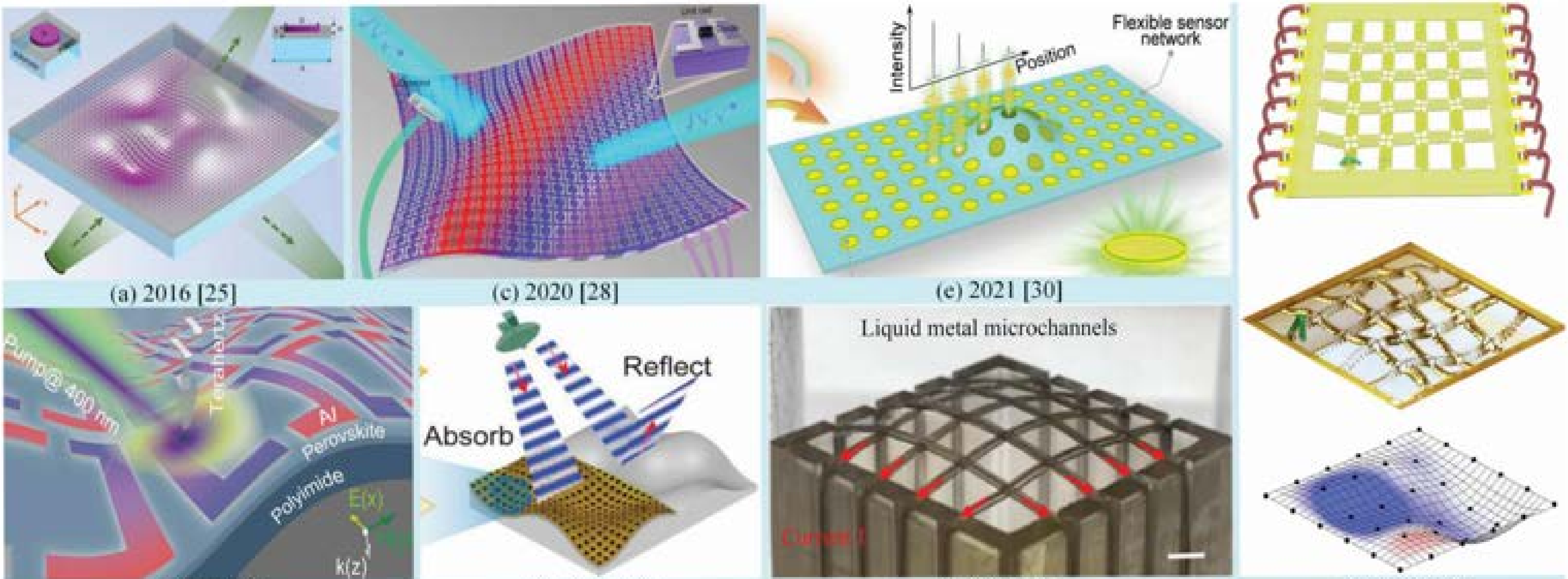

(a) 2016 [25] (c) 2020 [28] (e) 2021 [30]
(b) 2017 [27] (d) 2021 [29] (f) 2022 [31] (g) 2022 [32]

Conformal Metamorphic Metasurfaces

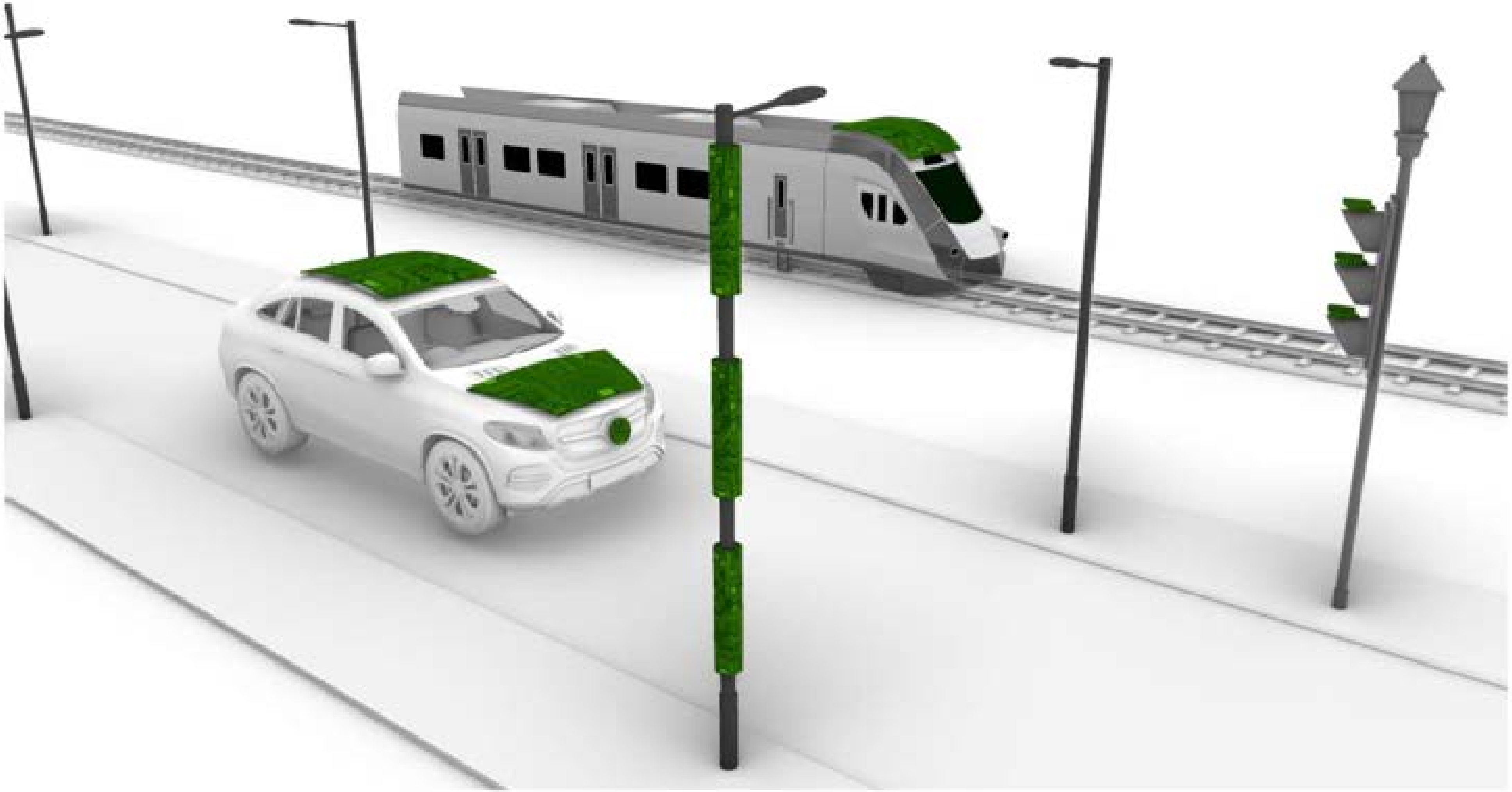

Conformal Metamorphic Metasurfaces

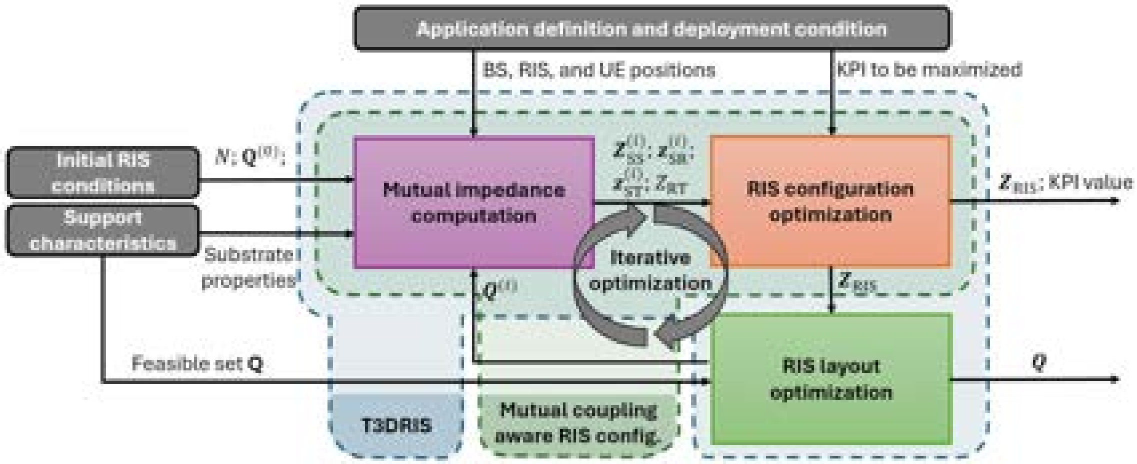

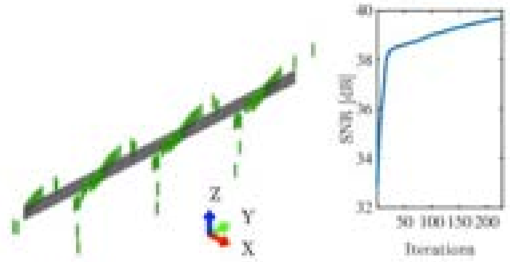

(a) ULA

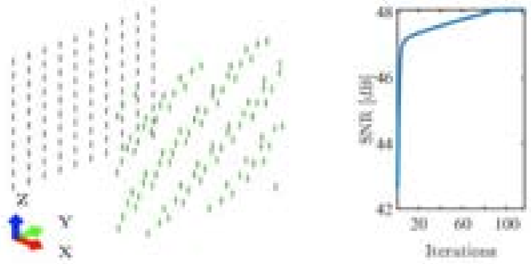

(b) UPA

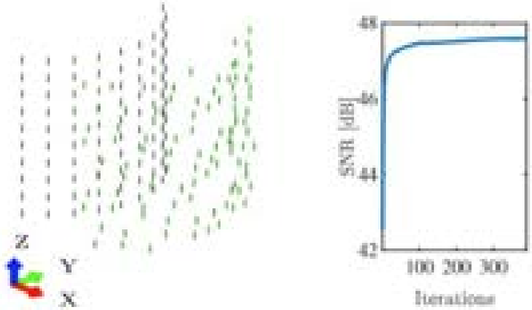

(c) Cylindrical

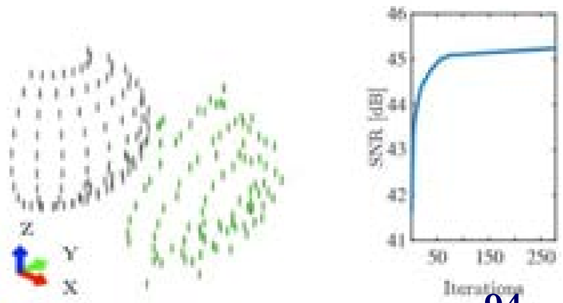

(d) Spherical

Multifunction Reconfigurable Surface → ISAC

nature communications

Article

https://doi.org/10.1038/s41467-025-57137-6

Integrated sensing and communication based on space-time-coding metasurfaces

Received: 14 May 2024

Accepted: 7 February 2025

Published online: 21 February 2025

Check for updates

Xiao Qing Chen[1,5], Lei Zhang[1,5], Yi Ning Zheng[1,5], Shuo Liu[1], Zhuo Ran Huang[1], Jing Cheng Liang[1], Marco Di Renzo[2,3], Vincenzo Galdi[4] & Tie Jun Cui[1]

Programmable metasurfaces (PMs), also called reconfigurable intelligent surfaces (RISs), are planar structures capable of dynamically manipulating electromagnetic waves in real-time. Regarded as a key enabling technology for implementing smart wireless propagation environments, PMs/RISs also serve as an ideal supporting platform for integrated sensing and communication (ISAC). Here, we propose two ISAC schemes based on a special type of PMs/RISs: space-time-coding metasurfaces (STCMs). By leveraging space-time-coding strategies, STCMs simultaneously control the propagation at the fundamental (carrier) frequency for reliable wireless communication and generate spatially distributed harmonics for sensing. The proposed schemes seamlessly integrate both communication and sensing on a shared hardware platform, eliminating the need for additional sensors. For experimental validation, we implemented an ISAC system using a 2-bit STCM operating at microwave frequencies. Experimental results align with theoretical predictions, confirming the practical viability and effectiveness of the proposed ISAC schemes for applications in communication, imaging, radar, and sensing systems.

ISAC Using STCM

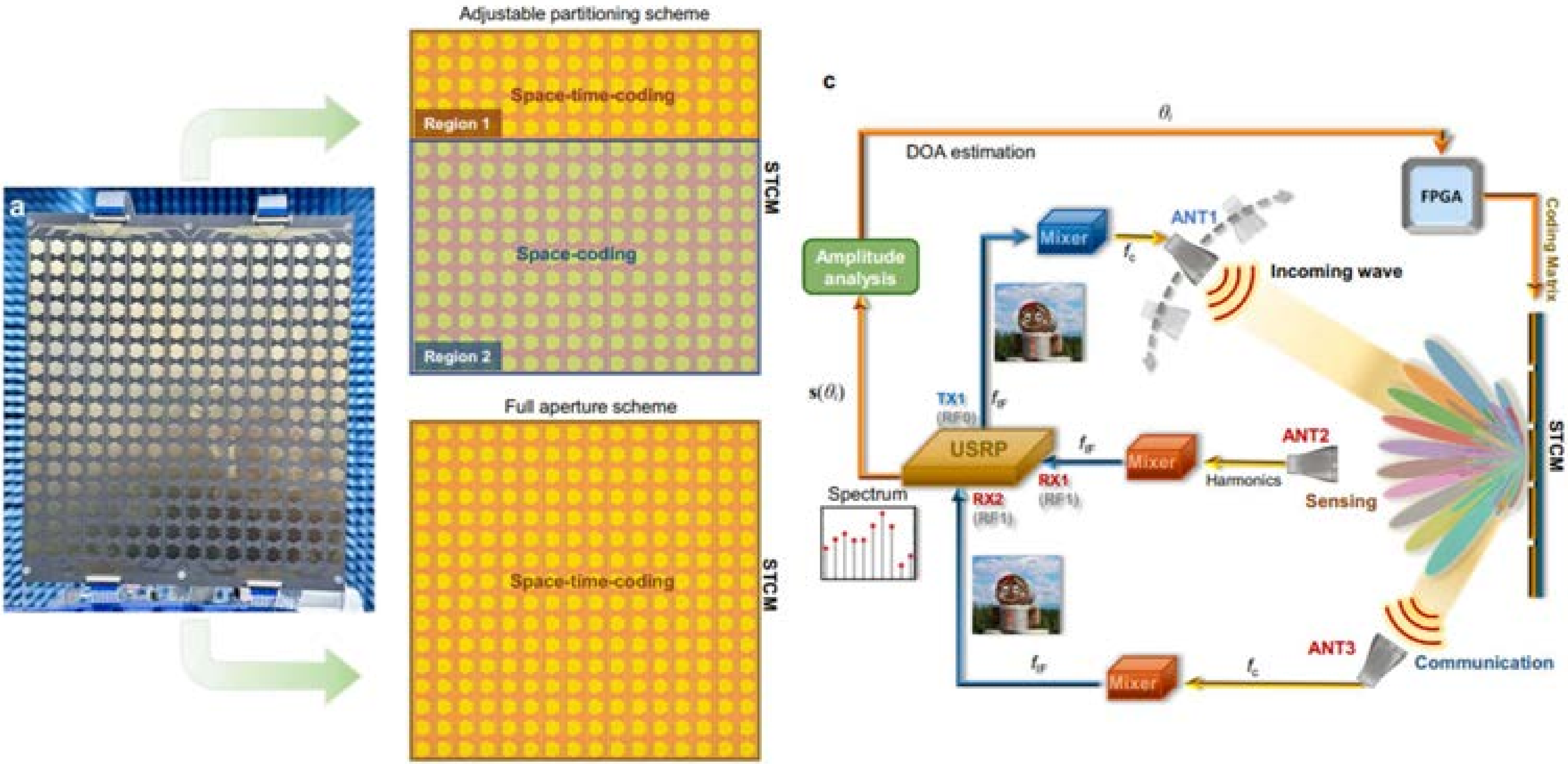

ISAC Using STCM

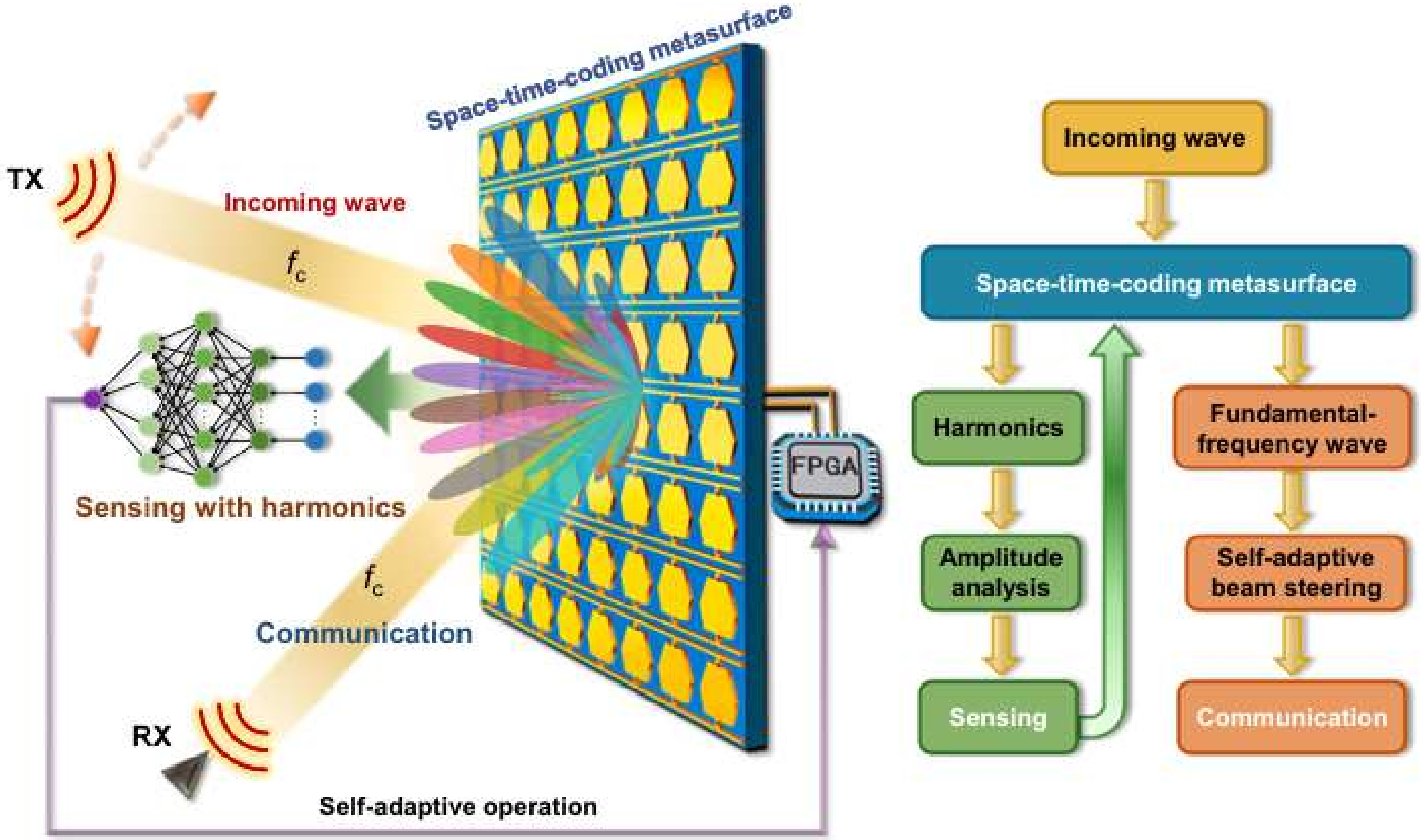

$$\boxed{f_{\mathrm{T}}^{v}(\theta,\theta_i)} = f_e(\theta)\sum_{n=1}^{N}\boxed{a_v^n}\exp\left(j(n-1)d\left[\boxed{k_v}\sin\theta + k_c\boxed{\sin\theta_i}\right]\right)$$

Scattered field of the harmonic v

Fourier coefficients of the time-periodic modulation signal

Angle of incidence

ISAC Using STCM

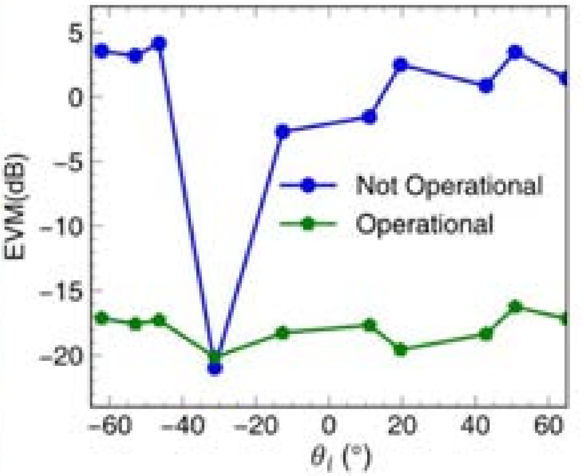

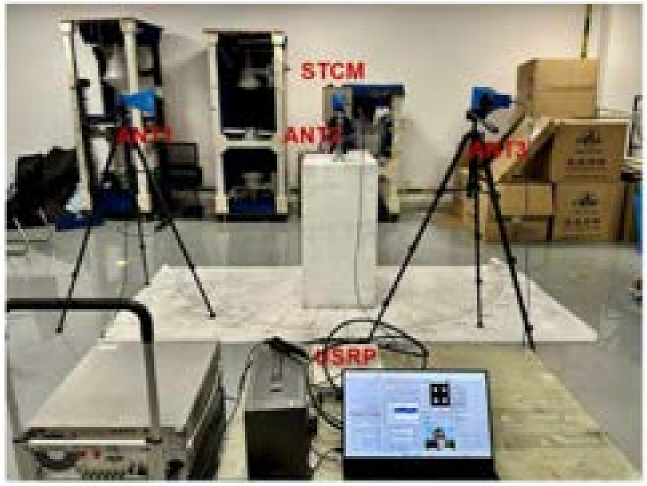

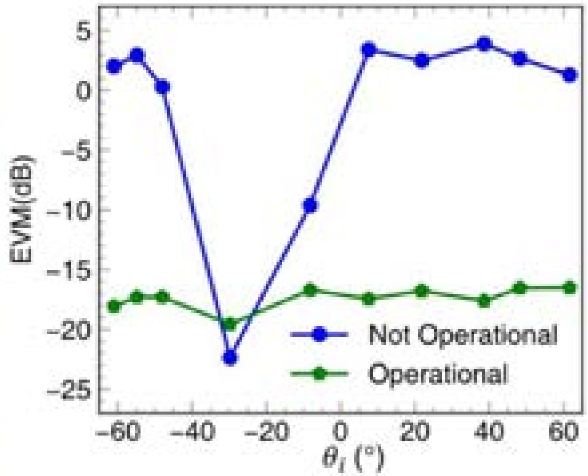

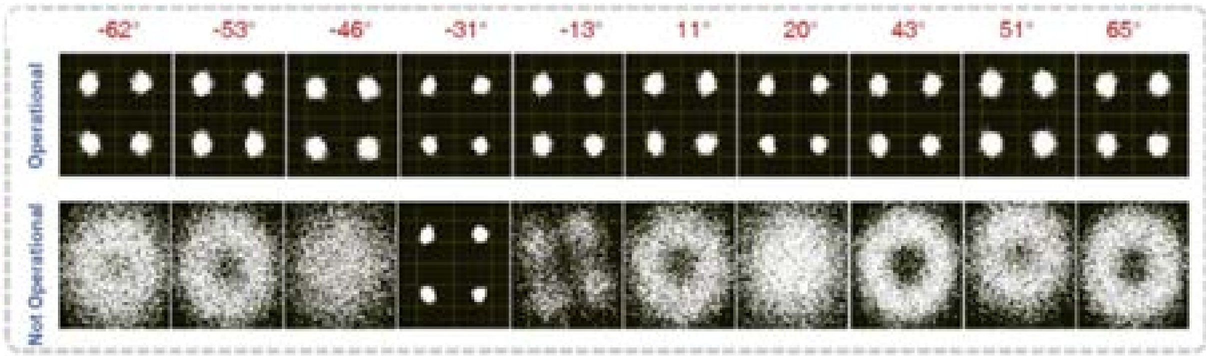

Thanks – ANR PEPR Networks of the Future

FRANCE 2030 PROGRAMME DE RECHERCHE RÉSEAUX DU FUTUR

The PEPR | Projects | News | Recruit | Results | Contact us

https://pepr-futurenetworks.fr/en/home/

Priority Research Programme and Equipment

Led by

cea | cnrs | Institut Mines-Télécom

Financed by

FRANCE 2030

Acted by

anr agence nationale de la recherche

Some numbers

500
permanent scientists

67
post-doctoral fellows to be recruited

34
research laboratories

104
doctoral students to be recruited

Stacked Intelligent Metasurfaces

Communication, Computing and Sensing in the Wave Domain

Marco Di Renzo

CNRS Research Director – CentraleSupélec, Paris-Saclay University, France
Chair Professor in Telecom Engineering, King's College London, UK
marco.di-renzo@universite-paris-saclay.fr, marco.di_renzo@kcl.ac.uk

HE-MSCA-DN-2021

ANR-23
CHR-2022

HE-JU-SNS-2023

COST ACTION

Télécom Paris – IP Paris
Seminaire ICE
May 6, 2025